Polyelectrolyte Complex Nanoparticle Nutrient delivery system for Microbial Enhanced Oil Recovery

By

Weiwei Li

B.Sc. Biotechnology and Bioengineering, University of Inner Mongolia, Hohhot, Inner Mongolia, China, 2007

M.Sc. Petroleum Engineering, New Mexico Tech, USA, 2010

Submitted to the graduate degree program in Department of Chemical and Petroleum Engineering and the Graduate Faculty of the University of Kansas in partial fulfillment of the requirements for the degree of Doctor of Philosophy.

Committee members:

_____

Susan Williams

(Chairperson)

_____

Jenn-Tai Liang

(Co-chairperson)

_____

Stephen Johnson

_____

Belinda Sturm

_____

Cory Berkland

_____

Reza Barati

_____

Karen Peltier

Date defended: _____

Abstract

Microbial enhanced oil recovery (MEOR) techniques stimulate naturally occurring reservoir microbes or inject specially selected consortia of natural bacteria into the reservoir. The stimulated microbes produce specific metabolites such as surfactants, polymers, acid or gases that lead to the extraction of oil trapped in capillary pores of the formation rock or in areas not swept by the classical or modern enhanced oil recovery (EOR) methods. Although the potential benefits of MEOR applications are considerable, improvement of oil recovery via the manipulation of microbial metabolism in the reservoir remains an unproven concept. One of the major issues of MEOR application is that biomass and extracellular polymeric substances produced in response to high injected nutrient concentrations can cause plugging close to the injection point (near wellbore plugging).

In this study, a novel approach to MEOR is discussed. Polyelectrolyte complex nanoparticles (PECs) were used to encapsulate and propagate nutrients, and release the nutrient substrate slowly, to enable stimulation of the microbes to occur over an extended distance and prevent near wellbore plugging.

In the present study, polyethylenimine-dextran sulfate (PEI-DS) polyelectrolyte complexes were used to entrap nutrients commonly used in microbial stimulation. Stability of PEC nanoparticles were tested over time. The toxicity of PEI and DS to a bacterial consortium isolated from Wellington oil field, Wellington, KS was also monitored by aerobic batch culture. The microbes survived at a DS concentration up to 6000 ppm and a PEI concentration up to 3000 ppm.

Bacteria growth, as revealed by plate counting, was delayed, compared to equivalent systems where the nutrient mixture was not entrapped (positive control group). This is consistent with the hypothesis that PEC nanoparticles delay the growth of microbes by entrapping their nutrient source. Compared to the positive control group, the entrapped nutrient group has a 10^2 magnitude decrease in microbial number for the first 72 hours; also the entrapped nutrient group requires at least 96 hours more to reach the stationary phase.

Acknowledgement

First and foremost, I would like to express my gratitude to my advisors: Prof. Jenn-Tai Liang and Prof. Stephen Johnson for their continuous motivation and support during the entire period of this study.

I would also like to thank Prof. Susan Williams for serving as my committee chair and help in editing my dissertation and arranging everything for my defence.

Deep appreciation is also extended to Prof. Belinda Sturm and Dr. Cory Berkland for their enlightening and insightful comments that greatly improved the whole research, especially in the cell incubation and nanoparticle.

I would also like to extend my appreciation to Prof. Reza Barati Ghahfarokhi for serving in my committee.

I would also like to thank Dr. Shengxue Xie for his great help in the sand pack experiments; Dr. Ying-Ying Lin, Dr. Huili Guan, Dr. Kaixu Song and Dr. Ying Wang for their insightful comments that greatly improved the whole research.

I greatly appreciate Dr. Karen Peltier for all her assistance with construction and operating laboratory equipment and procedures. I also thank all my fellow students in TORP for their help and friendship.

Finally, I would like to dedicate this document to my beloved parents and my wife,

Yan Gao, for their love and support.

Table of Contents

List of figures

List of tables

1. Introduction

Microbial enhanced oil recovery (MEOR) techniques stimulate naturally occurring reservoir microbes or inject specially selected consortia of natural bacteria into the reservoir. The stimulated microbes produce specific metabolites such as surfactants, polymers, acid or gases that lead to the extraction of oil trapped in capillary pores of the formation rock or in areas not swept by the classical or modern enhanced oil recovery (EOR) methods.[1] Although the potential benefits of MEOR applications are considerable,[2] improvement of oil recovery via the manipulation of microbial metabolism in the reservoir remains an unproven concept. One of the major issues of MEOR application is that biomass and extracellular polymeric substances produced in response to high injected nutrient concentrations can cause plugging close to the injection point (near wellbore plugging).[3]

1.1 Objectives and rationale of this study

In this study, a novel approach for MEOR is discussed. Polyelectrolyte complex nanoparticles (PECNPs) are used to encapsulate and propagate nutrients. It is hypothesized that PEC nanoparticles are capable of controlling the release of nutrients with the potential for application in microbial enhanced oil recovery. The general goal of this research is to develop nano-sized carriers capable of carrying nutrients to the reservoir, delaying the release of nutrients in order to enable stimulation of the microbes to occur over an extended distance and prevent near wellbore plugging.

The approach taken towards the objective of this research is threefold. In the first part, charged nanoparticles with high nutrient entrapment efficiency and high stability are

developed. In this part, we show that PEC nanoparticles can entrap and release nutrients. Negatively charged PEC nanoparticles are prepared by varying the volume ratio of polycations (polyethylenimine or cationic starch) and a polyanion (dextran sulfate). Peptone, a digested peptide typically used as a nutrient for microbes, is added into PEC nanoparticles as the third component. Particle size, zeta potential, and entrapment efficiency are tested to characterize the properties of the nanoparticles.

In the second part, the toxicity of nanoparticle compositions is analyzed by adding polyelectrolytes at concentrations required to deliver nutrients to the incubation media. The microbial generation time and cell growth rate of microbes in the toxicity tests are monitored and compared with these parameters of microbes incubated in the peptone media (positive control).

In the third part, when nutrients are entrapped in polyelectrolyte complex nanoparticles, the growth kinetics of both aerobic and anaerobic microbes are tested to evaluate the potential of nanoparticles in delaying the microbial growth.

The results of this research provide two nanoparticle systems that are capable of delaying the growth of microbes by entrapping the nutrients inside the polyelectrolyte complex nanoparticle. These systems can potentially be applied to solve the near wellbore plugging caused by biostimulation.

1.2 Dissertation organization

The following chapter (Chapter 2) is aimed at familiarizing the reader with some fundamentals and related testing methods for both microbial enhanced oil recovery and polyelectrolyte complex nanoparticles. Chapter 3 discusses the materials and methods used in this study. More detailed formulas and selection between multiple testing methods can be found in Appendix 1 and 2. The results of experiments are included in Chapter 4 with the comparison to the parallel studies. Chapter 5 contains the summary and conclusions, with future work listed in Chapter 6.

2. Literature review

In this section, microbial enhanced oil recovery (MEOR), polyelectrolytes, and self-assembled polyelectrolyte complex nanoparticles (PECNP) are reviewed. In Section 2.1, a general introduction to MEOR is presented. In Section 2.2, the relationship between reservoir and microbes is introduced. In Section 2.3, the classification and mechanism of MEOR are introduced. Section 2.4 presents a detailed review of the polymers and polyelectrolytes. Section 2.5 explains the mechanism of polyelectrolyte complex nanoparticles formation. In Section 2.6, the methods used to characterize nanoparticles are listed. Finally, in Section 2.7, the polyethylenimine/dextran sulfate nanoparticle system used in this study is introduced.

2.1 Microbial enhanced oil recovery: history and challenge

During crude oil production, oil recovery operations have been divided into three stages: primary, secondary, and tertiary. Primary recovery is the first stage of oil production; it is driven by the naturally existing displacement energy in the reservoir. Secondary recovery (water flooding, pressure maintenance, gas injection) is usually implemented after the primary recovery. Typically, 30% - 50% of oil recovery is considered to be produced by both primary and secondary methods.[2,4] Tertiary recovery is also known as enhanced oil recovery (EOR). During tertiary oil recovery, methods such as miscible gas injection, chemical flooding, and thermal injection are applied to displace residual oil. EOR allows another 5–15% of the reservoir's residual oil to be recovered.[5] The goal of the EOR methods is to recover more oil from the underground oil reservoir. The oil recovery can be calculated by Equation 2.1:

$$Oilrecovery = \frac{Oilproduced}{Originaloilinplace} \times 100\% \qquad \text{Equation 2.1}$$

However, many of the EOR processes are considered economically unattractive.[5-7] Thus, it is important to develop new approaches to improve the recovery of trapped oil in the reservoir. MEOR represents the use of naturally occurring or injected microorganisms to mobilize the residual oil and thus reduce its content and increase the sweep efficiency in the reservoirs. Gases, solvents, polymers, surfactant, organic acids, biomass and other compounds similar to those used in chemical enhanced oil recovery are all common products of microbial metabolism.[8-11] In some cases, MEOR has shown its potential to work as a tertiary oil recovery method.

Cheap nutrient substrates can be used to perform MEOR. From an economic point of view, the process itself is affordable compared to other EOR processes.[6,12] Also, MEOR processes can tolerate harsh environments in terms of pressure, temperature, pH and salinity.[13] Average bacterial cells range between 0.5 and 5.0 μm; the small size of bacteria allows them to penetrate through the reservoir's porous media.[14] In general, MEOR has many advantages, such as economical, biocompatibility, low toxicity, and biodegradability.[15] Therefore, MEOR offers a good alternative in improving the crude oil recovery.

The idea of MEOR was first proposed by Beckmann[16] when he published results on the possibility of using microbial metabolic processes to enhance oil recovery. ZoBell[17] was another pioneer in MEOR and demonstrated that the products of microbes had the potential to improve the oil production rate. From the classical works of

Beckmann and ZoBell, other advances made in MEOR were made from the 1950s to the 1980s.[18-22]Field testing and field applications of MEOR were presented in 1989,[14] scientific and technical understanding of the microbial enhanced oil recovery was also improved at the same time.[23]

From the 1990s through 2000s, significant interest in MEOR rose with increasing crude oil prices.[15,24-26] Donaldson[27]and Lazar[15] mentioned that searching for a cheaper and effective EOR method was the major driving force for the development of MEOR.A great deal of laboratory and field work had been done during this period.[24,25,28-30] Many of the results were promising. Microorganisms were investigated for both surface production of functional microbial metabolites and injection of microbes into a reservoir for in situ production of metabolic compounds.[31,32] Core samples or columns were utilized in the laboratory tests to approximate downhole conditions.[33] The metabolic substrates were tested to demonstrate the usefulness of biosurfactants in oil recovery from sandstone and carbonate. The movement and effectiveness of microorganisms and nutrients injected into the core samples were also analyzed.[9]

However, some results from field applications were unsuccessful.The oil production was not enhanced and other problems such as near wellbore plugging[34] occured. Donaldson *et al*.[27] suggested that it was because the biological, chemical and physical processes that occurred during in situ metabolism in the reservoir were not fully understood.

Hitzman[35] summarized several possible reasons that could be considered for the failure of field tests in MEOR studies. He claimed that one important reason was the difficulty in extrapolating the results from one microbial field trial to other reservoirs

since each reservoir had its unique properties and microbial population. Moreover, the interactions of the multiplying microorganisms with the reservoir matrix also caused physical and chemical changes in the reservoir which were hard to duplicate in the laboratory. Another major reason identified for the failure of field trials was insufficient consideration of the physical and chemical conditions which characterize petroleum reservoirs. Sheehy[8] also observed that the activity of bacteria are highly dependent on the temperature, pressure, pH, salinity, ionic strength, the source of energy and nutrients. Moreover, since there is no oxygen in the reservoir, the knowledge about the growth of microorganisms in oil under anaerobic conditions was required during the early days of MEOR.

Another common issue for MEOR is near wellbore plugging. The utilization of nutrients by microbes near the point of injection causes plugging of the pore space or pore throats. This plugging results in a reduction in petroleum hydrocarbon production. Jack and Steheier[34] suggested that filtration before injection, nonproduction of biopolymers during solution injection, or microbial adsorption to rock surface were required to prevent plugging. Moreover, dispersion/transportation of all necessary components to the target zone in the reservoir would also help avoiding plugging and save the energy and nutrients injected into the reservoir. A major goal of this dissertation is to demonstrate that utilizing polyelectrolyte complex technology to deliver the nutrients into the target zone will help prevent near wellbore bioplugging.

2.2 Reservoir and Microbes

2.2.1 Petroleum microbes

Many naturally occurring microorganisms can be found in the reservoir. Magot *et al*.[29]emphasized that anaerobic microorganisms are considered as true inhabitants. Anaerobes do not require oxygen for respiration, and for certain anaerobes, they may react negatively or even die in the presence of oxygen. Anaerobes can be classified into three categories according to the respiration type and action under oxygen: Obligate anaerobes, which cannot tolerate oxygen; Aerotolerant organisms, which cannot use oxygen, but tolerate its presence; Facultative anaerobes, which are able to grow either as aerobes or anaerobes determined by the nutrient availability and environmental conditions.[36] All three types of anaerobic microbes are found in the petroleum reservoir.[37]

Aerobic microorganisms that can use oxygen during respiration are also found in the reservoir.[36] The role of aerobes as true inhabitants is uncertain, and thus they are considered as contaminants. Contaminant microorganisms are probably transferred through fluid injection to the reservoir or during drilling devices.[29] Considering the anaerobic conditions in the reservoir and the difficulty in supplying oxygen, it is suggested that growing the naturally occurring anaerobic microbes in the reservoir is more practical.[38] Commonly used bacterial genera in MEOR are *Bacillus* and *Clostridium*.*Bacillus* species produce gas, surfactants, and acids; while *Clostridium* produce gases, surfactants, alcohols, and solvents. Only a few *Bacillus* species can produce biopolymers. Microorganisms and their products used for MEOR are listed in Table 2.1, reproduced from Bryant, 1989.[37] *Bacillus* and *Clostridium* are often able to

survive under extreme conditions such as high salinity, high temperature existing in the oil reservoirs.[21]

Table 2.1 Microbe in MEOR and their respiration type and products[37]

Genus	Respiration type	Products
Clostridium	Anaerobic	Gases, acids, alcohols and surfactants
Bacillus	Facultative	Acids and surfactants
Pseudomonas	Aerobic	Surfactants and polymers
Xanthomonas	Aerobic	Polymers
Leuconostoc	Facultative	Polymers
Desulfovibrio	Anaerobic	Gases and acids
Arthrobacter	Facultative	Surfactants and alcohols
Corynebacterium	Aerobic	Surfactants
Enterobacter	Facultative	Gases and acids

2.2.2 Microbes under the reservoir conditions

The action of microorganisms is complex when they respond to the surrounding environment.[39] The cells change physiological state in order to survive. Abilities, such as forming spores, can help microbes survive in the severe conditions. The spores are dormant, resistant forms of the cells, they are units of asexual reproduction that may be adapted for and survival in stressful environments such as high temperature, drying, and acid. The duration of the dormancy can be extremely long and yet the survival rate is high .In general, activities such as the substrate consumption, growth, and metabolite production of the microbes in the reservoir may change significantly compared to those under normal conditions (room temperature, pH ≈ 7, humidity >80%).[39-41]

Microorganisms existing in the reservoir are exposed to many different physical (temperature, pressure, pore size/geometry), and chemical (pH, oxidation potential, salinity) conditions.[42] Cellular activities such as growth, cell decay, chemotaxis, and cell attachment and detachment to pore walls are largely affected by these physical and chemical conditions.[30]

Temperature is one of the most important physical factors that affect the cellular process of microorganisms. The reservoir temperature can be up to 150 ℃, but most of the microorganisms isolated from reservoirs can only grow at temperatures below 82 ℃.[29] The growth of microorganisms depends on their enzyme function. High temperatures can denature the enzyme by disrupting the hydrogen bonding.[36,42] The effect of high pressure on microbes is more indirect because it first changes gene expression and protein synthesis, and then further influences the physiological and metabolic state of microbes.[29,42]

Pore size is the major limitation for microorganisms to penetrate the reservoir. In MEOR, bacteria are mainly applied because of their small size (near2 μm).[36] For tight reservoirs, bacteria might have the same radius as the pores. It is possible for bacteria to penetrate reservoirs with minimum pore diameters of at least 2 μm[42] but pore sizes of 6 μm to10 μm are preferred.[43]

The high pressure of the reservoir results in gases dissolved in the reservoir fluids which can influence the pH. pH values as low as 3 have been observed comparing to many other wells with a normal pH range of 6-8.[12] The surface charge of bacteria changes when they are exposed to an acidic environment, thus impacting their transportation in the reservoir. The bacterial growth rate is also reduced by acidity.[29,42]

The tolerance of bacteria to the acid environment is highly affected by their surface structure. Gram-positive bacteria usually survive the acid environment as they possess an acid resistance system which the gram-negative bacteria do not. The acid resistance system is a complex system consists of the use of proton pump, the change on cell membrane and production of alkali *etc*.[44]

In addition, Crescente *et al*.[45] mentioned that the transport of the bacteria also depends on its hydrophobicity. If the bacterial surface is solely hydrophobic, the bacteria tend to stick and transport together. Meanwhile, hydrophilic bacteria usually flow as single cells.

2.2.3 Microbes and their nutrient source

Nutrients are the largest expense in the MEOR processes, and it has been shown by Pommerville *et al*. that almost 30% of the cost for a microbial fermentation is from microbial media.[46] The microbial growth is determined by the presence of different nutrients. The microbes require three major nutrients for growth and metabolic production: carbon, nitrogen and phosphorous sources.[36] Some researchers suggest the general ratio of these three types nutrients should be C, 100: N, 10: P, 1. However, media optimization is necessary since the types of bioproducts are highly dependent on the nutrient types and concentrations.[36] Even some cheap raw materials, which contain all the necessary nutritional components for the microbial growth can also be applied as nutrients in the MEOR including molasses, cheese whey, and beef extract.[47,48]

Carbon and nitrogen determine the growth rate of microbes and they are generally considered as the limiting nutrients because of the large quantity of carbon and nitrogen consumed by the microbes. But in some cases, phosphate can also work as a limiting nutrients.[49] Moreover, if the nutrient concentration is too high, inhibition of cell growth by high concentration of substrate may occur.[50] Other essential nutrients are phosphorus, sulfur, potassium and magnesium, and they are required in much smaller amounts.[36] Trace elements such as iron, zinc and manganese are critical to cell function even though the amount required is small. The trace elements play a structural role in various enzymes and catalysts. However, as only tiny amount is required, the natural occurrence is abundant.[12] Other essential compounds for some organisms are vitamins and amino acids, which are required only in small amounts as they are important for enzymatic function.[36]

2.2.4 The growth of microbes

The growth of microbes is defined as the increase in the number of microorganisms rather than in the size of the individual cell. Malthus[51] derived the model of population growth. He suggested the variation of the x(t) or cell number with time can be described by a linear differential equation with a constant coefficient:

$$\frac{dx}{dt} = \mu x \qquad \text{Equation 2.2}$$

where μ is the specific growth rate of the population and is determined by the species and the environment. The specific growth rate can be calculated from Equation 2.3.[52]

$$\mu = \frac{d_x}{x d_t} \qquad \text{Equation 2.3}$$

The growth of microorganisms in batch culture can be modeled with four different phases: the lag phase, the log or exponential phase ,the stationary phase, and the death phase.

The lag phase occurs when a microorganism is introduced into fresh medium and a delay is observed in the growth of the number of microbes. During this period of time, the microbes adapt themselves to the new growth conditions.[53] In this phase, cellular metabolism is accelerated. Proteins, co-enzymes and vitamins needed for microbial growth are produced. Cells are increasing in size, but not able to replicate themselves, therefore,cell number does notincrease . The length of the lag phase depends directly on the previous growth condition of the organism. When the microorganism growing in a nutrient-rich medium is inoculated into a nutritionally poor medium, the organism usually takes alonger time to adapt the new environment than the microbes introduced from a nutrient-poor environment.

The log phase (logarithmic phase or the exponential phase) is characterized by cell doubling. At this stage, the logarithm of bacterial biomass increases linearly with time so that numbers of bacterial cells in a given interval of time is proportional to the biomass of bacteria present. Their metabolic activity increases and the organisms begin the DNA replication by binary fission at a constant rate. The time taken by the bacteria to double in number during log phase is known as the generation time. Generation time is controlled by different environmental conditions and by the nature of the microbial species. *E.coli* divides in every 20 minutes. Therefore its generation time is 20 minutes while the generation time of *Staphylococcus aureus* is 30 minutes.[54]

The log phase is followed by the stationary phase. The stationary phase describes the period of time in which the number of cells undergoing division is equal to the number of cells dying. The number of new cells is limited by factors such as the depletion of nutrient; the formation of growth inhibitor may also result in stationary phase.[54]

Finally, the death phase represents the death of microbial cells.Cell death can be caused by insufficient nutrients, the subsequent accumulation of metabolic waste products, severe temperature (too high or too low), accumulation of other toxic materials,low pH, dry enviroment,etc. During this phase, the microbe completely loses its ability to reproduce. Due to the unfavorable conditions bacteria begin to die rapidly at a uniform rate. The number of dead cells exceeds the number of live cells. Some organisms can survive in the environment by producing spores. A bacterial spore is a spore-like structure produced by certain Gram-positive bacteria, for example *Bacillus* and *Clostridium* during reproduction process. Spore formation is not the principal method of bacteiral reproduction but a method to counter environmental stresses such as nutrient starvation.[55]A scheme of all microbial growth phases is shown in Figure 2.1.

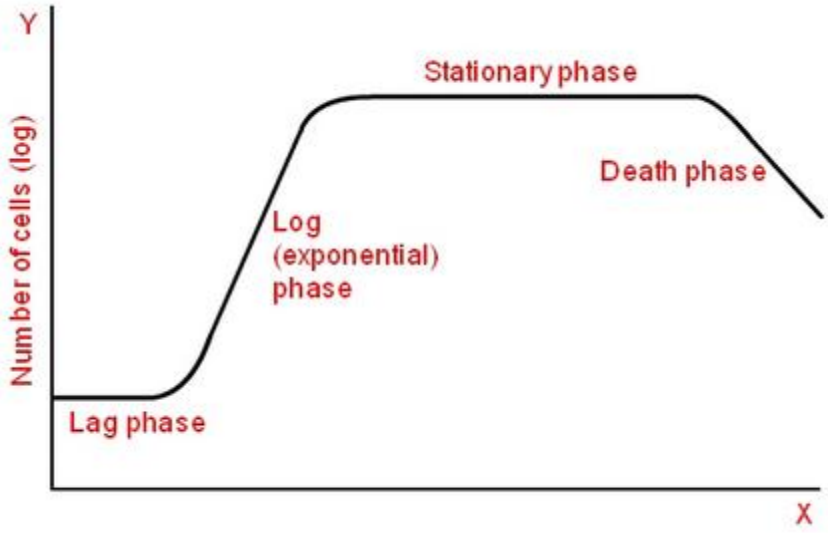

Figure 2.1 Typical microbial growth curve including growth phases[56]

2.3 Classification and mechanisms of MEOR

2.3.1 Classification of MEOR

The most active applications of the MEOR process can be subdivided into three categories: single-well stimulation, microbial flooding, and selective plugging. Single-well stimulation is the treatment at the wellbore zone to remove near-wellbore paraffin deposits or other chemicals leading to formation damage, or degrade heavy oil in the region around the wellbore. The scheme of single well treatment is demonstrated in Figure 2.2. During the treatment, the wells are shut-in for a period long enough to allow microbial growth and metabolites formation. The shut-in can last for a number of days or weeks.[12]

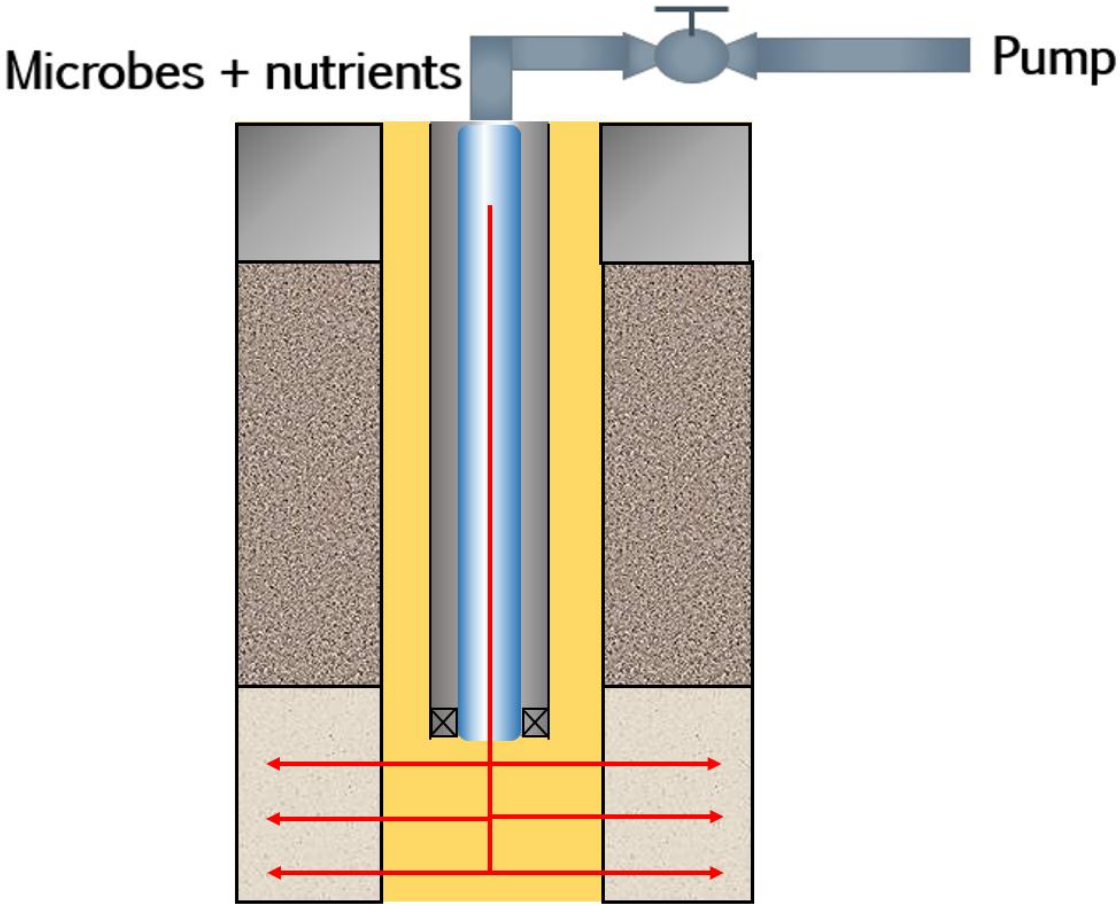

Figure 2.2 Single well MEOR treatment[57]

Microbial flooding is the most frequently used MEOR method.[5] As shown in Figure 2.3, nutrients with/without oilfield microbes will be injected through an injection well into the reservoir. With the growth of bacteria in the reservoir, metabolites (surfactant, polymers *etc.*) are produced, and the properties of reservoir fluids are modified by the bio-products. In this study, we mainly focus on the second application of MEOR: microbial flooding

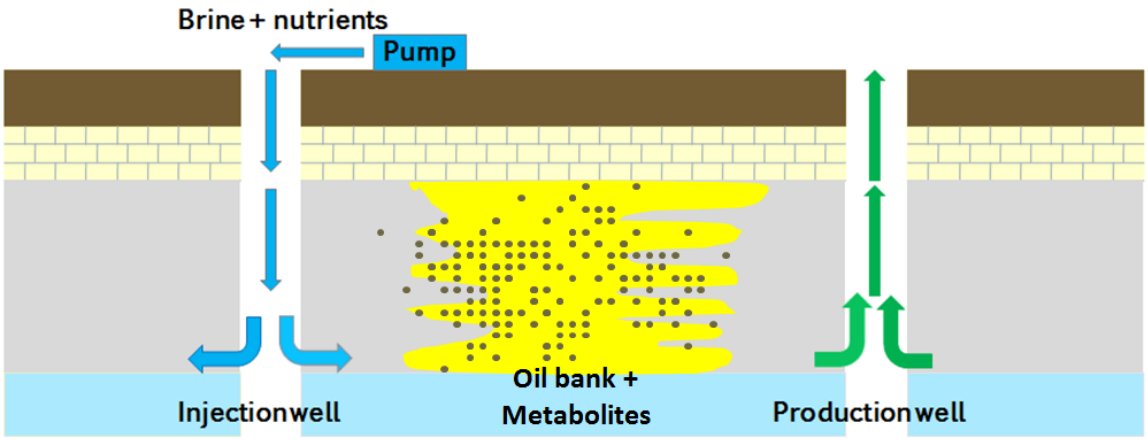

Figure 2.3 Scheme of microbial flooding

Microbial selective plugging is a method used to redirect the flow of water into low permeability regions by blocking water channels deep in the reservoirs. With this type of treatment, nutrients preferentially flow into the high permeability regions, thus stimulating biomass and polymer production in these regions, and reducing the permeability of the rock.[58]

2.3.2 Mechanism of MEOR

The MEOR process applies microorganisms that are already present in the reservoir or microorganisms that are biopolymer and/or biosurfactant producers. Incubation of naturally occurring downhole microorganisms is preferred to ensure the growth of microbes in a specific environment.[2,13,21]

The process of MEOR has been studied for over 50 years since 1947.[17] However, the mechanism is still unclear. Although many explanations were given in individual lab experiments, more information was required when same explanations were applied in the field tests.[59]

A generally accepted way to explain the MEOR mechanism is to discuss the functions of different bioproducts of incubated microbes in the reservoir.[12,59,60] During the MEOR process, naturally occurring microorganisms are mostly activated by injection of nutrient substrates, otherwise exogenous microorganisms are injected with their substrates or in between slugs of substrates. The microorganisms penetrate the reservoir, while they consume nutrients, reproduce themselves, and produce different important metabolites. These metabolites improve the oil recovery in different aspects: reduction of oil/water interfacial tension and alteration of wettability by surfactant production, selective plugging by microorganisms and bio-polymers, viscosity reduction and pressure improvement by gas production, and generation of acids that dissolve rock improving absolute permeability.

Table 2.2 shows a summary of these bioproducts and their application in oil recovery.

Table 2.2 Microbial bioproducts and their applications in oil recovery[61]

Product	Application in oil recovery
Biomass	Selective plugging, viscosity reduction, oil degradation, wettability alteration
Biosurfactants	Emulsification, interfacial tension reduction, viscosity reduction
Biopolymers	Selective plugging, mobility control, viscosity modification
Bio-solvents	Emulsification, viscosity reduction
Bio-acids	Permeability increase, emulsification
Biogases	Increased pressure, oil swelling, interfacial tension reduction, viscosity reduction, permeability increase

2.4 Polymer and polyelectrolyte

As mentioned in Section 2.1, one of the major chanllenges for MEOR is the plugging cause by the biostimulation of the microbes in the near-wellbore region. The objective of this research is to deliver the nutrients to the reservoir at a controlled rate. Polyelectrolyte nanoparticles, which are extensively applied as controlled release drug delivery system, are introduced to MEOR to achieve the objective of this research.

Polyelectrolytes are the main compositions of the polyelectrolyte complex nanoparticles (PECNPs). Thus, it is necessary to understand the behavior of these polyelectrolytes before discussing further on the formation of the PECNP.

2.4.1 Polymer and polyelectrolyte classification

Polymers are composed of many repeated small units called monomers. Based on their structures, polymers can be classified as linear, branched or network types. Based on the type of monomers, the polymers can be categorized into random, block, or graft copolymers.[62]

Polyelectrolytes (PE) are polymers containing multiple ionic groups. In polar solvents, such as water, the ionic groups in the polyelectrolytes can dissociate, release counterions into the aqueous phase, and make the polymer chains charged.[63]There are two opposite forces controlling the dissociation process: the counterions-releasing driving force, which push the oppositely charged counterions away from the PE chain and the electrostatic force, which attracts the counterions to the PE chain. Driven by those two forces around the polymer chain "free" and "condensed" counterions form in dilute solutions, similar to the electrical double layer for dilute colloids (Figure 2.4).[57,64,65]

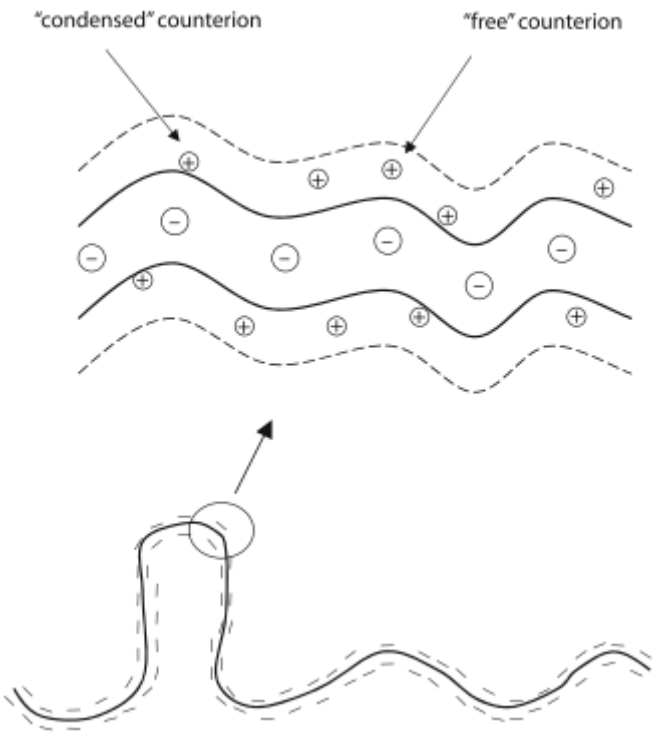

Figure 2.4 Schematic shows "condensed" and "free" counterions [63]

Some polyelectrolytes in the aqueous solution are completely dissociated into macroion and counterion in the whole pH range, e.g. sodium-polystyrene and poly(diallyl dimethyl ammonium chloride). Some polymers remain undissociated at a certain pH range. These polymers are defined as "weak" polyelectrolytes since they cannot exhibit typical polyelectrolyte characteristics in all pH ranges.[66] Typical examples are poly(acrylic acid) (PAA) and poly(ethylenimine) (PEI). PAA is undissociated at low pH while PEI is undissociated at high pH. Polyelectrolytes can also be classified according to their charges as polyanions, polycations, and polyampholytes (Figure 2.5).[67]

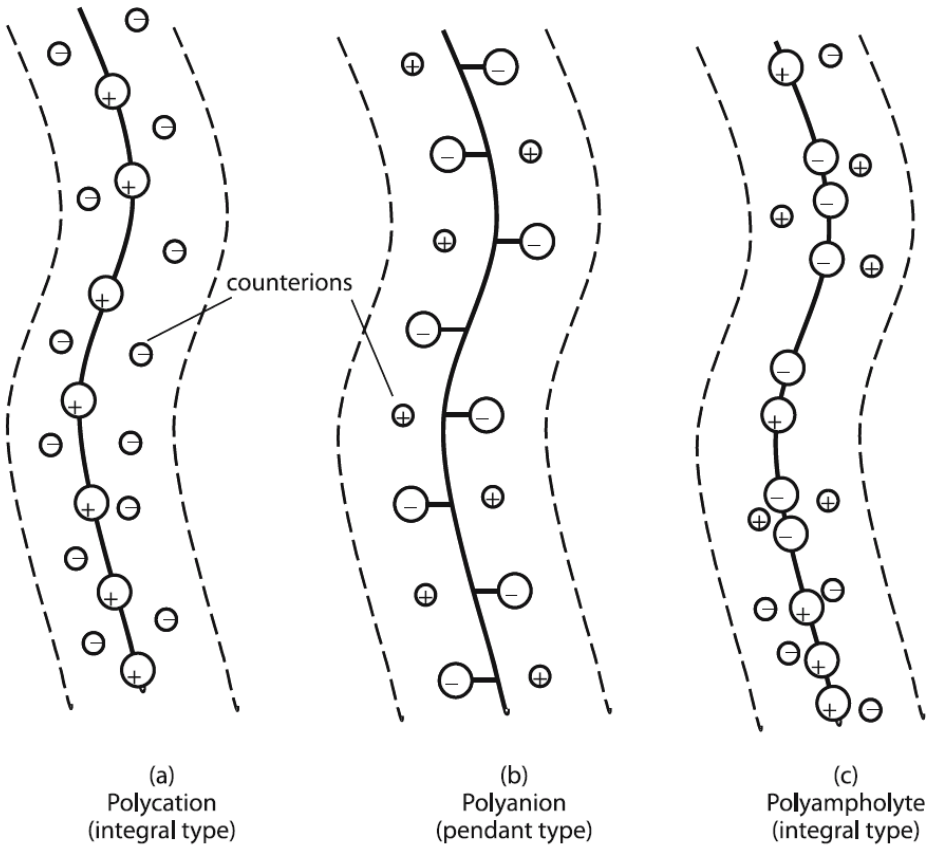

Figure 2.5 Classification of polyelectrolytes in terms of their charge[67]

Polyelectrolytes carrying both anionic and cationic groups are called "polyampholytes." Proteins are the typical examples of polyampholytes. They are positively charged in acid media and negatively charged in alkaline media. At their isoelectric point, they bear no charge.

2.4.2 Factors that affect polyelectrolyte properties

The ionic group on the polymer chains determines the charge of the polyelectrolyte. The possible ionic groups that can be attached to a polymer include the following functional groups:

-COO^-(carboxyl), -CSS^-(disulfide),-OSO_3^-(sulfate),-SO_3^-(sulfonate),-OPO_3^{2-} (phosphate),=NH^-(primary amine), ≡NH^- (secondary amine), -NR_3^-(tertiary amine)

One of the most important parameters that affect the behavior of polyelectrolytes, especially in solution, is the average distance between the charged groups. Equation 2.2 defines the relationship between the charge density and average distance:

$$\varepsilon = \frac{l_B}{b} \qquad \text{Equation 2.2}$$

Where ε is the ideal PE linear charge density, b is the average linear distance between neighboring charged groups, and l_B is the Bjerrum length, which is 0.71 nm in water at 35 ℃[63].

Ionic groups are linked to the polyelectrolyte ionicity, which expresses the proportion of charged groups in the macromolecule. In the particular case of polysaccharides such as guar gums and starches, a limited number of the hydroxyl groups present on each sugar unit are active for substitution reactions.[63] In this case, it is customary to use the degree of substitution to express the number of charged groups per monomer unit. For synthetic polyelectrolytes, the charge density is often used to express the molar percentage of charged monomers in the polymer. The charge density of these polyelectrolytes depends on the dosage and reactivity of the respective monomers used in the polymerization steps of the manufacturing process.

2.5Polyelectrolyte complex nanoparticles

2.5.1 Polyelectrolyte Complex Formation with Oppositely Charged Polyelectrolytes

Polyelectrolyte complex nanoparticles (PECNP) are formed by mixing oppositely charged polycations and polyanions, which offers the possibility to combine

physicochemical properties of at least two polyelectrolytes. Figure 2.6 shows the formation of PECNP by mixing oppositely charged polyelectrolytes. PECNPs are extensively used as drug delivery carriers.[68] In some of the applications, a third component such as metal ion,[69] DNA,[70] or protein[71] is entrapped in the nanoparticle system (Figure 2.6).

The driving force for PECNP formation is the strong electrostatic interactions between the oppositely charged polyelectrolytes. Inter-macromolecular interactions such as hydrogen bonding, Van der Waals forces, hydrophobic interactions are also involved in the formation of PECNP structures.[72]

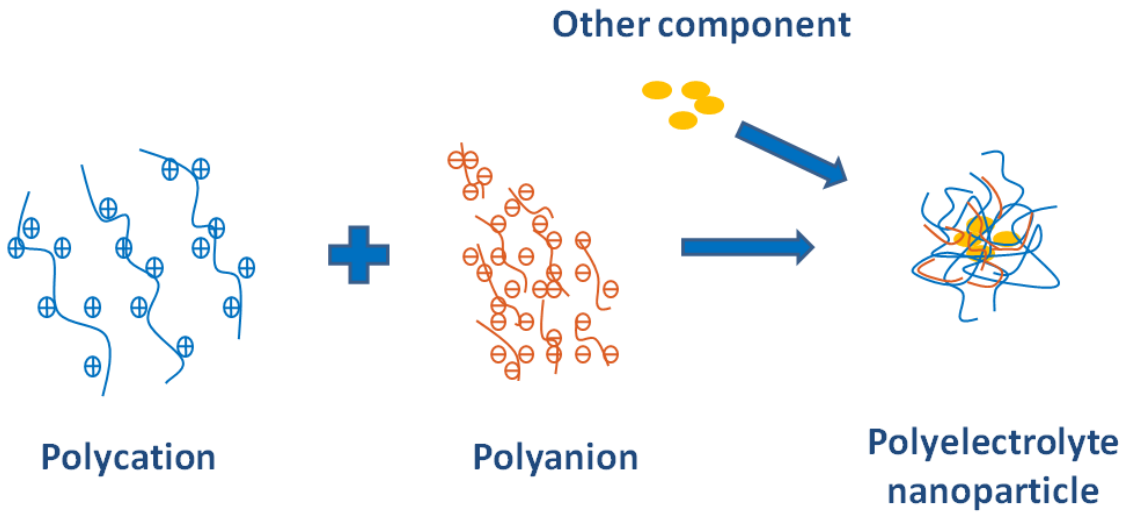

Figure 2.6 Scheme of polyelectrolyte complex formation (redrawn after Liang)[73]

2.5.2 Mechanism of polyelectrolyte binding

Electrostatic forces are considered to dominate the interactions between the polyelectrolyte chains.[74,75] The electrostatic interaction not only exists in the direct attraction between the oppositely charged polyelectrolytes, but also involves the release of counterions.[75] In this way, although the direct electrostatic force is enthalpic, the ion-exchange process for polyelectrolyte binding is usually accompanied by a significant entropy gain due to counterion release,[76,77] and the formation process is claimed to be athermal.

The process of the formation of PECNP is described by Hartig *et al*.[72]The first step is diffusion-controlled collision of polyion coils at very short times; then thermodynamic rearrangementoccurs, causing instability in the PECs.Generally, the conformational changes and disentanglements at long times determine this rearrangement of the already formed aggregates. Hartig *et al*.[72]also report that when strong polyelectrolytes with similar molar masses are mixed together, the final structure of the polyelectrolyte complex can be described by either the Ladder Structure or Scrambled-egg model. The Ladder Structure model has fixed ionic cross-links and the structure occurs via conformational adaptation. If two weak polyelectrolytes with different molecular dimension are mixed, a ladder-like structure occurs. (Figure. 2.7) Structures that form by the Scrambled-egg model are observed when strong polyelectrolytes with similar molar mass are mixed (Figure 2.7).

The ladder model assumes that two polyelectrolytes have suitable charge centers and charge densities that they can zip together in a cooperative fashion.[78,79] However, if the PEC complex is formed by polyelectrolytes both having relatively

high molecular mass and high charge density, the complexation will proceed from more than one site, a more crosslinked structure will be formed. In this situation, it may not be appropriate to assume that the polyelectrolyte chains can line up as highly regular "ladders" and the "scrambled egg" model is a better description of the complexation. Therefore, it was concluded that the structures of PECs mainly depend on the number and fitting accuracy of the charge centers on both polycation and polyanion.

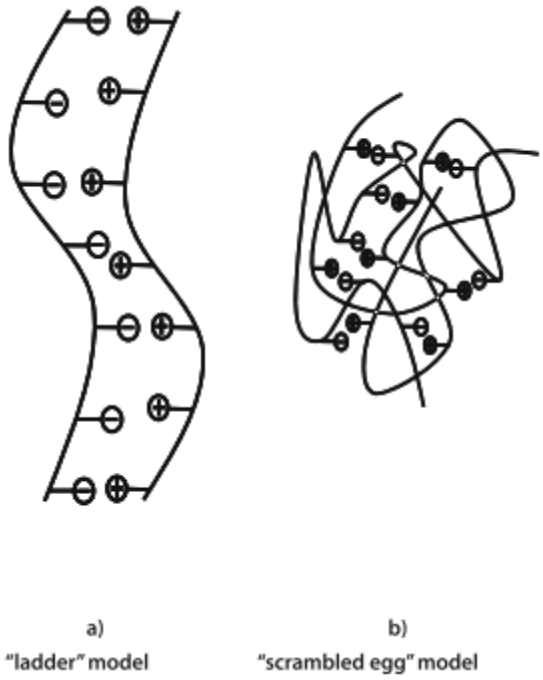

Figure 2.7 Polyelectrolyte complex models [72]

Vanerek and van de Van[80] suggested that the molecular weight of polyelectrolyte is one of the key factors in PECNP complex formation. They developed a PEC nanoparticle with cationic polyacrylamide (CPAM) and sulfonated Kraft lignin and found

that the molecular weight of CPAM determined the complex formation. They ascribed their results to the CPAM, with smaller molecular weight, being more easily adopted into lignin with coiled structure.

In general, PECs are readily obtained by controlling the concentration of each polyelectrolyte stock solution and the mixing ratio. Different structures of PECs form by changing the chemical composition of polymers as well as the molecular weight, chargedensity, and functional groups.[81] Self-assembly also depends on the ionic strength of the media and the solution pH. The ionic strength may enhance the nanoparticle formation at low concentration but inhibit the process at high concentration.[82] At lower concentrations, it favored the formation of these complexes through the decrease in the dimensions of the polyelectrolyte molecules (increase in surface charge density). However, as the ionic strength increases, small counterions screen and penetrate the PECs, the zeta potential decreases, and the PECs aggregate and eventually precipitate. The properties of the synthesized PECs such as surface charge and entrapment efficiency can be manipulated by adjusting the pH value in the stock solution, stirring rate, etc.

2.5.3 The entrapment and release of small components in PEC

The encapsulation of a third component (protein, DNA/RNA, metal ion etc.) by an oppositely charged PECNP system is also a polymer bonding process. Generally, low molecular weight molecules can be bound to macromolecules by all intermolecular forces, mainly ionic or complex bond or the combination of both.[83] Complex bonds are significantly more selective than ionic interactions.

The release of an entrapped third component is a diffusion process, where the entrapped low molecular weight molecules move from a region of high concentration (inside PECNP) to a region of low concentration (outside environment).The release can be triggered by stimuli such as temperature, pH, salt, magnetic field, or light.[84]

2.6 Characterization of polyelectrolyte complex nanoparticles

Since this polyelectrolyte complex nanoparticle will be applied into the petroleum industry and will be delivered under reservoir conditions, important properties of PEC nanoparticle include: particle charge, particle size, entrapment efficiency, and stability.

2.6.1 Particle charge

Usually, long-range interparticle interactions control the stability of colloidal system such as PEC nanoparticles. Therefore, nanoparticles with similar charge lead to a repulsive force andkeep nanoparticles suspending in the system.[63] Zeta potential is an extensively applied measurement to determine the electrokinetic potential at the effective shear plane between the dispersed particle and the stationary layer of fluid attached to the dispersed particle.[63] In zeta potential measurement, a double layer model is used to describe the individual particles dispersed in continuous solvents (usually water) with charged surfaces. Figure 2.8 shows a scheme of double layer model.[67] In this graph, the double layer consists of:

1. A layer of fixed dehydrated positively charged ions that are adsorbed onto the surface due to chemical interactions

2. A Layer of ions (“diffuse layer”) attached to the first layer composed of ions attracted by the surface charge and thermal motion, which is not firmly anchored.

Zeta potential is the total potential drop between the surface of the solid and the moveable liquid and the electrokinetic, zeta potential is measured at the diffuse layer.

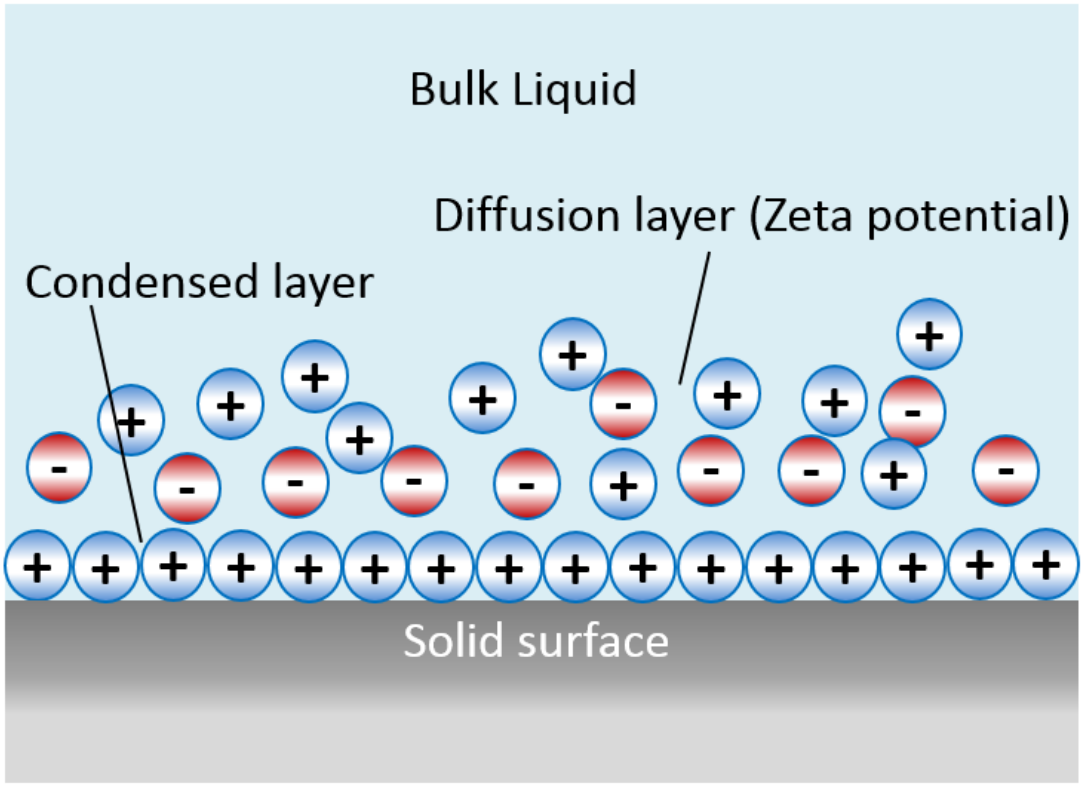

Figure 2.8 Diagram showing the double layer model[67]

As stated above, the zeta potential is the potential at the effective shear plane between the mobile and immobile part of the double layer. Therefore, the potential can be determined by the moving of one phase with respect to the other. The phase movement can occur when the counterions being moved by an electric field.[63]

Phase analysis light scattering (PALS) is utilized for the zeta potential measurement. It determines the small phase shifts in the scattered light that arise due to the movement of particles in an applied electric field. The measured phase change is proportional to the change in the position of the particles.

2.6.2 Particle Size

The most significant parameter of a PEC nanoparticle is the particle size since almost all other properties of the nanoparticle are influenced by its size. In field applications, PEC nanoparticles are preferred because smaller particles are capable to go through the small pores in the reservoir. Moreover, from the view of surface science, as the size of an object decreases the surface area to volume ratio increases. Furthermore, as the size scale of an object becomes small, the behavior of that particle is governed increasingly by the surface interactions rather than gravity.[63]

One common technique for determining the particle size and size distribution of colloidal systems is dynamic light scattering. When light hits small particles, the scattered light undergoes either constructive or destructive interference with the surrounding particles leading to the intensity of scattered light fluctuating over time. This fluctuation is due to Brownian motion of small particles.

There are two assumptions made in using the dynamic light scattering method. The first assumption is that the particles are in Brownian motion. The second assumption is that the particles used in the experiment are spherical particles with a diameter comparable to the molecular dimensions. Under these assumptions, the particle diameter can be calculated by the Stoke-Einstein equation,

$$D_B = \frac{k_B T}{6\pi\eta a} \qquad \text{Equation 2.4}$$

where a is the diameter of the particles, k_B is the Boltzmann constant (1.38×10^{-23} m^2 kg s^{-2} K^{-1}), T is the temperature in Kelvin, η is the viscosity of the particle suspension (Pa.s), and D_B is the diffusion constant.

2.6.3 Entrapment efficiency

Entrapment efficiency (EE) describes the loading efficiency of the component of interest in the PEC nanoparticle system. EE is defined as the ratio of the mass of the entrapped component to the mass of initial component added to the system. The method to measure EE is described in Chapter 3.

2.7 Polyethylenimine/Dextran Sulfate System

The oppositely charged polyethylenimine (PEI)/dextran sulfate (DS) system used in this study was first introduced by Tiyaboonchai, with zinc sulfate as a stabilizing agent.[68] Her system works as a delivery vehicle for pharmaceutical applications. She used a mild preparation technique, which means no organic solvents, heat or high shear forces

were applied to the system. The chemical formulas of PEI and DS are shown in Figure 2.9.

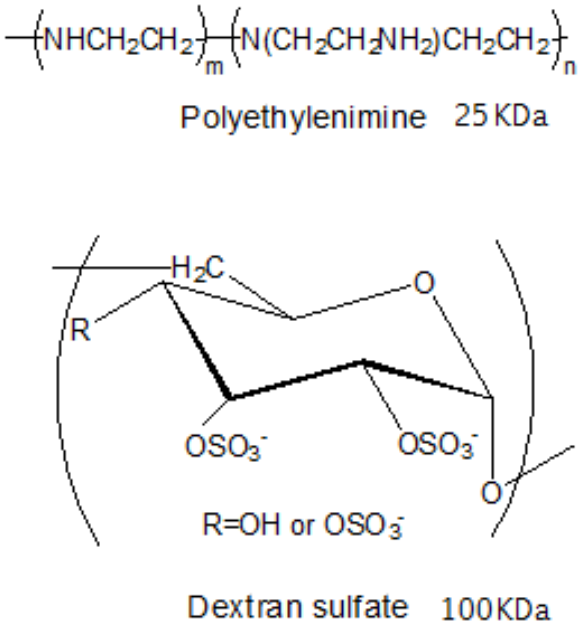

Figure 2.9 Chemical structure of PEI and DS[69]

2.7.1 Polyethylenimine

Polyethylenimine (PEI) is a polymer with monomer composed of the amine group and carbon aliphatic. PEI is produced by cationic ring-opening polymerization of ethylenimine, it can be obtained in a variety of molecular weights (a few hundred Daltons to 1500 kDa).There are two types of PEI: linear and branched. The linear polyethylenimine contains only secondary amines, in contrast to branched PEI, which contains primary, secondary and tertiary amino groups. The chemical structure of different types of amines is shown in Figure 2.10. Branched PEI is water-soluble at room temperature while linear PEI is only soluble in water above 55 ℃.[85,86]

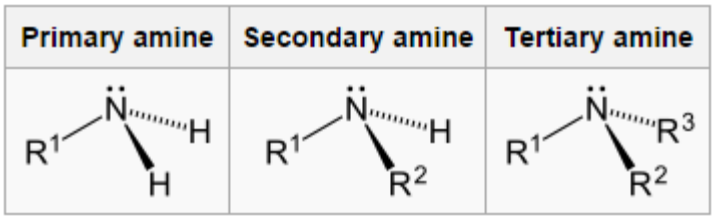

Figure 2.10 Scheme of primary, secondary and tertiary amines[74]

PEI is widely used in drug delivery as DNA or protein transportation vehicle because of its high charge density.[65,74] It is also used in the cell culture of weakly anchoring cells to increase attachment.[87] Tiyaboonchai[68] provided several reasons for choosing PEI as polycation including PEI: being a water-soluble cationic polymer, reported as having the highest loading efficiency among other cationic polymers used in the pharmaceutical industry, and being available in wide range of molecular weights and structures (linear and branched).

Since the nitrogen atoms must be protonated to achieve cationic charge, the cationic charge density of PEI is pH dependent. The charge density of PEI decreases with increasing pH.[88,89] In this research, PEI solutions with different stock pH (from 7 to 12) were tested to achieve optimized nitrogen nutrient entrapment efficiency.

Cells can uptake PEI through endocytosis without endosomal degradation because of its cationic nature[90] The PEI backbone is composed of nondegradable carbon–carbon linkages, so the effect of PEI accumulation within cellular has raised researchers' attention. It was observed that a higher concentration of PEI (> 6000 ppm) induced cellular toxic response in cultured mammalian cells.[87] However, the PEI concentration in

the nutrient delivery system is significantly lower than 6000 ppm. Meanwhile the polyanion in this system: dextran sulfate, is capable of decreasing the toxicity since the concentration of PEI is decreased by mixing with DS during the PEC complexation process. Moreover, the injection of nanoparticles in the field application is a dilution process. Brine is injected along with the nanoparticle suspensions in order to reduce the clay swelling. Therefore, the final concentration of PEI in the reservoir will be significant lower than the toxic concentration (The toxicity test of PEI on oilfield microbes is listed in Section 4.2).

2.7.2 Dextran sulfate

Dextran sulfate (DS) is the polyanion in this nutrient system. DS is a biodegradable and biocompatible polyanion with polysaccharide backbone and negatively charged sulfate groups.[91] DS has been employed in nanoparticle synthesis to encapsulate different biomolecules such as peptides and insulin.[91,92] The main advantage of using DS as a polyanion is the enhanced stability of PEC nanoparticles at different pHs since DS is not pH sensitive.

2.7.3 Cationic Starch

As discussed in Section 2.7.1, different biocompatible and biodegradable polysaccharides are applied as polyelectrolytes to reduce the toxicity of PEC nanoparticles. Cationic starch (CS) is one of the most commonly used polysaccharides in PEC nanoparticle synthesis. CS is a chemically modified starch, and was developed to solve the poor solubility and processing of natural starch.[93] Figure 2.11 shows the

chemical structures of CS. In this research, a CS/DS system is optimized as an alternative to the PEI/DS system.

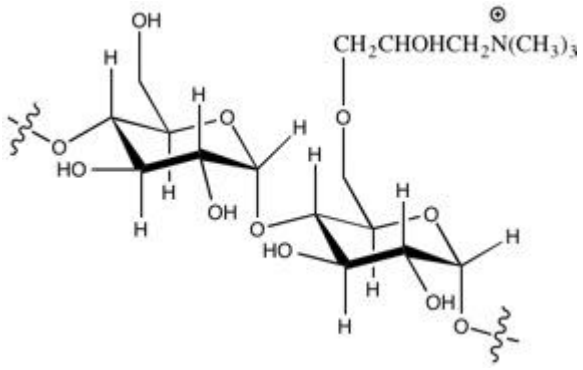

Figure 2.11 Chemical structure of Cationic Starch [68]

2.7.4 Modified PEI/DS polyelectrolyte nanoparticle system

As mentioned at the beginning of Section 2.7. The PEI/DS polyelectrolyte nanoparticle system was first introduced by Tiyaboonchai.[68] The reported mean particle size of her optimized nanoparticle system was about 270 nm. The particle size decreased as increasing PEI:DS ratio. Entrapment efficiency of peptone (EE) was tested by centrifugation. Increasing the amount of zinc sulfate added to the solution increased the EE with the best EE observed at PEI stock pH = 8.

Cordova *et al.*[69] modified the system presented byTiyaboonchaito delay hydrolyzed polyacrylamide (HPAM) gelation by encapsulating the chromium (III) crosslinker in PEC nanoparticles. After adjusting the mixing ratio of 1% w/w PEI to 1%

w/wDS, PEC nanoparticles with a diameter less than 200 nm were formed. Mixing ratios above 1:1 v/v (PEI: DS mass ratio of 2.22) were needed to generate positively charged nanoparticles. Results showed that Cr-loaded nanoparticles successfully delayed the gelation time for HPAM (4.5 days) compared to the gelation time of the control system with no PECs at 30 minutes.

Barati *et al.*[71] further modified the PEI-DS system for controlled release of enzymes breakers (pectinase) in hydraulic fracturing fluid cleanup. The optimized PECNP system had an average particle size of 460 nm. The highest enzyme entrapment efficiency was about 75%. The degradation of borate-crosslinked guar gel by pectinase loaded in polyelectrolyte nanoparticles was delayed by up to 12 h, compared to about 2 h for equivalent systems where the pectinase was not entrapped.

It is hypothesized that the well developed PEI-DS nanoparticle system has the potential of entrap the nutrients (ammonium and phosphate salt, protein, and polysaccharide), and deliver the nutrients in a contolled manner to prevent the near wellbore plugging. Base on the previous research, we will extend the study of nanoparticle system on the ability of nanoparticle system to entrap nutrients, the effect of polyelectrolytes on the oilfield microbes, the effect of salt on the nanoparticles and the retension of nanoparticles in the sand pack.

3. Materials and Experimental Procedures

3.1 Materials

3.1.1 Polyelectrolytes

Polycations (different molecular weight of polyethylenimine branched with Mw =800 Da, 2000Da, and 25 kDa from SIGMA) and a polyanion (dextran sulfate sodium salt with Mw =500 kDa from SIGMA, 9011181) were obtained from Fisher Scientific (Pittsburgh, PA). The other polycation (cationic starch with Mw at a range of 50-500kDa) was obtained from Cargill Inc., Minneapolis, MN. The structureand properties of PEI and DS are described in the literature review Section 2.7.

3.1.2 pH Modifiers

Sodium hydroxide (1 M or 0.1 M) and hydrochloric acid (4 N) were used as pH modifiers. They were both obtained from Fisher Scientific (Pittsburgh, PA).

3.1.3 Nutrient sources

Nitrogen, carbon and phosphate are the three major nutrients that microbes require for the reproduction of themselves as we discussed in Section 2.2.3. Ammonium chloride (>99.5% purity) was obtained from Fisher Scientific (Pittsburgh, PA) and was initially used as sole nitrogen source that was entrapped in the nanoparticle. Bacteriological peptone [LP0037, 14% w/w nitrogen, from Oxoid Inc. (Hampshire, UK)] was then used as nitrogen provider in this research as the stability of ammonium-based nanoparticle was poor. Peptone is a complex water-soluble product that contains protein

and other protein derivatives. It is obtained by digesting protein (such as soy or meat) with an enzyme (pepsin or trypsin) and is used chiefly in nutrient media in bacteriology. Dextrose (D-glucose) (>99.5% purity) was used as a carbon source to provide carbon nutrients in the experiments. Dextrose was obtained from Fisher Scientific (Pittsburgh, PA). The chemical structure of dextrose is listed in Figure 3.2. Potassium phosphate (>99.9% purity) was obtained from Fisher Scientific (Pittsburgh, PA), it was used as the sole phosphate source in this research.

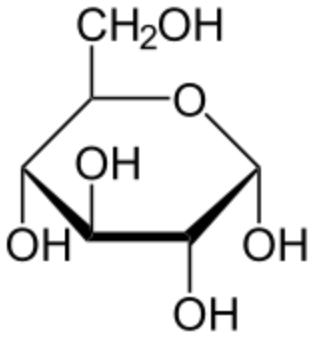

Figure 3.1 Chemical structure of dextrose[69]

3.1.4 Cultures

Pseudomonas putida was initially used as model bacterium in the experiment. *P, putida* is a Gram-negative, rod-shape soil bacterium, which can degrade petroleum hydrocarbon and survive with oil as primary carbon source.[94] Tuleva *et al*.[95] reported that *P. putida* was also found as a biosurfactant (rhamnolipid) producer when the bacteria grew with hexadecane as the sole carbon nutrient.

The pure culture of *P. putida* (ATCC Number: 39213) was purchased from American Type Culture Collection (Manassas, VA). The freeze-dried pure culture was revived and incubated in 15 ml liquid sodium benzoate medium at 34 ℃ for 72 hours. The incubated *Pseudomonas putida* was then streak plated with solid sodium benzoate medium, incubated at 34 ℃ for 72 hours. A single colony was then picked and transferred to liquid media.

The microbial species used throughout this work were mixed cultures isolated from the production sites of Wellington oilfield (Wellington, KS) by B. L. Huff.[96] Aerobic microbes were collected from the produced water tank; the anaerobic microbes were collected from the producing pipe. The aerobic microbe cultures were maintained followed Gray's method.[97] Aerobic cultures were maintained in liquid peptone media (Section 3.1.4) at 4 °C and subcultured every two weeks. Freezer stocks were kept at −20 °C. Experimental inoculation was prepared by withdrawing 20 µl of liquid culture and transferring it to 20 ml liquid peptone media at 37 °C for 24 hours (log phase). Experimental media were then inoculated with 20 µl of the resulting culture and incubated as previously described, unless otherwise specified. The anaerobic cultures followed the almost same procedure, except they were incubated in the anaerobic conditions (anaerobic chamber).

3.1.5 Microbial media

3.1.5.1 Incubation media

Sodium benzoate medium with benzoate as the sole carbon source was used for *Pseudomonas putida* incubation. The sodium benzoate medium was prepared by mixing

diammonium phosphate [>99.9% purity, Fisher Scientific (Pittsburgh, PA)], dipotassium phosphate [>98.0% purity, Fisher Scientific (Pittsburgh, PA)], magnesium sulfate[>99.5% purity, Fisher Scientific (Pittsburgh, PA)], bacteriological yeast extract [>95.0% purity, Oxoid Inc. (Hampshire, UK)], and bacteriological sodium benzoate [>99.0% purity, Oxoid Inc. (Hampshire, UK)] with RO water to a final mass of 1000 g. The recipe for sodium benzoate medium is listed in Table 3.1.

Table 3.1 Sodium benzoate medium

	Concentration (g/kg)
$(NH_4)_2HPO_4$	1.5
K_2HPO_4	1.2
$MgSO_4$	0.2
Yeast extract	0.5
Sodium benzoate	3.0
H_2O	993.6

The aerobic peptone medium (complete medium) was made according to the directions provided by the manufacturer's manuals from Oxoid.10 g peptone [>95.0% purity, Oxoid Inc. (Hampshire, UK)], 20 g sodium chloride [>99.9% purity, Fisher Scientific (Pittsburgh, PA)], 2.5 g potassium phosphate [>99.5% purity, Fisher Scientific (Pittsburgh, PA)], and 5 g dextrose [>95.0% purity, Oxoid Inc. (Hampshire, UK)] were dissolved in RO water to a final mass of 1000 g. In this recipe, peptone serves as the sole nitrogen source, dextrose as the sole carbon source, and potassium phosphate as sole phosphate source. The only difference for the anaerobic medium is that 0.66 g/kg sodium nitrate [>99.5% purity, Fisher Scientific (Pittsburgh, PA)] was added as the electron

acceptor. All media were sterilized by autoclaving at121 ℃ for 15 min. Solid peptone media was made by adding 10 g/kg agar [bacteriological grade, Oxoid Inc. (Hampshire, UK)] into the aerobic or anaerobic liquid peptone media.

3.1.5.2 Selective media

Two selective media were used in this research. The first selective medium was toxicity test medium which was used to test the toxicity of polyelectrolytes to the model bacteria. The toxicity test medium was prepared by adding polyelectrolytes at the same concentration as in the nanoparticle system. In a typical experiment to test the toxicity of DS to mixed aerobic microbial culture, 6 g/kg Dextran sulfate was added to the aerobic peptone media. Table 3.2 shows the recipe for this specific media. Other toxicity test media formulas are listed in Appendix 1.

Table 3.2 DS toxicity test media (aerobic mixed culture)

	Concentration (g/kg)
Peptone	10.0
NaCl	5.0
KH_2PO_4	2.5
Dextrose	5.0
H_2O	977.5

The second selective media was new nutrient source media which was designed to check whether the polyelectrolytes have the potential to be a sole carbon, nitrogen, or phosphate provider. New nutrient source media was prepared by replacing the carbon or

nitrogen source in the incubation media by the polyelectrolytes. Both old and new nutrient source media have the same concentration of carbon or nitrogen. In a typical experiment to test the potential of PEI as a sole nitrogen source to incubate aerobic mix culture, 10 g/kg peptone was replaced by 4.4 g/kg PEI. Table 3.3 shows the recipe for this specific media. Other new nutrient source media formulas are listed in Appendix 1.

Table 3.3 Peptone media (aerobic mixed culture) with PEI as sole nitrogen source

	Concentration (g/kg)
PEI	4.4
NaCl	5.0
KH_2PO_4	2.5
Dextrose	5.0
H_2O	983.1

3.1.6 Synthetic seawater

Synthetic seawater (SSW) was prepared by mixing potassium chloride, sodium chloride, calcium chloride, magnesium chloride, magnesium sulfate, and sodium bicarbonate with RO water to a final mass of 1000 g. The recipe for SSW is listed in Table 3.4.[98] All chemicals not specifically identified were purchased from Fisher Scientific and are ACS grade.

Table 3.4 Synthetic sea water[98]

	Concentration (g/kg)
NaCl	23.50
KCl	0.73
$CaCl_2.6H_2O$	1.47
$MgCl_2.6H_2O$	10.63
$MgSO_4$	3.92
$NaHCO_3$	0.19
H_2O	959.57

3.1.7 Sands for sand pack test

Ottawa sand F-110 (fine sand) and Berea sand werekindly offered by Shengxue Xie (University of Kansas, Tertiary Oil Recovery Project). Ottawa sand was obtained from U.S. Silica (Frederick, MD), Berea sand was purchased from Cleveland Quarries Co. (Amherst, OH). Berea sand was crushed and sieved through a #50 Sieve (300 μm aperture).

3.1.8 Protein staining reagents

To measure the concentration of peptone during the sand pack analysis, Thermo Scientific Pierce Coomassie Plus (Bradford Protein Assay[99]) reagent was initially used as a staining solution to stain peptone. Coomassie Plus reagent for Bradford Protein Assay was obtained from Fisher Scientific (Pittsburgh, PA); the UV absorbance wavelength is 595 nm.[99] Due to the testing limitations of the Bradford protein assay, other modified methods were also used to better analyze the protein concentration, namely UV absorbance analysis, modified Bradford assay and modified UV absorbance.

Modified Bradford Assay was used to better analyze the peptone concentration during the sand pack tests as the sample concentrations were beyond the detection limitation of Coomassie Plus. When nanoparticle concentration is less than 12%, the method is invalid. The UV absorbance wavelength of modified Bradford Assay is 595 nm. Bradford reagents were prepared by dissolving different amount of Coomassie Brilliant Blue G-250 in 5 g 95% ethanol [>94% purity, Honeywell Corp. (Muskegon, Ml)], add 10 g 85% (w/v) phosphoric acid [Tech grade, Sigma-Aldrich (St. Louis, MO)]. After the dye had completely dissolved, the resulting solution was diluted with RO water to 100 g. The formulas of modified Bradford reagents are listed in Table 3.5.

Table 3.5 Modified Bradford reagents

	Coomassie blue G-250	**95% ethanol**	**85% phosphoric acid**	**H_2O**
0.5 × Bradford	0.05 g	5.00 g	10.00 g	84.95 g
1 × Bradford	0.10 g	5.00 g	10.00 g	84.90 g
1.5 × Bradford	0.15 g	5.00 g	10.00 g	84.85 g
2 × Bradford	0.20 g	5.00 g	10.00 g	84.80 g

3.2 Methods

3.2.1 Preparation of PECNPs

Polyelectrolyte nanoparticles were prepared with different PEI: peptone volume ratios from 1:10 to 10: 1 (mass ratio 1:100 to 1:1) or CS: peptone volume ratios from 1:10 to 10:1(mass ratio 1:100 to 1:1), different addition order, and different PEI pH.

During the stock preparation, the pH of 1% w/w aqueous solution of PEI stock was adjusted to 7, 8, 9, 10, 11, or 12 with 6N HCl or 1N NaCl. The pH of 1% w/w aqueous solution of DS stock was about 7.8, the pH of 10% w/w aqueous solution of peptone was approximately 5.4, and the pH of 0.5% w/w aqueous solution of CS stock was around 6.2.

During the PEI/DS/peptone nanoparticle preparation, PEI, DS and peptone stock solution were mixed at different volume ratios. The DS volume was fixed at 10 ml, while the PEI/peptone ratio was optimized to find highest entrapment efficiency. PEI was added dropwise to DS while stirring. The solution was then stirred for 10 min at 600 rpm unless otherwise indicated. Peptone solution was added dropwise either before or after PEI was added. Peptone-loaded nanoparticles were used as the nitrogen source in polymer systems at a final concentration of 0.6% w/w peptone. In different PEI/DS/peptone nanoparticle recipes, the DS volume was fixed to 10 ml. The PEI volume ranged from 0.5 ml to 10 ml in 0.5 ml increments. The peptone volume also changed from 0.5 ml to 10 ml in 0.5 ml increments.

PEI/NH_4^+/DS and CS/DS/peptone were prepared by following the same procedure. Table 3.6 and 3.7 show the PEI/DS/peptone nanoparticle recipes (PEI stock pH = 10) with varying PEI volume and fixed peptone volume at 1ml or 2 ml. Table 3.8 shows the CS/DS/peptone nanoparticle recipes with varying CS volume and fixed peptone volume at 3ml. The mass ratio of PEI: DS: peptone or CS: DS: peptone in the final preparation was also calculated and listed in Table 3.6-3.8.

Table 3.6 Nanoparticle systems with different ratios of PEI, DS, and peptone and order of addition (peptone volume = 1 ml)

Group	1% w/w PEI (ml)	PEI pH	1% w/w DS (ml)	10% w/w peptone (ml)	Mass ratio (PEI: peptone: DS)	Order of addition
P101-1	0.5	10	10	1	0.5:10:10	DS, peptone, PEI
P101-2	0.5	10	10	1	0.5:10:10	DS,PEI, peptone
P101-3	1	10	10	1	1:10:10	DS, peptone, PEI
P101-4	1	10	10	1	1:10:10	DS,PEI, peptone
P101-5	1.5	10	10	1	1.5:10:10	DS, peptone, PEI
P101-6	1.5	10	10	1	1.5:10:10	DS,PEI, peptone
P101-7	2	10	10	1	2:10:10	DS, peptone, PEI
P101-8	2	10	10	1	2:10:10	DS,PEI, peptone
P101-9	2.5	10	10	1	2.5:10:10	DS, peptone, PEI
P101-10	2.5	10	10	1	2.5:10:10	DS,PEI, peptone
P101-11	3	10	10	1	3:10:10	DS, peptone, PEI
P101-12	3	10	10	1	3:10:10	DS, peptone, PEI
P101-13	3.5	10	10	1	3.5:10:10	DS,PEI, peptone
P101-14	3.5	10	10	1	3.5:10:10	DS, peptone, PEI
P101-15	4	10	10	1	4:10:10	DS,PEI, peptone
P101-16	4	10	10	1	4:10:10	DS, peptone, PEI
P101-17	4.5	10	10	1	4.5:10:10	DS,PEI, peptone
P101-18	4.5	10	10	1	4.5:10:10	DS, peptone, PEI
P101-19	5	10	10	1	5:10:10	DS,PEI, peptone
P101-20	5	10	10	1	5:10:10	DS, peptone, PEI
P101-21	5.5	10	10	1	5.5:10:10	DS,PEI, peptone
P101-22	5.5	10	10	1	5.5:10:10	DS, peptone, PEI
P101-23	6	10	10	1	6:10:10	DS, peptone, PEI
P101-24	6	10	10	1	6:10:10	DS,PEI, peptone
P101-25	7	10	10	1	7:10:10	DS, peptone, PEI
P101-26	7	10	10	1	7:10:10	DS,PEI, peptone
P101-27	7.5	10	10	1	7.5:10:10	DS, peptone, PEI
P101-28	7.5	10	10	1	7.5:10:10	DS,PEI, peptone
P101-29	8	10	10	1	8:10:10	DS, peptone, PEI
P101-30	8	10	10	1	8:10:10	DS,PEI, peptone
P101-31	8.5	10	10	1	8.5:10:10	DS, peptone, PEI
P101-32	8.5	10	10	1	8.5:10:10	DS,PEI, peptone
P101-33	9	10	10	1	9:10:10	DS, peptone, PEI
P101-34	9	10	10	1	9:10:10	DS, peptone, PEI
P101-35	9.5	10	10	1	9.5:10:10	DS,PEI, peptone
P101-36	9.5	10	10	1	9.5:10:10	DS, peptone, PEI
P101-37	10	10	10	1	10:10:10	DS,PEI, peptone
P101-38	10	10	10	1	10:10:10	DS, peptone, PEI

Table 3.7 Nanoparticle systems with different ratio of PEI, DS, and peptone and the order of addition (peptone volume = 2 ml)

Group	1% w/w PEI (ml)	PEI pH	1% w/w DS (ml)	10% w/w peptone (ml)	Mass ratio (PEI: peptone: DS)	Order of addition
P102-1	0.5	10	10	2	0.5:10:20	DS, peptone, PEI
P102-2	0.5	10	10	2	0.5:10:20	DS,PEI, peptone
P102-3	1	10	10	2	1:10:20	DS, peptone, PEI
P102-4	1	10	10	2	1:10:20	DS,PEI, peptone
P102-5	1.5	10	10	2	1.5:10:20	DS, peptone, PEI
P102-6	1.5	10	10	2	1.5:10:20	DS,PEI, peptone
P102-7	2	10	10	2	2:10:20	DS, peptone, PEI
P102-8	2	10	10	2	2:10:20	DS,PEI, peptone
P102-9	2.5	10	10	2	2.5:10:20	DS, peptone, PEI
P102-10	2.5	10	10	2	2.5:10:20	DS,PEI, peptone
P102-11	3	10	10	2	3:10:20	DS, peptone, PEI
P102-12	3	10	10	2	3:10:20	DS, peptone, PEI
P102-13	3.5	10	10	2	3.5:10:20	DS,PEI, peptone
P102-14	3.5	10	10	2	3.5:10:20	DS, peptone, PEI
P102-15	4	10	10	2	4:10:20	DS,PEI, peptone
P102-16	4	10	10	2	4:10:20	DS, peptone, PEI
P102-17	4.5	10	10	2	4.5:10:20	DS,PEI, peptone
P102-18	4.5	10	10	2	4.5:10:20	DS, peptone, PEI
P102-19	5	10	10	2	5:10:20	DS,PEI, peptone
P102-20	5	10	10	2	5:10:20	DS, peptone, PEI
P102-21	5.5	10	10	2	5.5:10:20	DS,PEI, peptone
P102-22	5.5	10	10	2	5.5:10:20	DS, peptone, PEI
P102-23	6	10	10	2	6:10:20	DS, peptone, PEI
P102-24	6	10	10	2	6:10:20	DS,PEI, peptone
P102-25	7	10	10	2	7:10:20	DS, peptone, PEI
P102-26	7	10	10	2	7:10:20	DS,PEI, peptone
P102-27	7.5	10	10	2	7.5:10:20	DS, peptone, PEI
P102-28	7.5	10	10	2	7.5:10:20	DS,PEI, peptone
P102-29	8	10	10	2	8:10:20	DS, peptone, PEI
P102-30	8	10	10	2	8:10:20	DS,PEI, peptone
P102-31	8.5	10	10	2	8.5:10:20	DS, peptone, PEI
P102-32	8.5	10	10	2	8.5:10:20	DS,PEI, peptone
P102-33	9	10	10	2	9:10:20	DS, peptone, PEI
P102-34	9	10	10	2	9:10:20	DS, peptone, PEI
P102-35	9.5	10	10	2	9.5:10:20	DS,PEI, peptone
P102-36	9.5	10	10	2	9.5:10:20	DS, peptone, PEI
P102-37	10	10	10	2	10:10:20	DS,PEI, peptone
P102-38	10	10	10	2	10:10:20	DS, peptone, PEI

Table 3.8 Nanoparticle systems with different ratio of CS, DS, and peptone and the order of addition (peptone volume = 3 ml)

Group	1% w/w PEI (ml)	PEI pH	1% w/w DS (ml)	10% w/w peptone (ml)	Mass ratio (PEI: peptone: DS)	Order of addition
C3-1	0.5	10	10	3	0.5:10:30	DS, peptone, PEI
C3-2	0.5	10	10	3	0.5:10:30	DS,PEI, peptone
C3-3	1	10	10	3	1:10:30	DS, peptone, PEI
C3-4	1	10	10	3	1:10:30	DS,PEI, peptone
C3-5	1.5	10	10	3	1.5:10:30	DS, peptone, PEI
C3-6	1.5	10	10	3	1.5:10:30	DS,PEI, peptone
C3-7	2	10	10	3	2:10:30	DS, peptone, PEI
C3-8	2	10	10	3	2:10:30	DS,PEI, peptone
C3-9	2.5	10	10	3	2.5:10:30	DS, peptone, PEI
C3-10	2.5	10	10	3	2.5:10:30	DS,PEI, peptone
C3-11	3	10	10	3	3:10:30	DS, peptone, PEI
C3-12	3	10	10	3	3:10:30	DS, peptone, PEI
C3-13	3.5	10	10	3	3.5:10:30	DS,PEI, peptone
C3-14	3.5	10	10	3	3.5:10:30	DS, peptone, PEI
C3-15	4	10	10	3	4:10:30	DS,PEI, peptone
C3-16	4	10	10	3	4:10:30	DS, peptone, PEI
C3-17	4.5	10	10	3	4.5:10:30	DS,PEI, peptone
C3-18	4.5	10	10	3	4.5:10:30	DS, peptone, PEI
C3-19	5	10	10	3	5:10:30	DS,PEI, peptone
C3-20	5	10	10	3	5:10:30	DS, peptone, PEI
C3-21	5.5	10	10	3	5.5:10:30	DS,PEI, peptone
C3-22	5.5	10	10	3	5.5:10:30	DS, peptone, PEI
C3-23	6	10	10	3	6:10:30	DS, peptone, PEI
C3-24	6	10	10	3	6:10:30	DS,PEI, peptone
C3-25	7	10	10	3	7:10:30	DS, peptone, PEI
C3-26	7	10	10	3	7:10:30	DS,PEI, peptone
C3-27	7.5	10	10	3	7.5:10:30	DS, peptone, PEI
C3-28	7.5	10	10	3	7.5:10:30	DS,PEI, peptone
C3-29	8	10	10	3	8:10:30	DS, peptone, PEI
C3-30	8	10	10	3	8:10:30	DS,PEI, peptone
C3-31	8.5	10	10	3	8.5:10:30	DS, peptone, PEI
C3-32	8.5	10	10	3	8.5:10:30	DS,PEI, peptone
C3-33	9	10	10	3	9:10:30	DS, peptone, PEI
C3-34	9	10	10	3	9:10:30	DS, peptone, PEI
C3-35	9.5	10	10	3	9.5:10:30	DS,PEI, peptone
C3-36	9.5	10	10	3	9.5:10:30	DS, peptone, PEI
C3-37	10	10	10	3	10:10:30	DS,PEI, peptone
C3-38	10	10	10	3	10:10:30	DS, peptone, PEI

3.2.2 Size and zeta potential measurement of PECNPs

The mean particle size and zeta potential of the nanoparticles were measured by a ZetaPALS zeta potential analyzer (Brookhaven Instruments Corp., Long Island, NY). Samples of the nanoparticles for mean particle size measurements were diluted approximately 40× by volume with deionized water. The average of three measurements of each sample was detected by light scattering at 90°.

Samples for zeta potential measurements were diluted approximately 20× with 1.0 mM KCl solution. Triplicate measurements were averaged for each analysis. The zeta potential was estimated with the Smoluchowski approximation[100] from the electrophoretic mobility of the nanoparticles.

3.2.3 Separation of the nanoparticles

Samples of the nutrient-loaded nanoparticles were centrifuged at 15,000 g for 90 min at 25°C.It is hypothesized that nanoparticles with entrapped nutrients were centrifuged down to the bottom of the tubes as sediments, only free polyelectrolytes and nutrients could be found in the supernatant. Supernatants were then separated from the nanoparticles for entrapment efficiency measurements.

3.2.4 Resuspension of CS/DS/Peptone nanoparticle

It is observed that CS/DS/peptone nanoparticle has the property that sonication in RO water can resuspend the centrifuged nanoparticle precipitates. 20 ml of CS/DS/peptone NP was first centrifuged to collect the nanoparticle precipitates. The precipitates were then resuspended by adding 10 ml of RO water. Samples were vortexed

at 18,000g for 5 min at 25 ℃, then sonicated for 20 min. The supernatant with free CS, DS, and peptone was removed by performing centrifugation steps several times. The residual free peptone in thesuspended nanoparticle solutions was found to be negligible (less than 2%). With the resuspension process, the effect of free components (free polyelectrolytes and free peptone) of the nanoparticles can be eliminated.

3.2.5 Entrapment efficiency measurement

The entrapment efficiency (EE) is defined as the ratio of nutrient concentration entrapped in NP to the total nutrient concentration in the system (Equation 3.1).

$$EE = \frac{C_T - C_S}{C_T} \times 100\% \qquad \text{Equation 3.1}$$

where C_T is the total nutrient concentration added to the nanoparticle system and C_S is the concentration of nutrient in the supernatant after centrifugation. C_T- C_S is the concentration of nutrient entrapped in the centrifuged precipitates.

The ammonium concentration in supernatant was obtained by using an Accumet 13-620-509 ammonium electrode with Accumet XL250 pH/mV/Temp/ISE meter from Fisher Scientific (Pittsburgh, PA). For the ammonium concentration tests, the multifunctional meter was set to mV mode. Ammonium chloride solutions with different ammonium concentration (100, 200, 500, 750, 1000mg/kg) werepreparedas standard solutions. The electric potential of each ammonium chloride solution was tested. The linear regression of electric potential and ammonium concentration was generated as a calibration curve(Figure 3.3) to determine the ammonium concentration of unknown samples[101].

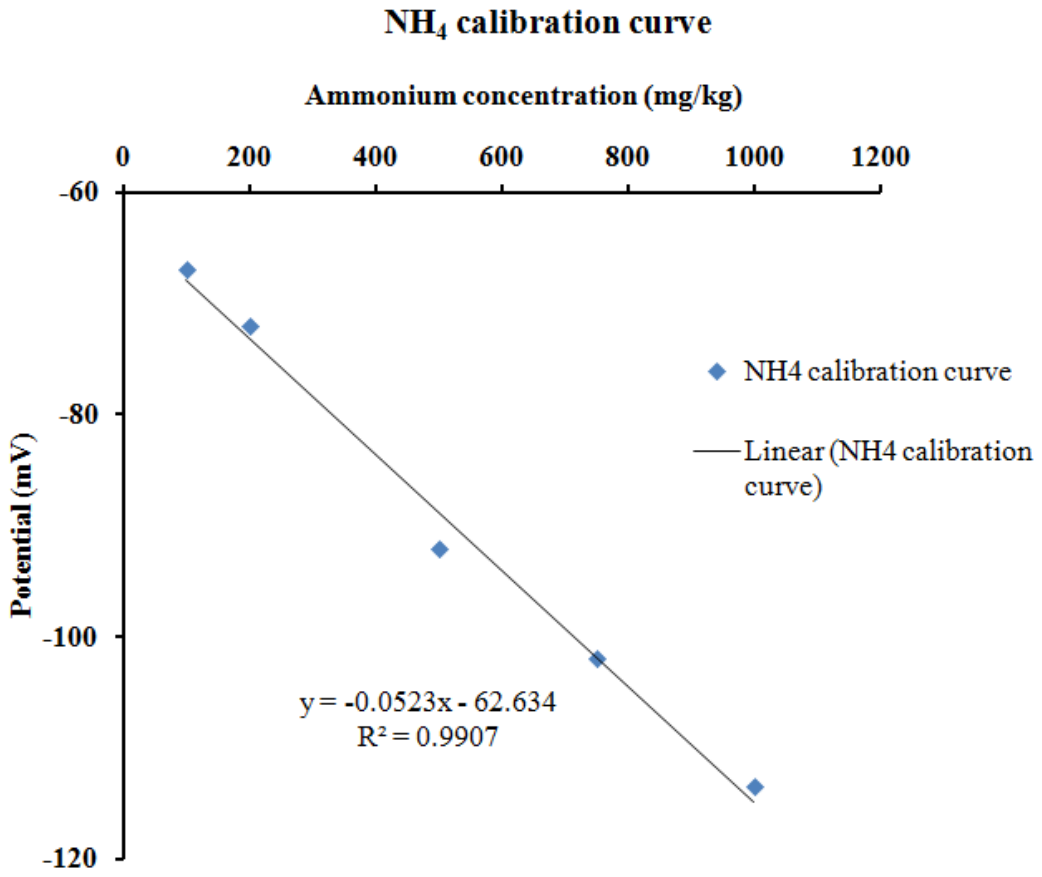

Figure 3.3 Standard calibration curve for ammonium concentration

Peptone concentration in the supernatant was determined by using a standard spectrophotometric method[102] with a UV-Vis Spectrophotometer (PerkinElmer Inc.. Waltham, MA). UV absorbance at 270 nm was used to estimate the concentration of peptone in solution, the visible/UV absorbance spectrum of peptone can be found in Appendix 2. A standard calibration curve was generated by correlating the UV absorbance to the peptone concentration (Figure 3.4). The calibration curve in Figure 3.4 was analyzed at a pH of 7.4 which was the final pH of PEI-NP prepared at a PEI stock

solution pH of 10. Other calibration curves with different pH, temperature and salinity are listed in Appendix 4.

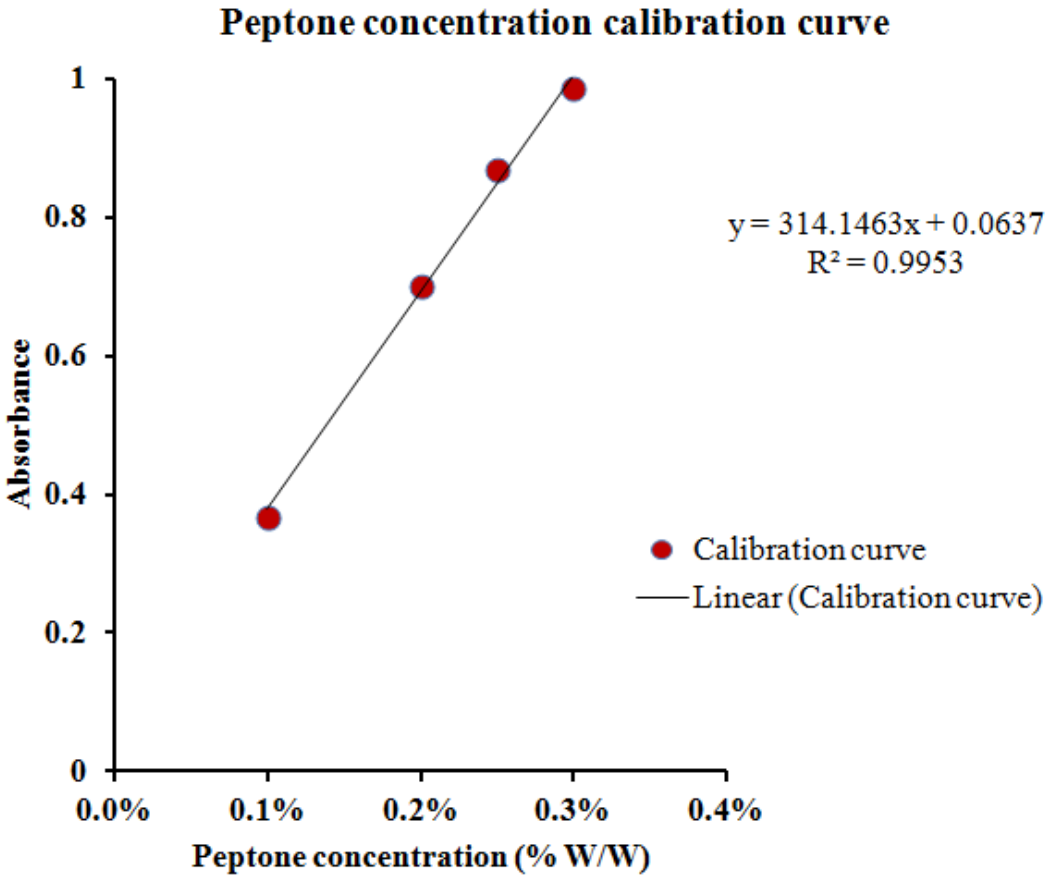

Figure 3.4 Standard calibration curve for peptone concentration at 270 nm (the calibration curve is tested at 25 ℃, pH = 7.4)

3.2.6 The stability of the nanoparticle

The size and zeta potential were measured periodically to demonstrate the stability of the nanoparticles over time. For each nanoparticle recipe, the mean particle size and zeta potential were analyzed every 12 hours. Recipes with little variation in particle size and charge over time are considered to be stable.

The changes of entrapment efficiency were also monitored over time to study the release of nutrients by the PECNP. EE was tested every 12 hours. The effect of temperature on the EE of PECNP was analyzed since the diffusion of entrapped peptone may be accelerated by the high temperature. The samples for EE test were incubated at both 25 ℃ and 40 ℃ Samples were then returned to 25 ℃for analysis in order to eliminate the effect of higher temperature (40 ℃) on the samples during the analysis.

The electrostatic interaction of polyelectrolytes may be screened by the salts in the brine resulting in disassociation of the PECNP. The stability of nanoparticle in brine was analyzed to validate the ability of PECNP to survive in the oilfield, where high salinity brine exists. Both particle size and zeta potential were used as indicators for the stability analysis of nanoparticle.

For all the stability test, triplicate sample (three individual samples prepared by the same procedure) were tested to determine the standard deviation.

3.2.7Incubation and survival tests of model microbes

3.2.7.1 Incubation of *Pseudomonas putida*

Freeze-dried *Pseudomonas putida* was revived and streak plated to obtain single colonies by following the method described in Section 3.1.4. The bacteria from a single colony were then incubated at 37 for 24 hours (Log phase), Appendix 3 Figure A3.1 shows different phases of *P. putida* growth curve. 20 µl of *Pseudomonas putida* suspension obtained during log phase growth was transferred to different selective media.

3.2.7.2 Toxicity of polyelectrolytes to *Pseudomonas putida*

Each polyelectrolyte was added separately into sodium benzoate media at a maximum polymer concentration in the nanoparticle system, namely 3000 mg/kg PEI, 6000 mg/kg DS and 2000 mg/kg CS. The formula of each toxicity test medium can be found in Section 3.1.5 and Appendix 1. The incubated bacteria were then serially diluted to a countable concentration before plating. The number of colony forming units (CFU) was recorded every 24 hours. The maximum CFU (C_{max}) at the stationary phase, generation time (c), and growth rate (b) were analyzed and compared with the data from groups of microbes incubated in the complete media. Complete medium represents the incubation medium described in Section 3.1.5.1, in which no potentially toxic polyelectrolyte was added and sufficient nutrients were included. The method to calculate generation time and growth rate is described in Section 3.2.8. Figure 3.5 shows the procedure of the incubation and survival tests of *Pseudomonas putida*.

3.2.7.3 Test of polyelectrolytes as sole nutrient source for *Pseudomonas putida*

Polyelectrolytes were tested for their potential as a nutrient source for *Pseudomonas putida* in order to decrease the application cost of the nutrient delivery nanoparticle system. The concentration of nitrogen or carbon in the complete sodium

benzoate medium was calculated. PEI containing the same N concentration was added into the media to replace the conventional nitrogen nutrient $(NH_4)_2HPO_4$, and DS or CS containing the same carbon concentration was used to replace dextrose in the complete media. The formulas of new nutrient media are listed in Appendix 1.

3.2.7.4 Incubation and survival tests of oilfield aerobic mixed culture

The incubation and toxicity test for the aerobic mixed culture followed the same procedure as the incubation of *Pseudomonas putida*, except the streak plating was not necessary during the incubation. The formula of the complete aerobic peptone media and polyelectrolyte toxicity test media for the aerobic mixed culture are listed in Appendix 1. The growth phases of aerobic oilfield mixed culture is listed in Appendix 3 Figure A3.2.

Similar to the tests for the *Pseudomonas putida*, during the tests of polyelectrolytes as sole nutrient source for the aerobic mixed culture, the PEI was tested as the potential nitrogen source to replace peptone, and DS or CS were analyzed as alternatives for dextrose. Generation time (*c*) (Equation 3.2), and growth rate (*b*) (Equation 3.3) were used as parameters for the growth of microbes. The calculation of *c* and *b* will be introduced in Section 3.2.8.

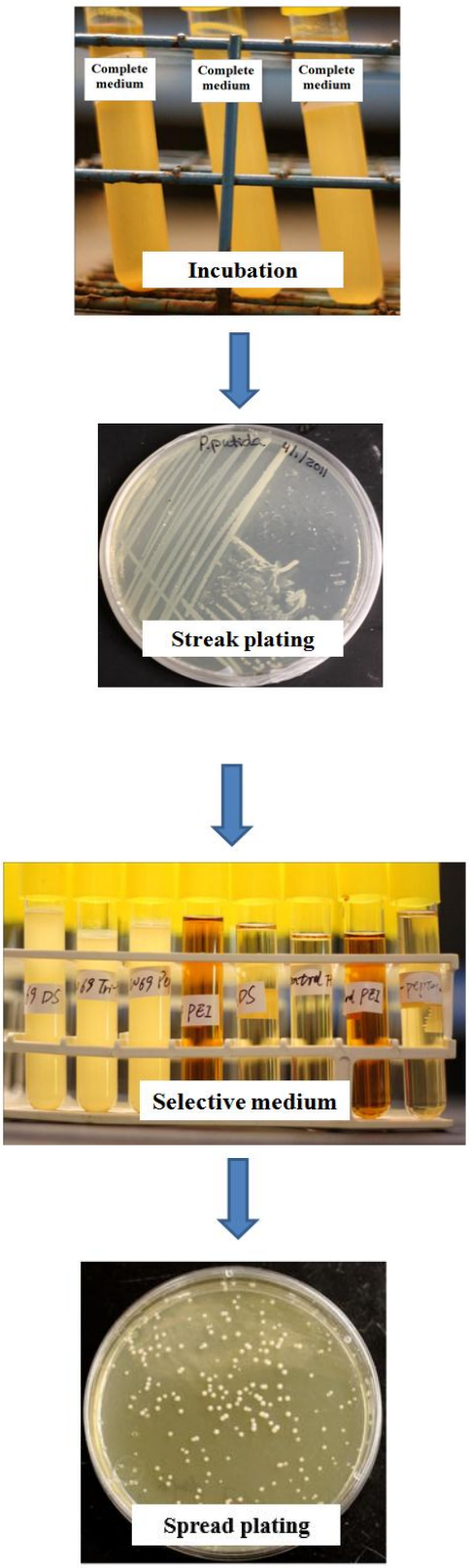

Figure 3.5 Procedure of the incubation and survival tests of *Pseudomonas putida*

3.2.7.5 Incubation of oilfield anaerobic mixed culture

The anaerobic mixed culture was incubated in an anaerobic chamber filled with anaerobic gas mix (5% H_2, 5% CO_2, and 90% N_2). 20 µl of anaerobic mixed culture was inoculated in 20 ml serum vials with sealed stoppers in the anaerobic chamber. The number of microbes was recorded by plating method in the anaerobic solid media every 24 hours. Figure 3.6 shows the anaerobic mixed culture incubated in the 20 ml serum vials in the anaerobic chamber.

Figure 3.6 Anaerobic mixed culture incubated in the anaerobic chamber

3.2.7.6 Survival tests of anaerobic mixed culture

The toxicity of polyelectrolytes and their potential to serve as anew nutrient source of the anaerobic mixed culture were tested in the anaerobic chamber. The incubated anaerobic mixed microbes from log phase (144 hour's incubation) were transferred to the different selective media listed in Appendix 1. Appendix 3 Figure A3.3 shows different phases of anaerobic mixed culture growth curve.

3.2.8 Generation time and growth rate

Generation time and growth rate are two parameters used in this research to compare the microbial growth between groups incubated with selective media and the positive control group. Microbial growth curves were obtained by plate counts every 24 hours. The number of colony forming units (CFU) in a bacterial suspension was determined by serial dilution and plate plating.

Generation time, c (min) was calculated from the exponential section of the growth curve using the equations described by V.L. Gray *et al*[103]:

$$c = \frac{T}{n} \qquad \text{Equation 3.2}$$

where $n = 3.3 \times (\log N - \log N_0)$ and $T = t - t_0$, t = the incubation time at the end of exponential phase, t_0 = the incubation time at the beginning of exponential phase, n = number of generations and N = number of cells. The mean average and standard deviation of c for both aerobic and anaerobic microbes in each media were calculated.

Growth rate, b [log(number of microbes)/hour] was calculated from the exponential growth phase using the equations demonstrated by C. R. Rao[104]:

$$b = \sum y_i g_i / \sum g_i^2 \qquad \text{Equation 3.3}$$

where y = observations on growth at different time points, g = the time interval between the (i - 1)-th and i-th time points. The mean and standard deviation of g for both aerobic and anaerobic microbes in each media were calculated.

3.2.9 Delayed growth test

The microbial growth condition was monitored when nanoparticles were applied to the complete media to test the delay of microbial growth by the PECNP. A 10 ml optimized PECNP suspension was mixed with 10 ml of incomplete peptone media (without N source, peptone or both N and C source, peptone and dextrose). Oilfield microbes were then inoculated into the media-suspension mixture. The microbial incubation followed the procedure mentioned in Section 3.2.7. The growth of positive controls and negative controls were monitored tested during the test. Positive controls are groups of microbes incubated in complete media (aerobic peptone medium or anaerobic peptone medium) to find the maximum growth kinetics for the microbes; negative controls are groups of complete media without microbes stored at same experimental condition (Section 3.2.7) to check whether there is contamination of other microbe species during the experiment. The number of microbes was recorded every 12 hours for aerobic microbes and every 24 hours for anaerobic microorganisms. Triplicate samples (three individual samples prepared by the same procedure) were prepared for each time point.

3.2.10 Nanoparticle retention test in porous media

Retention is the amount of nanoparticles retained in porous media during transport. A test of nanoparticle retention in the porous media was performed by using sand pack analysis. Both tracer tests and sample tests were conducted. Tracer tests were performed to calculate the pore volumes of the sand packs. Tracers, usually chemical compounds, are commonly used in porous media to investigate subsurface flow and transport processes by moving at the same rate as water. A tracer should have negligible effect on the transport properties of the injection fluids (e.g., density and viscosity). Moreover, a tracer should follow the injection fluids through a formation without loss or delay. Furthermore, the analyzing method of a tracer should be selective and sensitive.[105,106] The tracer used in this research is 1% w/w KNO_3. The mass loss of nanoparticle suspension while penetrating through sand packs was calculated from the sample test results. Retention was calculated from the equation below:

$$Retention = \frac{M_{NPIN} - M_{NPOUT}}{M_{sand}} \qquad \text{Equation 3.4}$$

Where M_{NPIN} is the mass of nanoparticle injected, M_{NPOUT} is the mass of nanoparticle collected at the effluent of the sand pack, M_{NPIN} - M_{NPOUT} is the mass loss of nanoparticle in porous media during transport, and M_{sand} is the mass of sand in the sand pack.

3.2.10.1 Sand pack preparation

As mentioned in Section 3.1.7, Ottawa and Berea sand were used in the retention tests. Prior to using, both sandsweresieved through a #50 sieve. A sand pack holder was

assembled as shown in Figure 3.7. The sand pack holder consisted of three parts: ①25 cm glass sand holder (tubing), ②plastic holder seals, and ③pressure gauge. The sand pack holder was prepared according following the procedure.

1. The mass of the empty sandpack holder and accessories was measured as M_1.

2. The bottom of the tubing was sealed with plastic cap. The plastic cap was assembled with a 37 μm mesh disk and a 15 μm mesh disk. Figure 3.8 shows the set-up.

3. Fine sand was slowly added through a powder funnel while vibrating.

4. The inside thread of the glass tubing was cleaned by cotton swabs to ensure the successful seal.

5. The mass of holder with sand was recorded as M_2. The mass of sand was calculated as:

$$M_{sand} = M_2 - M_1 \qquad \text{Equation 3.5}$$

6. A syringe was connected to sand pack to fill the tubing with brine. The mass of holder with sand and brine was recorded as M_3.

7. The mass of brine was calculated by:

$$M_{brine} = M_3 - M_1 \qquad \text{Equation 3.6}$$

8. Porosity was calculated by the following Equation 3.6:

$$\emptyset = \frac{V_{pore}}{V_{bulk}} = \frac{V_{brine}}{2\pi r^2 L} = \frac{\frac{M_{brine}}{\rho_{brine}}}{2\pi r^2 L} \quad \text{Equation 3.7}$$

Where,

L = Length (cm), r = radius (cm), V = Volume (cm^3), M = Mass (g), ρ = density, (g/cm^3)

Φ = Porosity

9. The pore volume (PV) could be estimated by Equation 3.7,

$$PV = V_{bulk} - V_{sand} = 2\pi r^2 l - \frac{M_{sand}}{\rho_{sand}} \quad \text{Equation 3.8}$$

Where ρ_{sand} = sand density ≈ 2.77 g/cm^3 (S. Johnson, pers. comm.).Since the 2.77 g/cm^3 is the average density of the sand, the calculated PV by Equation 3.7 is inaccurate. However, this estimated PV value provides information of how much volume of brine/tracer should be injected during the tracer test.

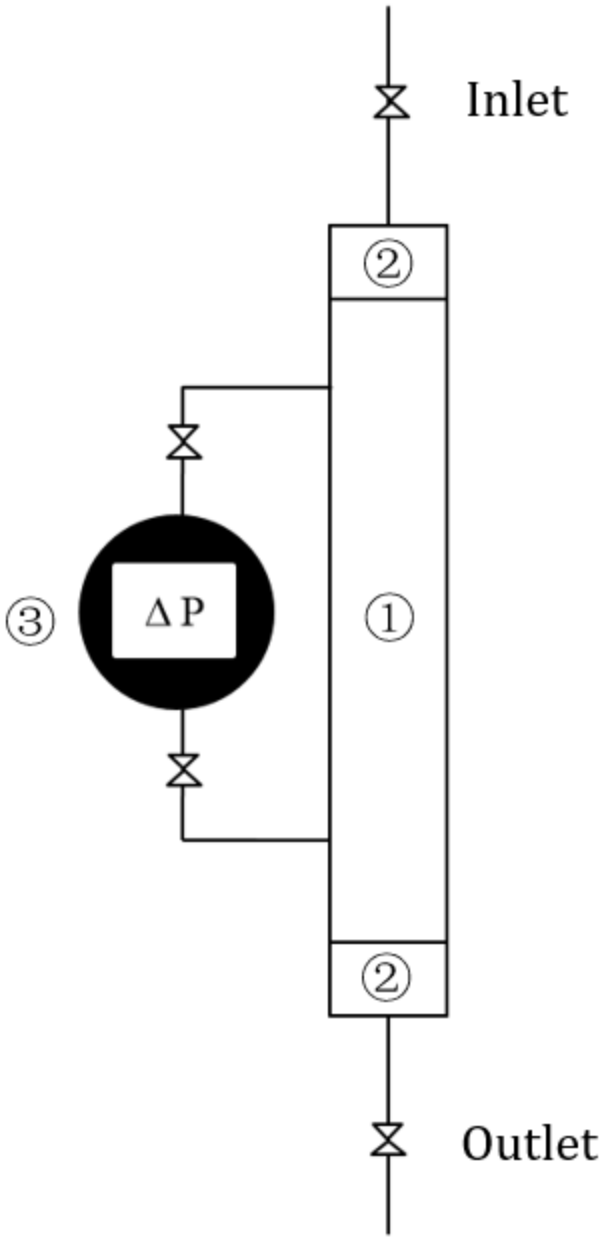

Figure 3.7 Schematic of sand pack holder (① glass sand holder ② plastic seal ③ pressure gauge)

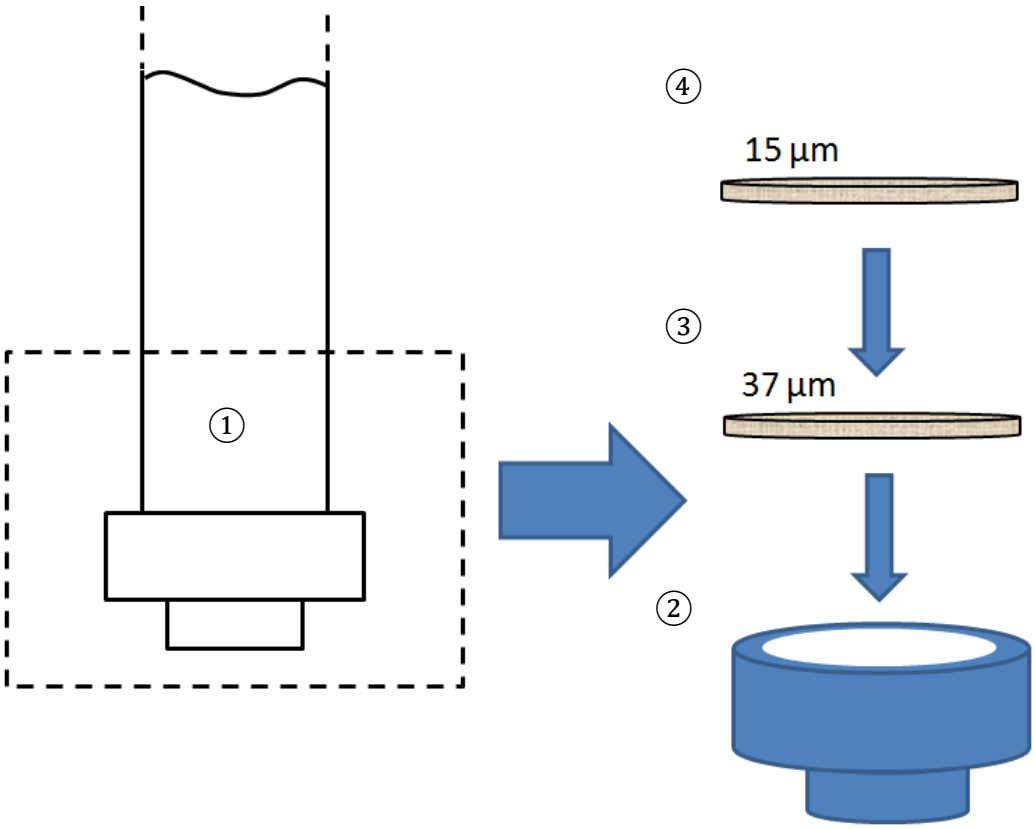

Figure 3.8 Schematic of sand pack holder (① glass sand holder ② plastic seal ③37 µm mesh disk④15 µm nylon mesh disk)

3.2.10.2 Tracer test

Tracer tests were performed to determine the pore volume (PV) of the sand pack. The tracer test used 1% w/w KNO_3 as tracer. The tracer concentration was determined by UV/Vis spectrometer at a wavelength of 302 nm. The normalized tracer concentration (C/C_o) was calculated by the following equation:

$$\frac{C}{C_o} = \frac{A_t - A_{min}}{A_{max} - A_{min}}$$ Equation 3.8

Where C/C_o is the normalized concentration of tracer, A_t is the absorbance time t, and A_{min} and A_{max} are the minimum and maximum absorbance of tracer test effluent samples at wavelength of 302 nm. The procedure is described below:

1. The tracer test system was connected together as shown in Figure 3.9.
2. Brine was pumped from brine/tracer transfer cylinder (Figure 3.10) at a rate of 5 ml/s to the sand pack holder (Figure 3.11) by an ISCO 1000D syringe pump. Effluent was collected and stored in 2 ml centrifuge tubes.
3. After injecting approximately 2 PV (Section 3.2.9) of the brine, the influent was switched to the tracer. After injecting 2~3 PV of tracer, the influent was then switched back to brine. The effluent samples were stored until another 1 PV was collected.
4. Absorbance of the effluent samples from the sand pack was determined by an in-line UV/Vis analyzer at 302 nm.
5. A graph of normalized tracer concentration (Equation 3.8) against the injection volumes was plotted to calculate the pore volume of the sand pack. As shown in Figure 3.12, the area below the curve up to 1 PV is equal to that above the curve from 1 PV to $C/C_o = 1$. In a perfectly homogeneous pack, $C/C_o = 0.5$ at exactly one PV.

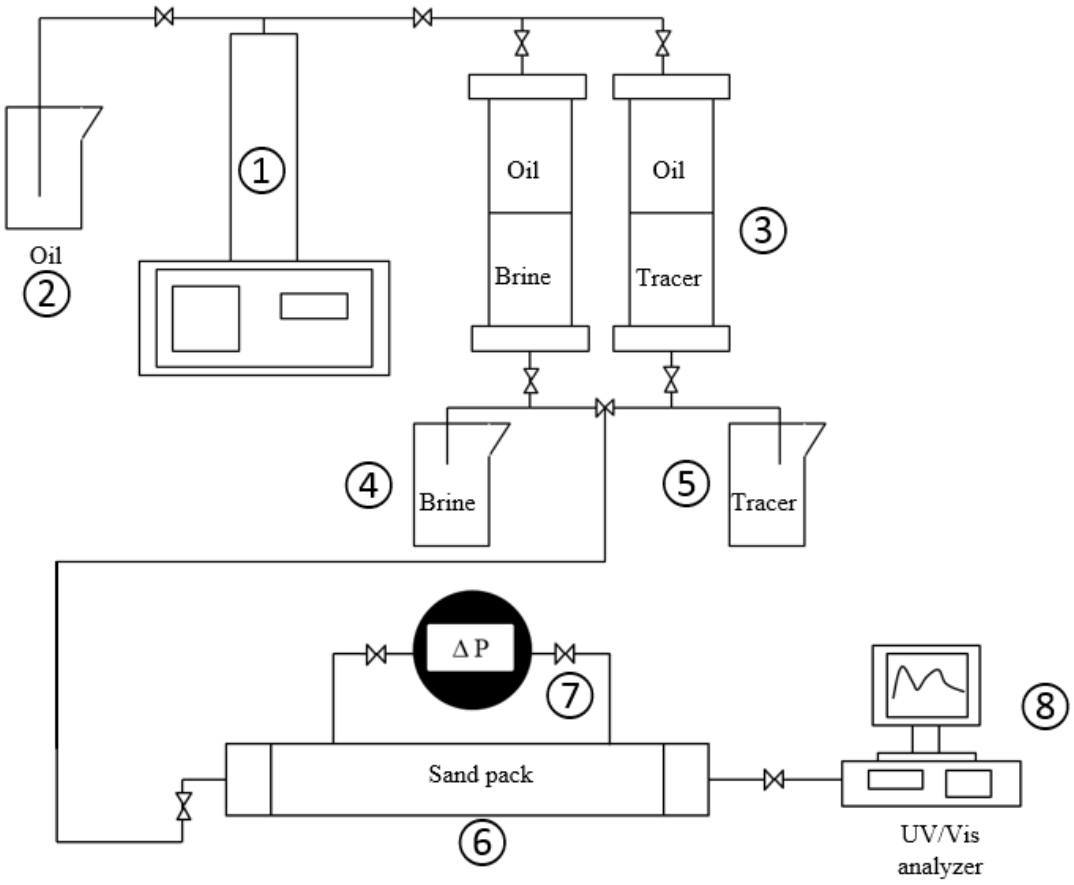

Figure 3.9 Schematic of tracer test set-up [① ISCO pump ② oil refill ③brine/tracer transfer cylinder④ brine refill ⑤tracer refill ⑥ sand pack holder ⑦ pressure gauge ⑧ Data logger (UV-Vis analyzer)]

Figure 3.10 Transfer cylinders containing oil/brine and oil/tracer solutions

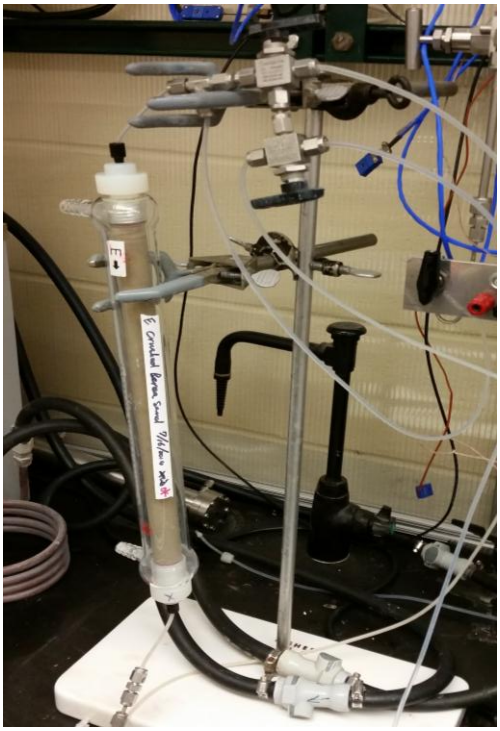

Figure 3.11 Sand pack holder with Berea sand filled

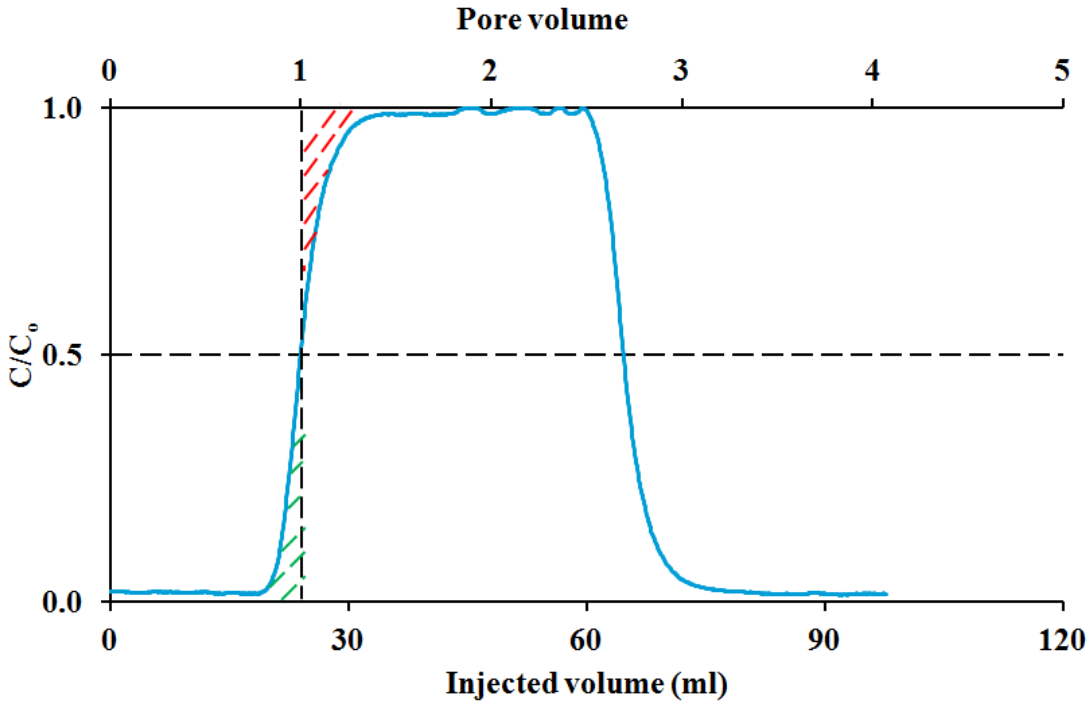

Figure 3.12 Specimen tracer curve. The area below the curve up to 1 PV (shaded in green) is equal to that above the curve from 1 PV to C/Co =1 (shaded in red) in a sand pack

3.2.10.3 Sample test

Both the PEI/DS/peptone nanoparticle suspension and the CS/DS/peptone NP suspension were tested for retention in the sand pack system. The sample test followed the process listed below:

1. The sample test system was connected as shown in Figure 3.13.
2. 1 PV of synthetic sea water (SSW) was injected through a 50 ml syringe by a PHD 2000 Syringe Pump (Harvard Apparatus Inc., Holliston, MA) at a rate of 5

ml/s to rinse the sand pack (Figure 3.14). The effluent solution was collected in 2 ml centrifuge tubes; each tube was fill with approximately 1.8 ml sample.

4. 8 PVs of NP suspension was then injected into the sand pack at the same rate. After the injection, the sand pack saturated with NP suspension was then stored overnight (8 hours). Then the influent was switched back to brine, then continued storing the effluent samples till another 4 PV.

5. The collected effluent samples were tested by both modified Bradford assay and UV absorbance analysis. The testing agent of modified Bradford assay can be found in Section 3.1.8. The testing methods for nanoparticle concentration are included in Appendix 2.

6. Graphs of C/C_o vs. pore volume injected were plotted to calculate the retention of the nanoparticle (Equation 3.9).

$$Retention = \frac{C_S \times V_t - \sum_{i=1}^{n} C_n \times V_n}{M_{sand}} \qquad \text{Equation 3.9}$$

Where C_s is the peptone concentration of SSW diluted nanoparticle suspension, V_t is the total injected volume of SSW diluted nanoparticle suspension, C_n is the peptone concentration in each effluent sample, and V_n is the volume of each effluent sample. $C_s \times V_t$ represents the total mass of nanoparticle injected, and the sum of $C_n \times V_n$ represents the total mass of nanoparticle collected at the effluent.

7. The recovery of nanoparticle was calculated by:

$$Recovery = \frac{\sum_{i=1}^{n} C_n \times V_n}{C_S \times V_t} \times 100\% \qquad \text{Equation 3.10}$$

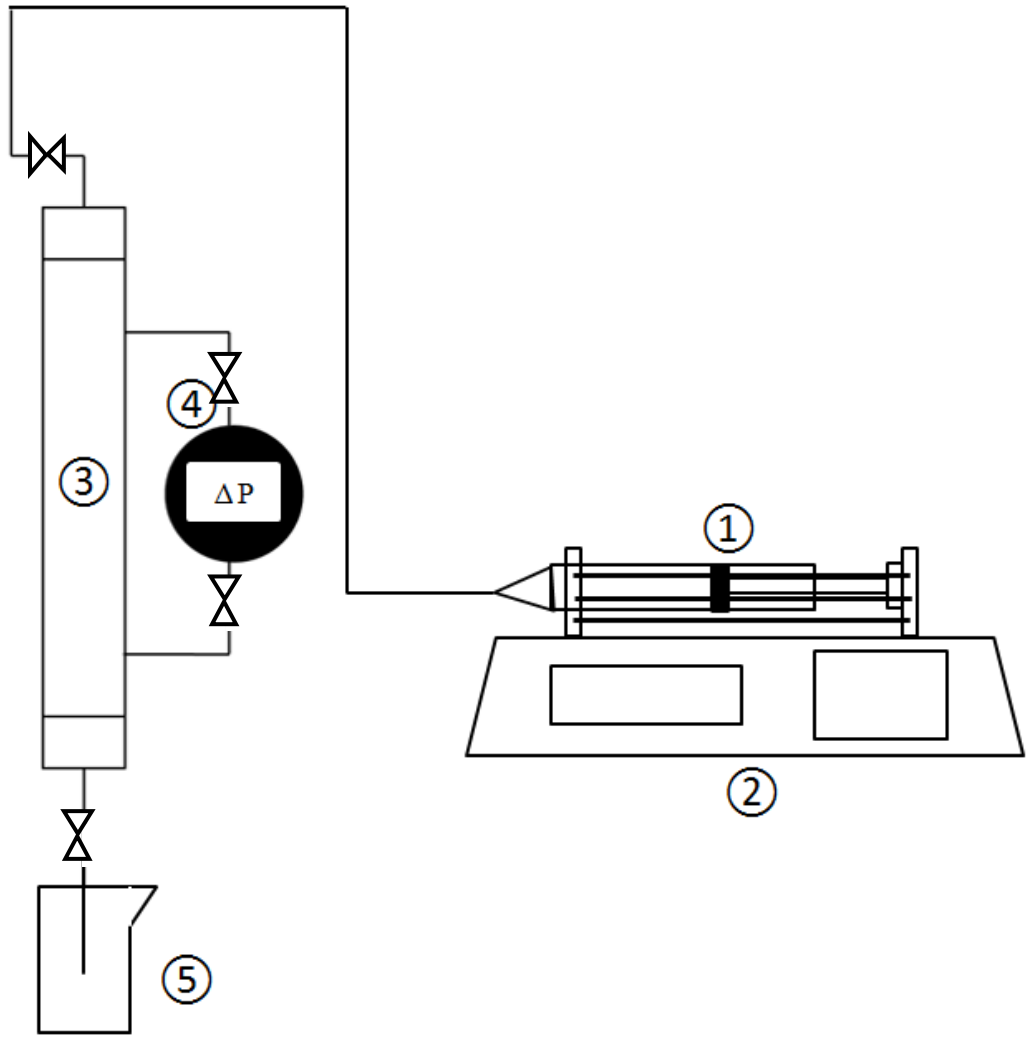

Figure 3.13 Schematic of sample test set-up (① 50 ml syringe containing nanoparticle solution or brine, ② syringe pump ③ sand pack holder, ④ pressure gauge, ⑤ effluent collection)

Figure 3.14 Injection of nanoparticle samples with PHD 2000 syringe pump (Harvard Apparatus Inc. Holliston, MA) (Flow rate: 5 ml/min)

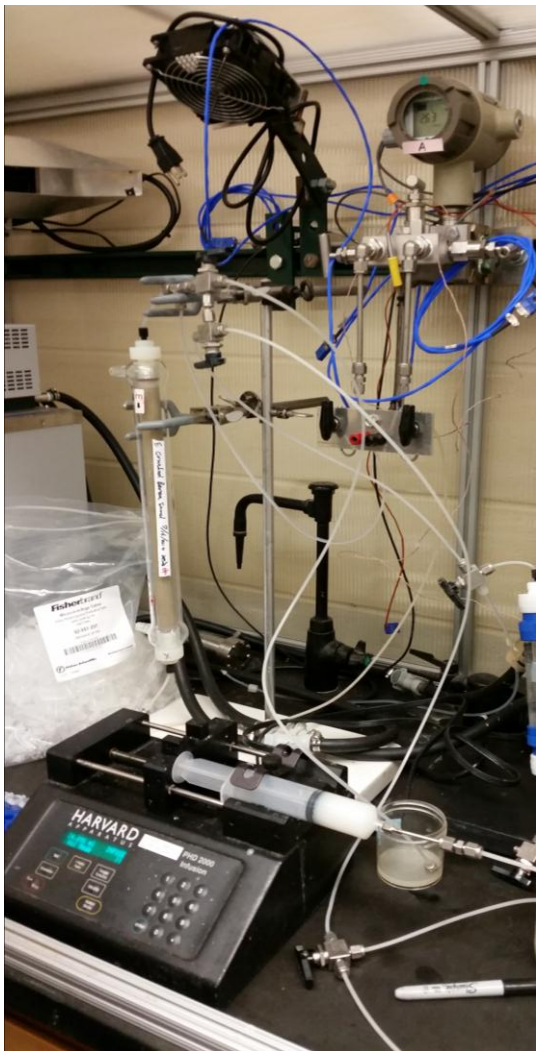

Figure 3.15 Sandpack test set-up

3.2.11 The selection of sandpack sample (NP concentration) testing method

In this section, different methods of PEI/DS/peptone and CS/DS/peptone nanoparticle concentration and peptone concentration in the sand pack sample test (retention analysis) are discussed. UV absorbance analysis was initially applied; and then protein staining analysis were conducted; finally modified Bradford assay and modified UV absorbance analysis were selected as standard method to measure the retention of PECNP in the porous medium.

3.2.11.1 Procedures of each NP concentration testing method

Among all the tests mentioned in this section, nanoparticle group P101-11 (PEI pH = 10, PEI : peptone : DS mass ratio = 3:10:10, Addition order: DS-peptone-PEI) was used as sample NP to validation all the testing methods.

3.2.11.1.1 UV absorbance analysis

A Full scan (200 nm to1100 nm wavelength) of 10% w/w PEI-NP suspension, 0.1% w/w peptone solution, 1% w/w PEI solution, 1% DS w/w solution and synthetic sea water was analyzed by UV-Vis analyzer to determine the absorbance peak of nanoparticle suspension and peptone solution. Figure 3.16 shows the results of the full scan, absorbance peak of both NP suspension and peptone solution were observed at 270 nm. In UV absorbance analysis, different concentrations of P101-11 NP was mixed with SSW with a mass ratio of 1:1. Then the NP suspension was tested for UV asorbance at 25 ℃ and a final pH of 7.8. A plot of NP absorbance at 270 nm vs. different concentration of PEI-NP was plotted to test whether there is linear regression between UV absorbance and PEI-NP concentration (Figure 3.17).

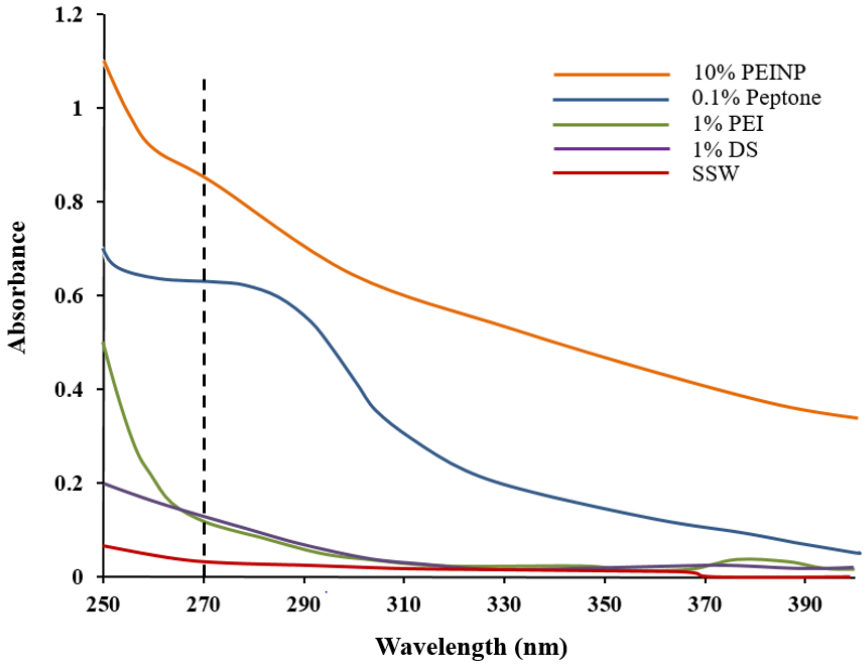

Figure 3.16 The UV absorbance full scan of different solutions

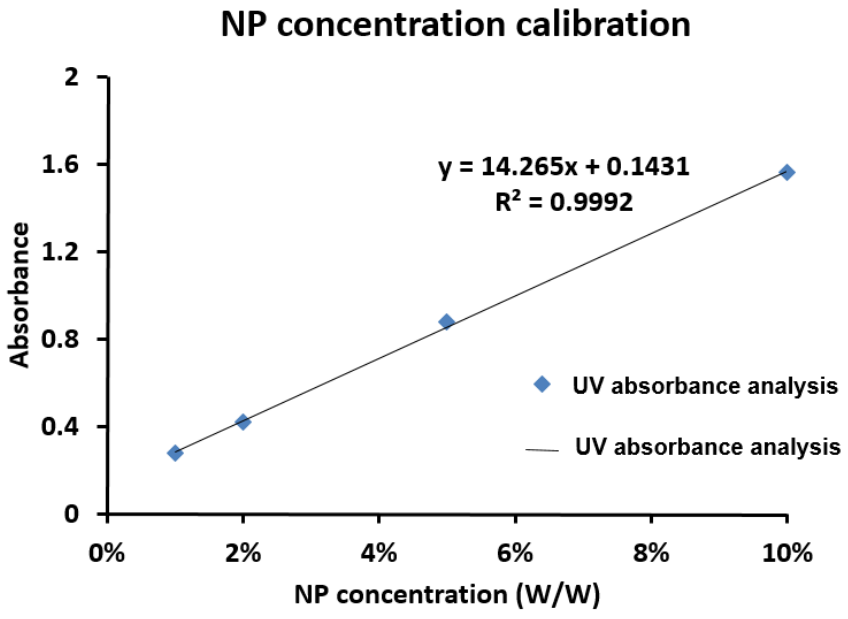

Figure 3.17 The UV absorbance calibration curve for peptone

3.2.11.1.2 Modified UV absorbance analysis

UV absorbance analysis (270 nm) was approved efficient in peptone concentration measurement in Section 3.2.5. Also, as shown in Figure 3.16, CS and SSW didn't affect the UV absorbance of peptone at 270 nm wavelength. Although both PEI and DS have a low absorbance at 270 nm, when converting the absorbance of PEI and DS to peptone concentration by the calibration curve, the converted [peptone] is less than 0.05% w/w. The effect of PEI and DS to peptone concentration was considered neglected. In this method, 4% hydrogen peroxide (H_2O_2) was applied to digest nanoparticles into free components (PEI, DS, peptone or CS, DS, peptone), UV absorbance analysis was then applied to test the concentration of free peptone. The sample analysis followed the process listed below:

1. 0.25 ml H_2O_2 was added into 0.75 ml NP sample at room temperature.
2. Samples were then stored in oven at 75 ℃ for 3 hours.
3. UV absorbance (270 nm wavelength) of each sample was tested at room temperature.
4. Analyzed UV absorbance data was then normalized by subtracting the UV absorbance of 1% H_2O_2 (0.0573). $H_2O_2$was also pre-treated by heating at 75 ℃ for 3 hours.

Figure 3.18 is the standard curve prepared for modified UV absorbance analysis.

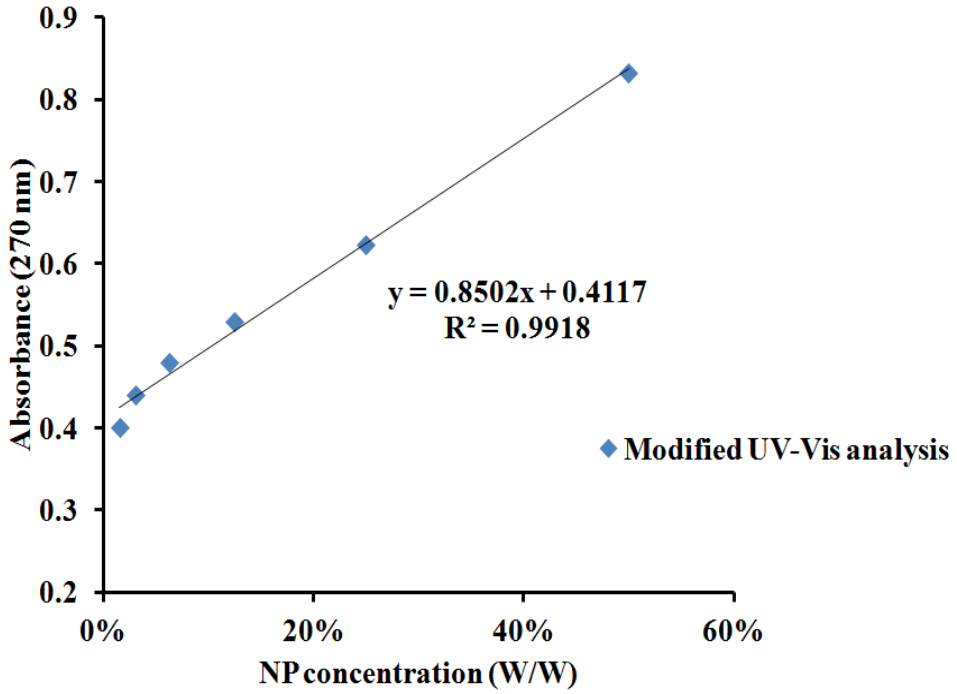

Figure 3.18 The modified UV absorbance calibration curve for peptone concentration from H_2O_2 digested NP

3.2.11.1.3 Coomassie Plus method (Bradford assay)

The Bradford protein assay is a spectroscopic analytical procedure used to measure the concentration of protein in a solution. It is based on an absorbance shift of the dye Coomassie Brilliant Blue G-250 in which under acidic conditions the red form of the dye is converted into its blue form to bind to the protein being assayed.[107]

Coomassie Plus (Bradford protein assay) reagent was obtained from Fisher Scientific (Pittsburgh, PA). The digestion of NP followed the method mentioned in Section 3.2.11.1.2.

0.75 ml of the digested sample and 0.25 ml of the Coomassie plus reagent were mixed with pipette and incubated for 10 minutes. The mixed solution was then transferred to the UV absorbance analysis, the absorbance testing wavelength was 595 nm.

3.2.11.1.4 Modified Bradford assay

The formula of Coomassie Plus reagent (Bradford assay reagent) was modified for more accurate analysis and broader testing range. The recipe of modified Bradford assay reagents is listed in Section 3.1.8. The sample preparation and incubation of modified Bradford assay follows the same procedure mentioned in previous section (3.2.11.1.3). Figure 3.19 is the optimized standard curve for modified Bradford assay.

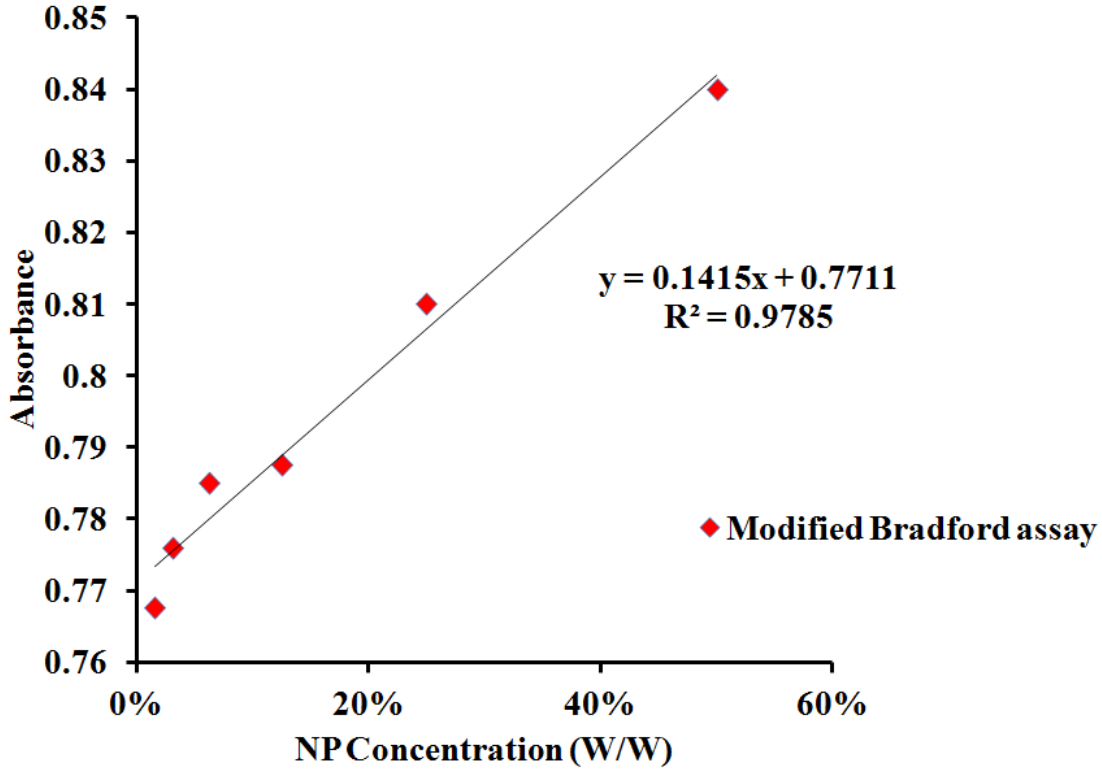

Figure 3.19 The calibration curve for modified Bradford assay

3.2.11.2 The validation of each NP concentration testing method

3.2.11.2.1 UV absorbance analysis

Figure 3.20 is the comparison of UV absorbance of both peptone and PEI-NP which contains same peptone concentration. It is observed from the plot that at each peptone concentration, the absorbance of peptone has significantly lower value than that of PEI/peptone/DS nanoparticle that contains same peptone concentration. This phenomenon can be explained by the turbidity of nanoparticle suspension.

Turbidity is a measure of water clarity that caused by particle suspending in water and decreasing the passage of light through the water. Turbidity is a good indicator of the particle concentration. Optical density is a typical application of turbidity to estimate microbial concentration in a suspension since the absorbance is proportional to the concentration of the absorbing species in the sample.[108] Jason and Linden[109] also suggested that the turbidity of suspended particles in water affects the light absorbance results. The increase of absorbance in Figure 3.21 is possibly caused by the turbidity of suspended nanoparticles in the system.

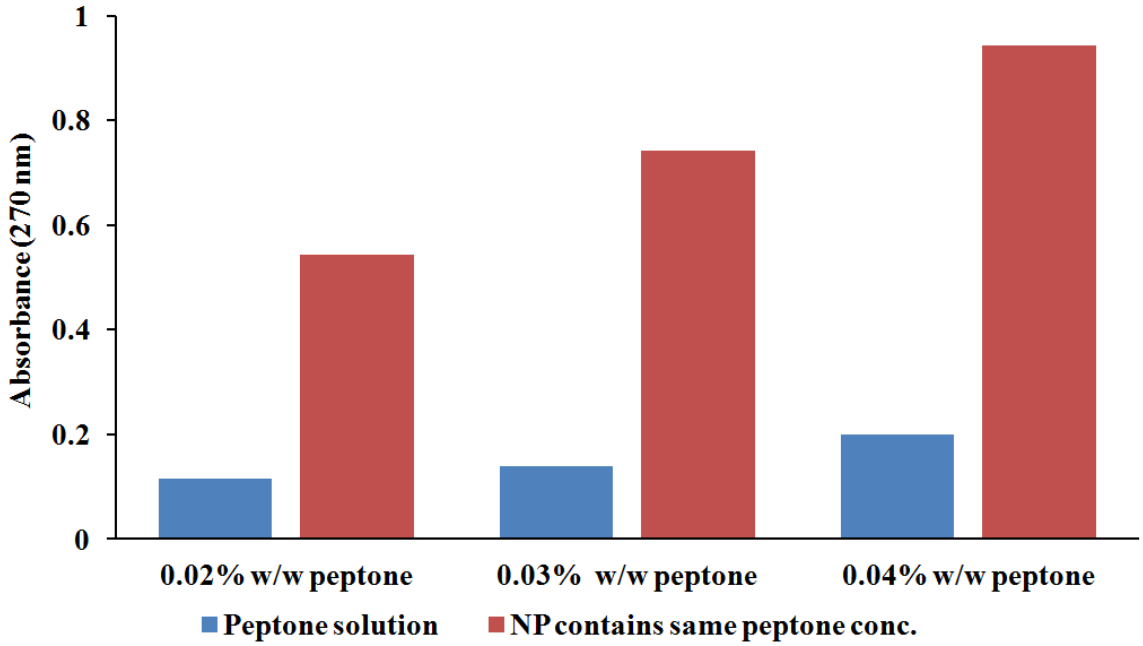

Figure 3.20 The comparison of absorbance of the peptone solution with PEI-NP contains the same peptone concentration at 270 nm wavelength

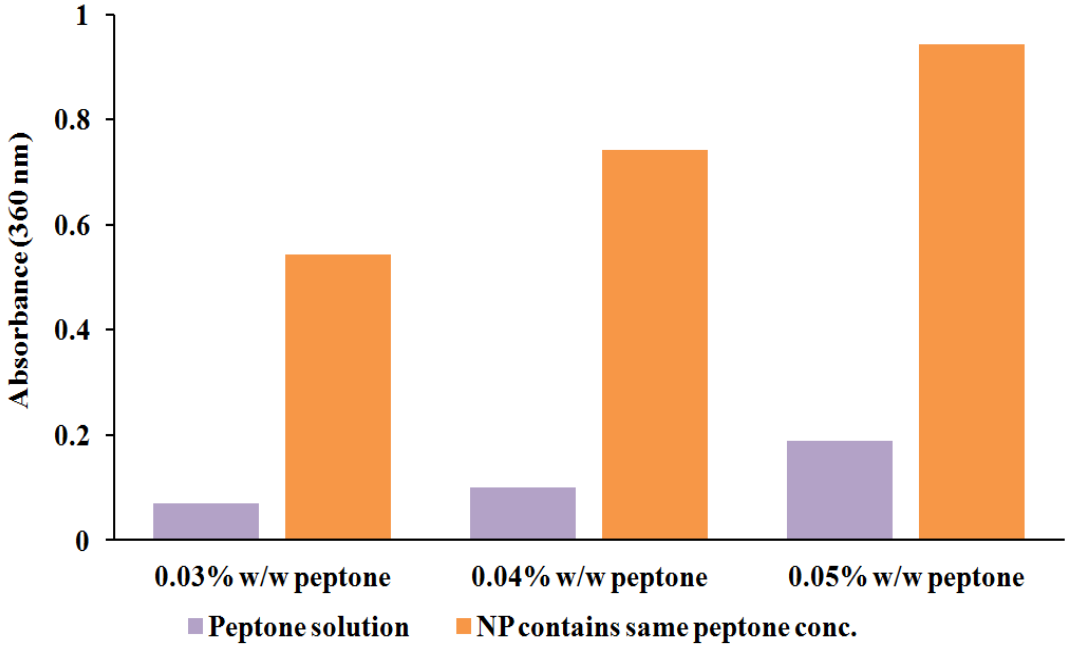

Figure 3.21 The comparison of absorbance of the peptone solution with PEI-NP contains the same peptone concentration at 360 nm wavelength

A sand pack test was applied to test the validation of UV absorbance analysis. As nanoparticles penetrate through the porous medium, the loss of nanoparticles occurs due to the absorption of NP in the porous medium. The loss of nanoparticles will cause the decrease of turbidity in the system. Also in the nanoparticle system, free peptone and PEI-NP coexist, both of which contribute to the UV absorbance. It is possible that a system with low PEI-NP concentration and high free peptone concentration has the same absorbance as the system which contain higher PEI-NP concentration and lower free peptone concentration. The UV absorbance may not accurately measure the retention of nanoparticle, and unsmoothed sand pack results will occur (Figure 3.22). UV absorbance analysis is proven invalid method for NP retention measurement.

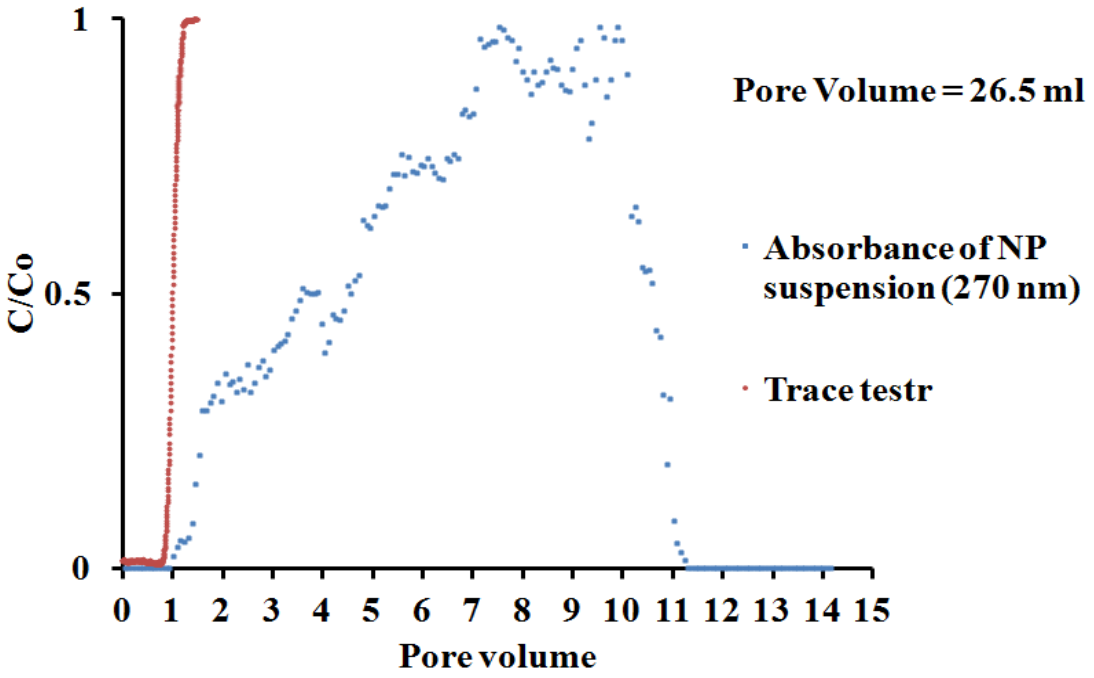

Figure 3.22 The sand pack results by UV absorbance analysis (unsmoothed curve represents UV absorbance method is invalid)

3.2.11.2.2 Modified UV absorbance analysis

Since the UV measurement of nanoparticle concentration is invalid, degradation of NP into free components is required. In the modified UV absorbance method, the nanoparticles in the collected sand pack effluent samples were digested by hydrogen peroxide into free peptone and polyelectrolytes. The digested samples were then tested for UV absorbance at 270 nm. Figure 3.23 is the comparison of UV absorbance of peptone solution, digested PEI-NPs that contains same peptone concentration, and PEI-NP, results have been further normalized by subtracting the absorbance of 4% H_2O_2. It is observed in the bar chart that the absorbance of normalized PEI-NP is significantly identical to the absorbance of peptone, the difference is less than 5%.

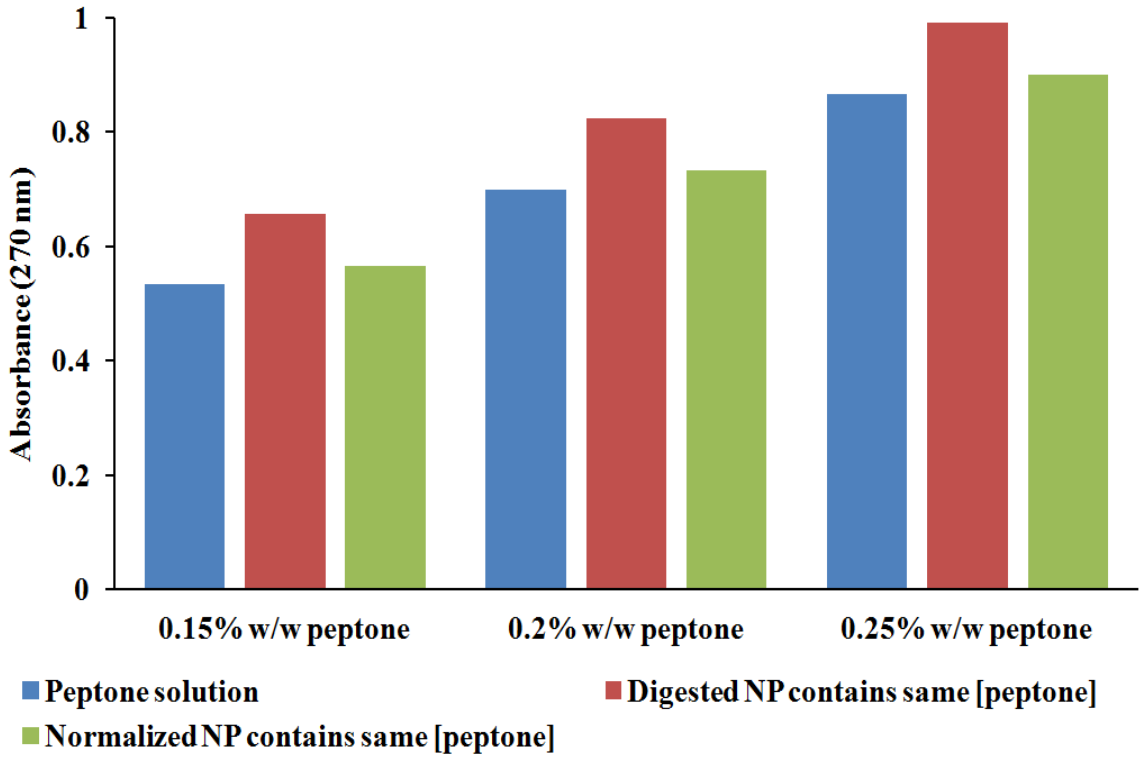

Figure 3.23 The comparison of absorbance of the peptone solution with PEI-NP contained the same peptone concentration and normalized digested PEI-NP

3.2.11.2.3 Coomassie Plus method (Bradford assay)

A plot of UV absorbance of digested PEI-NP at a wavelength of 595 nm vs. PEI-NP concentration (w/w) is generated as Figure 3.24. When the PEI-NP concentration is lower than 6%, the absorbance vs. concentration curve reaches a plateau, which indicates the limitation of this testing method. Therefore, the Coomassie Plus analysis is not capable of testing the retention of PEC nanoparticles.

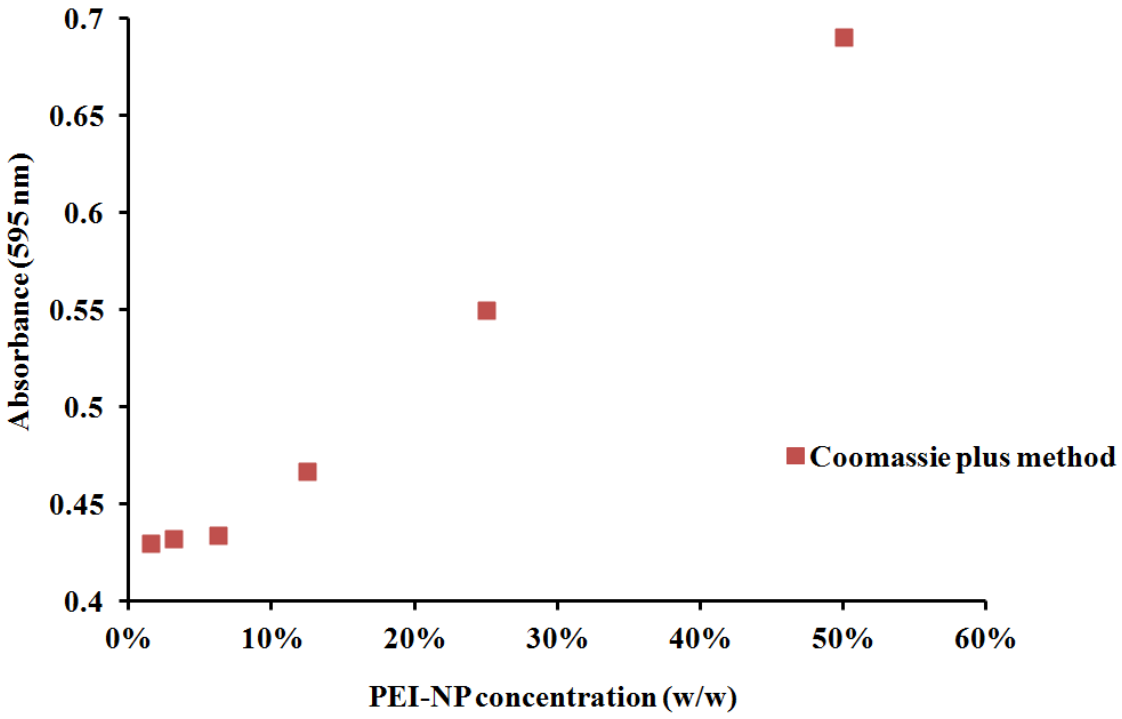

Figure 3.24 The standard curve of Coomassie Plus analysis (The plateau below 6% w/w PEI-NP concentration shows the limitation of Coomassie plus analysis)

3.2.11.4 Modified Bradford assay

Different concentrations of Coomassie brilliant blue G-250 has had been dissolved into RO water to form different Bradford assay reagents. The recipes of modified Bradford assay are listed in Table 3.5.

Figure 3.25 is the test of the capability of different modified Bradford reagents as peptone stain. It is observed that when 1.5 ×Bradford reagent is used as stain, the absorbance vs. concentration curve has the most linear-like regression. Moreover, the 1.5 ×Bradford reagent is capable of testing a PEI-NP concentration as less as 1.6%.

In summary, 1.5 ×Bradford reagent is selected as a secondary indicator to test the retention of nanoparticle in the porous medium.

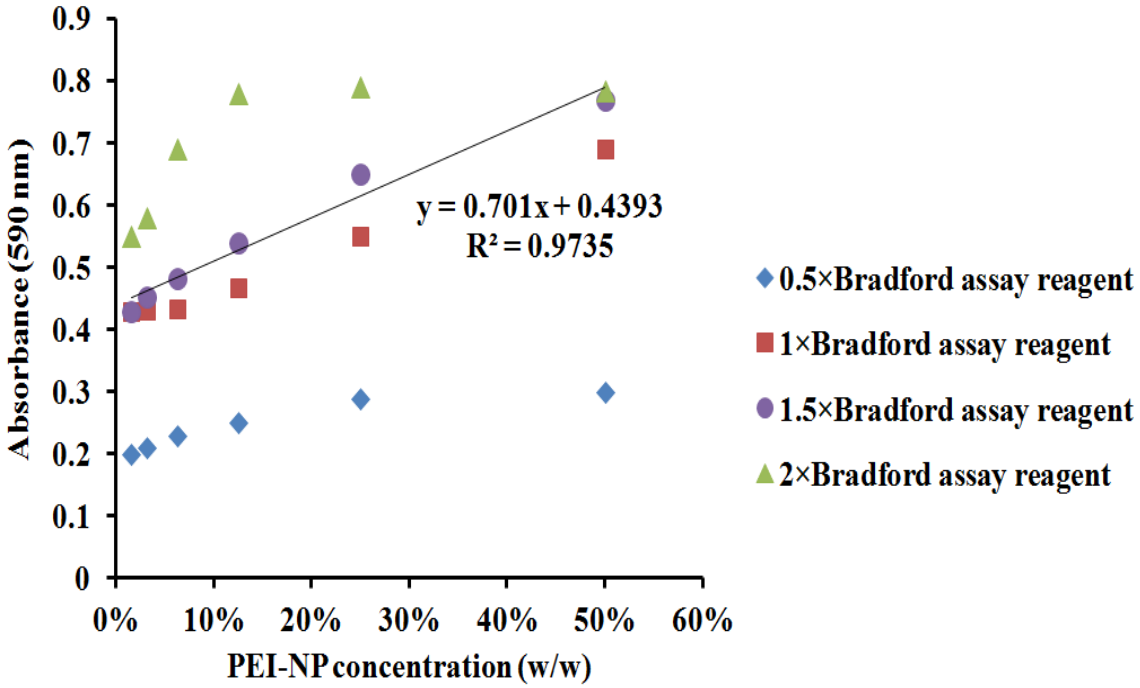

Figure 3.25 The test of different Bradford reagent as peptone stain

The repeatability error of modified UV absorbance and modified Bradford assay were calculated. The error of repeatability is calculated by the following equation:

$$error\ of\ repeatability = \frac{2 \times N_{avgstd}}{N_{avg}} \times 100\% \qquad \text{Equation 3.11}$$

Where N_{avgstd} is the average standard deviation of 3 readings of the same sample tested, Navg is the average of 3 readings of the same sample tested.

Table 3.9 shows the repeatability of different methods on same digested PEI-NP sample, the sample concentration is 12.5% v/v nanoparticle suspension. The average error of repeatability from 3 sets of data (12.5%, 25% and 50% w/w nanoparticle suspension) for each method can be found in Table 3.10. It is observed that both repeatability errors of modified UV method and modified Bradford method are lower than 5%, therefore, both methods are selected as analytical methods for Sandpack sample test.

Table 3.9 The repeatability of different method

Testing method	Testing results	Repeatability error
Modified UV absorbance	0.513	2.15%
	0.524	
	0.517	
Modified Bradford assay absorbance	0.476	2.47%
	0.478	
	0.467	

Table 3.10 The error of repeatability of different methods

Testing method	Average repeatability error
Modified UV absorbance	1.67%
Modified Bradford assay	2.36%

4. Results and discussion

4.1 Characterization and optimization of the nanoparticles

4.1.1 PEI/NH_4/DS nanoparticle

The preparation of PEI/NH_4^+/DS nanoparticle followed the method described in Section 3.1. Table 4.1 is an example of the PEI/NH_4^+/DS nanoparticle recipes at different PEI:NH_4^+ratio and the order of addition.

Table 4.1 Nanoparticle systems with different CS: peptone ratio and the order of addition (NH_4Cl volume = 1 ml, PEI pH = 10)

Group	1% w/w PEI (ml)	PEI pH	1% w/w DS (ml)	15% w/w NH_4Cl (ml)	Mass ratio (PEI:DS:NH_4^+)	Order of addition
N101-1	1	10	10	1	1:10:15	DS, NH_4^+, PEI
N101-2	1	10	10	1	1:10:15	DS,PEI, NH_4^+
N101-3	3	10	10	1	3:10:15	DS, NH_4^+, PEI
N101-4	3	10	10	1	3:10:15	DS,PEI, NH_4^+
N101-5	5	10	10	1	5:10:15	DS, NH_4^+, PEI
N101-6	5	10	10	1	5:10:15	DS,PEI, NH_4^+
N101-7	7	10	10	1	7:10:15	DS, NH_4^+, PEI
N101-8	7	10	10	1	7:10:15	DS,PEI, NH_4^+

The optimization of nanoparticles followed the criteria below:

1. The size of the nanoparticle should be small to penetrate into the narrow pores in the reservoir.

2. Large zeta potential is preferred to increase the repulsive force that helps to keep the nanoparticle from aggregating and precipitating.

3. Higher EE is required to decrease the amount of free peptone in the PECNP system.

The size, zeta potential and entrapment efficiency of different nanoparticles is shown in Table 4.2. Precipitation occurs when the PEI: NH_4^+ ratio is 1:1. The size of nanoparticle increases as the concentration of PEI increases. The zeta potential become less negative as the PEI: NH_4^+ ratio increases. The highest entrapment efficiency is observed at PEI: NH_4^+ ratio of 3:1 and addition order of DS/NH_4^+/PEI. The nanoparticle group N101-3 was selected as optimized ammonium nanoparticle for its relatively higher EE, zeta potential, and relatively lower particle size. The size, zeta potential, and EE were measured periodically to demonstrate the stability of the nanoparticles over time. The stability test results showed that the average changesin the size and zeta potential of ammonium nanoparticle are greater than 20% in 5 hours.The entrapment efficiency drops from approximately 50% to 14% in 3 hours.

Comparing to the PEI-DS system developed by Cordova[69] and Barati[71], the entrapped third component of this research, ammonium, has less ionic charge than the multivalent chromium and lower molecular weight than enzyme. The interaction between ammonium and PEI-DS is loose. The highly soluble and low molecular weight properties of ammonium allow it to easily diffuse out of the nanoparticle, which explains the huge EE decrease of the PEI-$NH4^+$-DS in the first 3 hours. The observation shows that the PEI/ NH_4^+/DS nanoparticle is an unstable polyelectrolyte complex system, the system may release the entrapped nutrients before they pass the near wellbore region.

Table 4.2 Mean particle size and zeta potential of different PEI/$NH4^+$/DS nanoparticles (PPT: precipitation)

Group	Particle size (nm)	zeta potential (mV)	Entrapment efficiency
N101-1	PPT	PPT	PPT
N101-2	PPT	PPT	PPT
N101-3	55	-21.2	55.2%
N101-4	PPT	PPT	PPT
N101-5	79	-24.7	19.85%
N101-6	82	-25.9	10.22%
N101-7	90	-22.1	24.8%
N101-8	87	-24.7	5.85%

4.1.2 PEI /peptone/DS nanoparticle

The size and zeta potential of PEI/DS/peptone NP was measured with varied formulas with different PEI:DS ratio and addition order, which was shown in Chapter 3. The measured mean particle size and zeta potential of different recipes in Table 3.6-3.8 arelisted in Table 4.2-4.4.

The optimization of nanoparticles followed the criteria below:

1. The size of the nanoparticle should be small to get into the narrow pores in the reservoir.

2. Large zeta potential is preferred to increase the repulsive force that helps keeping the nanoparticle from aggregation and precipitation.

3. Higher EE is required to decrease the amount of free peptone in the PECNP system.

TABLE 4.3 Mean particle size and zeta potential of different PEI/DS/peptone PECNP, PEI pH =10, peptone volume = 1ml (PPT: precipitation)

Group	Particle size (nm)	Zeta potential (mV)
P101-1	432	-37.8
P101-2	387	-33.2
P101-3	495	-35.8
P101-4	454	-37.3
P101-5	502	-33.9
P101-6	451	-10.2
P101-7	521	-29.6
P101-8	481	-18.4
P101-9	495	-30.8
P101-10	441	-20.5
P101-11	483	-28.9
P101-12	387	-25.8
P101-13	477	-28.4
P101-14	403	-23.7
P101-15	452	-27.9
P101-16	387	-10.8
P101-17	489	-27.3
P101-18	421	-14.7
P101-19	521	-26.7
P101-20	PPT	PPT
P101-21	PPT	PPT
P101-22	PPT	PPT
P101-23	PPT	PPT
P101-24	PPT	PPT
P101-25	PPT	PPT
P101-26	PPT	PPT
P101-27	PPT	PPT
P101-28	PPT	PPT
P101-29	PPT	PPT
P101-30	PPT	PPT
P101-31	PPT	PPT
P101-32	PPT	PPT
P101-33	PPT	PPT
P101-34	PPT	PPT
P101-35	PPT	PPT
P101-36	PPT	PPT
P101-37	PPT	PPT
P101-38	PPT	PPT

TABLE 4.4 Mean particle size and zeta potential of different PEI/DS/peptone PECNP, PEI pH =10, peptone volume = 2 ml (PPT: precipitation)

Group	Particle size (nm)	Zeta potential (mV)
P102-1	503	-37.8
P102-2	442	-33.2
P102-3	494	-35.8
P102-4	454	-27.3
P102-5	462	-33.9
P102-6	452	-10.2
P102-7	488	-29.6
P102-8	419	-18.4
P102-9	550	-30.8
P102-10	499	-20.5
P102-11	PPT	PPT
P102-12	PPT	PPT
P102-13	PPT	PPT
P102-14	PPT	PPT
P102-15	PPT	PPT
P102-16	PPT	PPT
P102-17	PPT	PPT
P102-18	PPT	PPT
P102-19	PPT	PPT
P102-20	PPT	PPT
P102-21	PPT	PPT
P102-22	PPT	PPT
P102-23	PPT	PPT
P102-24	PPT	PPT
P102-25	PPT	PPT
P102-26	PPT	PPT
P102-27	PPT	PPT
P102-28	PPT	PPT
P102-29	PPT	PPT
P102-30	PPT	PPT
P102-31	PPT	PPT
P102-32	PPT	PPT
P102-33	PPT	PPT
P102-34	PPT	PPT
P102-35	PPT	PPT
P102-36	PPT	PPT
P102-37	PPT	PPT
P102-38	PPT	PPT

From Table 4.3, precipitation occurs when the PEI : DS mass ratio is higher than 5:10. The size of PEI/DS/peptone NP does not change significantly with the changing PEI/DS/peptone ratio.The particle sizes are approximately in the range of 400-600 nm when the addition order is DS-peptone-PEI. However, when the addition order changes to DS-PEI-peptone, smaller nanoparticles are produced. Barati[67] reported a similar observation on the PEI-pectinase-DS nanoparticle. One possible reason for this phenomenon is that both PEI and DS are highly charged high molecular weight polymers. The interaction between PEI and DS is stronger than the interaction between peptone and DS. When mixing PEI/DS together first, the loading of peptone in the PECNP may decrease resulting in a PECNP that is smaller in particle size. The entrapment efficiency results show a decline when the addition order changes from DS-peptone-PEI to DS-PEI-peptone, which agrees well with this hypothesis (Table 4.5).

It is also observed from Table 4.3 and 4.4 that zeta potential become less negative when more PEI is added in the system. Since PEI is a positively charged polymer, with a fixed DS volume, increasing the PEI loading in the PECNP will result in the increase of positive ion concentration in the nanoparticle and the overall surface charge of nanoparticle will be less negative. When the positive ion concentration and negative ion concentrations were equal, precipitation caused by charge neutralization was observed.

TABLE 4.5 Entrapment efficiency of PEI/DS/peptone nanoparticle by different addition order, PEI pH =10

PEI-DS-peptone ratio	Entrapment efficiency by addition order	
	DS-peptone-PEI	DS-PEI-peptone
1:10:1	6.30%	1.30%
2:10:1	15.40%	5.10%
3:10:1	38.70%	11.20%
3:10:2	23.10%	13.40%

Table 4.6 is a matrix of entrapment efficiency of peptone in different PEI/DS/peptone nanoparticles. The highest EE (38%) was achieved when the PEI/DS mass ratio was 3:10 and the peptone/DS (V/V) ratio was 1:1 (Group P101-11). Also, the particle size of Group P101-11was relatively small, and zeta potential was more negative. So Group P101-11is the optimized system among all the PEI-NP groups. The entrapment efficiency of optimized PEI/peptone/DS nanoparticle in this research (38.7%) is lower than the EE of optimized PEI/pectinase/DS nanoparticle (73%) designed by R. Barati.[67] This difference is likely due to the fact that the molecular weight of pectinase (50K-90K)[111] is higher than that of peptone (2k-20K), which makes pectinase more able to be entrapped in the nanoparticle. Moreover, the chromium nanoparticle developed by Cordova[69] has the highest entrapment efficiency among all three nanoparticles (93-94%). The possible explanation could be the multivalent charge on the chromium ion. Chromium has more surface charge, and a smaller size than protein (peptone and pectinase), the interaction between chromium and polyelectrolyte is stronger. Thus higher EE can be observed on PEI-chromium-DS nanoparticle.

Table 4.6 The entrapment efficiency (EE) of different PEI/DS/peptone PECNP (PEI pH = 10)

Matrix for EE	Mass ratio of PEI											
Mass ratio of peptone	0.5	1	1.5	2	2.5	3	3.5	4	4.5	5	5.5	6
5	3.3%	2.1%	0.4%	0.7%	15.2%	19.5%	2.2%	4.1%	1.7%	3.1%	3.7%	3.4%
10	8.4%	5.8%	26.6%	18.5%	21.4%	38.7%	10.3%	3.2%	16.3%	9.7%	5.2%	11.2%
15	2.5%	13.5%	23.7%	16.2%	14.3%	30.5%	18.5%	0%	0%	13.6%	1.4%	0%
20	3.1%	12.0%	13.5%	8.9%	18.7%	11.7%	11.4%	0%	0%	0.1%	0%	0%
25	0.8%	3.2%	3.4%	11.3%	8.1%	6.3%	6.1%	0%	0%	0%	0%	0%
30	0.7%	2.1%	2.1%	1.7%	1.9%	3.6%	5.2%	0%	0%	0%	0%	0%
35	0%	0%	0.3%	0%	0%	1.5%	3.8%	0%	0%	0%	0%	0%
40	0%	0%	0%	0%	0%	0.2%	0.3%	0.2%	0%	0%	0%	0%

4.1.3 CS/peptone/DS nanoparticle

The effect of CS : peptone ratio and order of addition on the mean particle size and zeta potential of the CS/DS/peptone nanoparticle is shown in Table 4.7.

Table 4.7 Mean particle size and zeta potential of different CS/DS/peptone PECNP (peptone volume = 3 ml, PPT: precipitate)

Group	Particle size (nm)	Zeta potential (mV)
C3-1	483	-32.8
C3-2	521	-30.5
C3-3	547	-26.9
C3-4	551	-26.6
C3-5	547	-27.4
C3-6	522	-26.7
C3-7	536	-25.1
C3-8	511	-24.3
C3-9	495	-27.1
C3-10	421	-28.3
C3-11	433	-25.6
C3-12	451	-27.1
C3-13	467	-26.4
C3-14	485	-27.5
C3-15	479	-26.9
C3-16	487	-26.1
C3-17	439	-26.3
C3-18	456	-25.4
C3-19	447	-29.4
C3-20	429	-28.7
C3-21	425	-27.5
C3-22	460	-27.1
C3-23	485	-26.4
C3-24	523	-26.1
C3-25	PPT	PPT
C3-26	PPT	PPT
C3-27	PPT	PPT
C3-28	PPT	PPT
C3-29	PPT	PPT
C3-30	PPT	PPT
C3-31	PPT	PPT
C3-32	PPT	PPT
C3-33	PPT	PPT
C3-34	PPT	PPT
C3-35	PPT	PPT
C3-36	PPT	PPT
C3-37	PPT	PPT
C3-38	PPT	PPT

It is observed from Table 4.7that the size and zeta potential of CS/DS/peptone NP do not change significantly with the different CS/DS/peptone ratio or the addition order. The mean particle size is 481 nm and average zeta potential is -27.1 mV. Similar to the PEI/DS/peptone nanoparticle, when the addition order change to CS-DS-peptone, the EE decreases.

The entrapment efficiency by the CS/peptone ratio is shown in Table 4.8. The highest EE (21%) was achieved when the CS/DS mass ratio was 5:10, and peptone/DS mass ratio was 30:10. The entrapment efficiencies of PEI pH = 7, 8, 9, 11 and 12 are listed in Appendix 2.

Table 4.8 The entrapment efficiency (EE) of CS/DS/peptone PECNP

Matrix for EE	Mass ratio of CS											
Mass ratio of peptone	0.5	1	1.5	2	2.5	3	3.5	4	4.5	5	5.5	6
5	0%	0%	0%	1.2%	1.1%	0.5%	5.7%	10.4%	0%	0%	0%	0%
10	0%	0%	2.2%	1.1%	0.8%	0.8%	10.2%	15.4%	10.4%	2.8%	2.7%	0%
15	0%	1.3%	1.2%	1.1%	1.4%	0.8%	6.3%	8.1%	8.3%	6.5%	4.2%	1.5%
20	0%	2.1%	1.6%	3.7%	1.5%	6.2%	5.7%	1.7%	3.4%	10.4%	7.7%	0.7%
25	0%	1.7%	7.4%	1.7%	1.2%	9.5%	6.2%	7.4%	9.7%	14.2%	11.4%	1.6%
30	0%	0%	1.3%	1.3%	1.3%	11.3%	11.3%	1.0%	12.2%	21.1%	6.7%	0.8%
35	0%	1.5%	1.1%	1.3%	1.4%	14.6%	12.4%	1.1%	10.7%	8.3%	4.3%	0.9%
40	0%	0%	1.3%	1.3%	1.7%	1.6%	1.1%	1.0%	7.2%	0%	1.1%	0%

Although the entrapment efficiency of CS/peptone/DS nanoparticle is very low (EE < 22%), the CS /peptone/DS NP has an interesting property which has been seldom reported. After the nanoparticles are spun down by centrifugation force, the nanoparticles can be resuspended in the aqueous phase by adding RO water to the recovered pellets. Since during the resuspension process the free peptone in the supernatant was discarded after the first centrifugation, when the resuspended nanoparticle was spun down by centrifugation, the free peptone concentration in the resuspended nanoparticle system can be calculated by the equation below:

$$C_f = C_T - C_{ss} \qquad \text{Equation 3.11}$$

Where C_f is the free peptone concentration in the resuspended system, C_T is the total peptone before resuspension, C_{SS} is the peptone in the supernatant after resuspension.

The free peptone concentration after resuspension is less than 0.1% of the original amount of peptone in the system, which indicated that the resuspension process removes the free components in the system; the effect of free peptone on the growth of oilfield microbes was eliminated during the resuspension process, at the expense of a much lower overall nutrient loading. Figure 4.3 shows the process of resuspension.

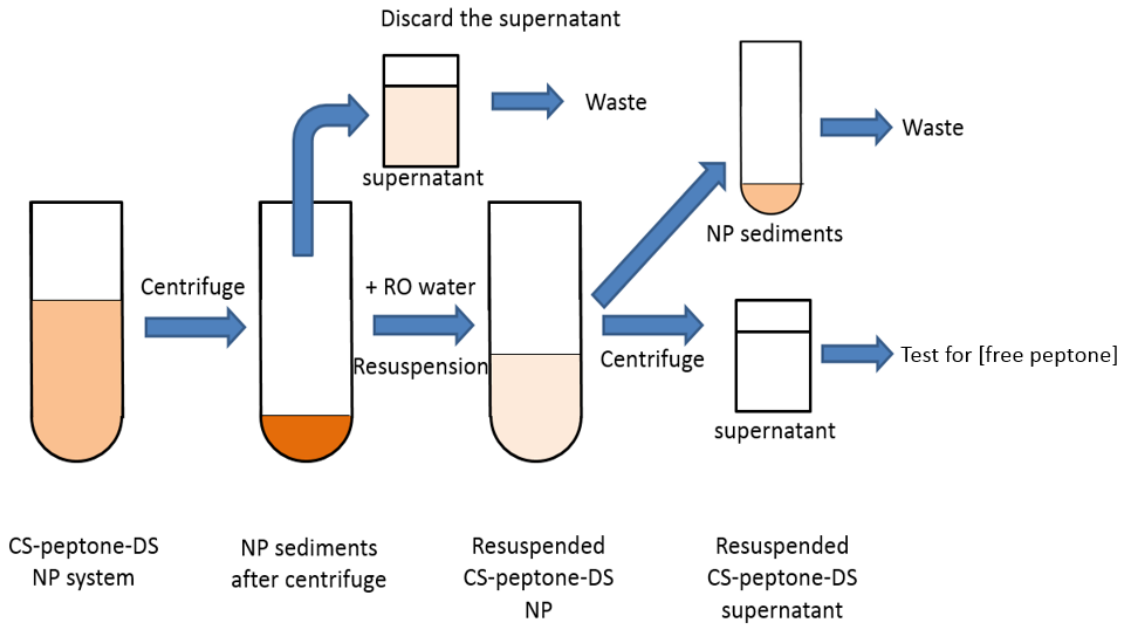

Figure 4.3 The resuspension process of CS-peptone-DS nanoparticle

4.1.4 Ability of PEC nanoparticles maintain their properties

Size and zeta potential were measured in triplicate samples periodically to determine the ability of the nanoparticles to maintain their properties over time. The change of particle size and zeta potential of the optimized PEI-NP group P101-11 and CE-NP group C3-21 is shown in Figure 4.4-4.5. No significant changes were observed in the size and charge of these nanoparticles over time. The optimized PEI-based and CS-based nanoparticles maintained the same properties up to 48 hours. This finding is in line with what Tiyaboonchai[68] reported when loading Amphotericin B, an antifungal drug, with PEI-DS nanoparticles.

The change of entrapment efficiency of peptone was also monitored in triplicate samples over time in anaerobic conditions. The effect of temperature on EE was also tested. PEI/DS/peptone nanoparticle suspensions were placed in an anaerobic chamber at 25 ℃ and 40 ℃ (Figure 4.6 and 4.7). The higher temperature accelerated the release of peptone. The EE of PEI-based NP dropped to 21% after 36 hours at 40 ℃. In contrast, the EE of same nanoparticle stored at 25 ℃ is 34%. After 48 hours at 40 ℃, the EE decreased to 8%. A similar decrease of EE with increasing temperature is also observedon CS-based NP. The EE of CSNP after 36 hours at 25 ℃ and 40 ℃ are 18% and 8.5%, respectively. Significant reduction in EE was observed after 48 hours at 40 ℃, with an EE of 4.6%. Both the PEI-based and the CS-based nanoparticles released more than 70% of the entrapped peptone at 48 hours. The increase in temperature grants the entrapped peptone molecules more kinetic energy and the peptone molecules diffuse through the nanoparticle at a faster rate than the peptone molecules at low temperature. Hence, the EE decreases as the temperature increases.

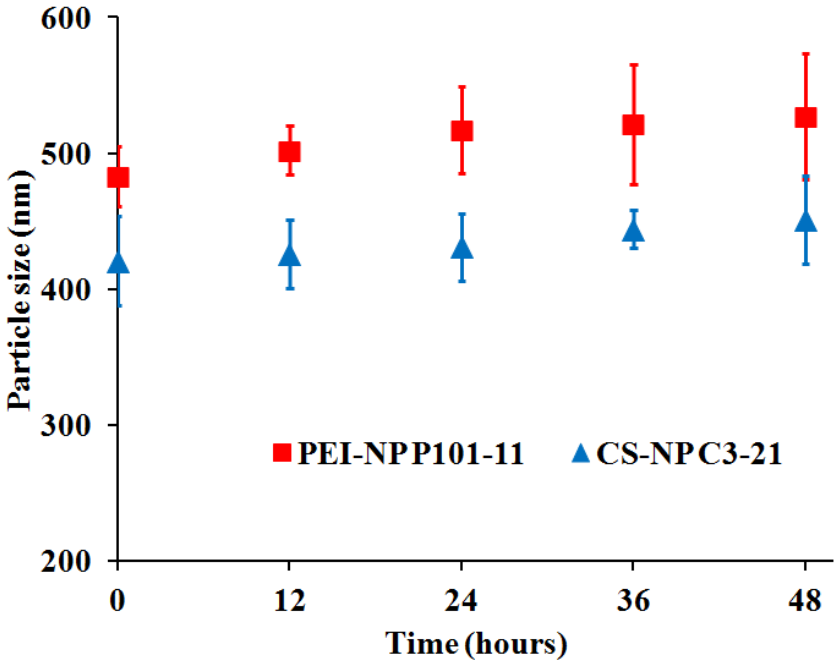

Figure 4.4 The stability of PECNP (particle size) during incubation at 25 ℃

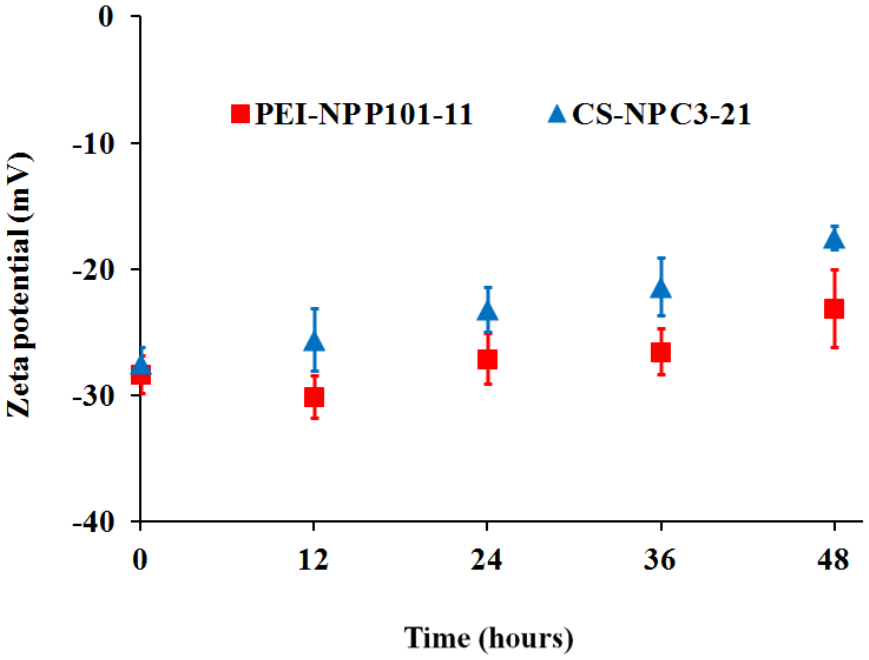

Figure 4.5 The stability of PECNP (zeta potential) during incubation at 25 ℃

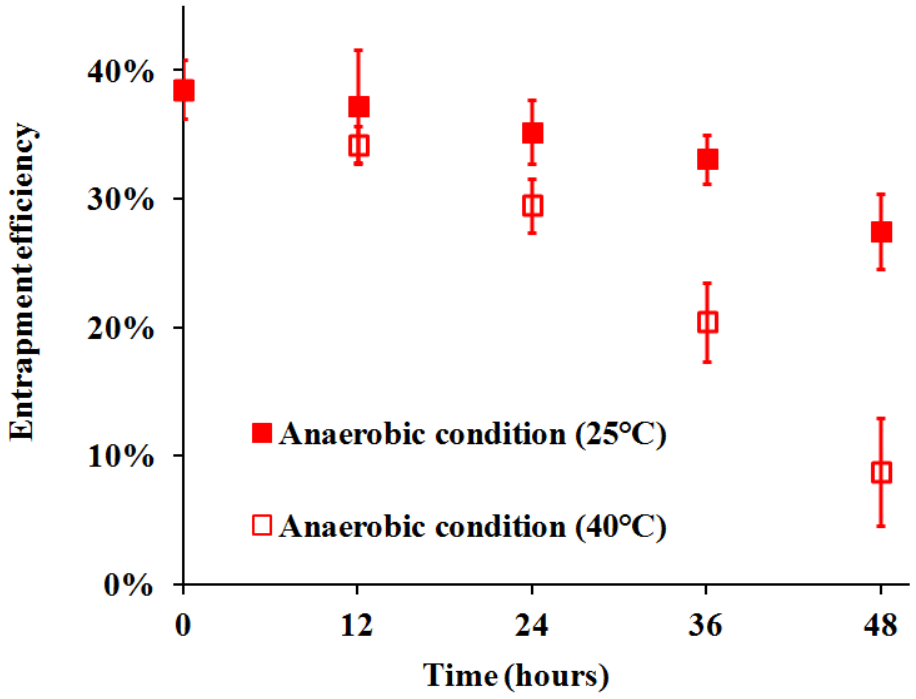

Figure 4.6 The effect of temperature on EE of PEI/DS/peptone NP (P101-11)

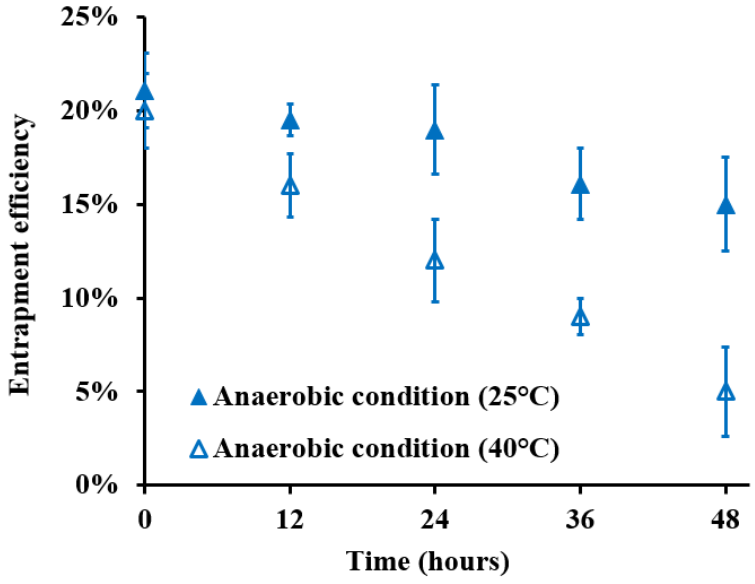

Figure 4.7 The effect of temperature on EE of CS/DS/peptone NP (C3-21)

4.1.5 The effect of PEI pH on the properties of PECNP

Tiyaboonchai[112] indicated that the cationic density of PEI is pH dependent with the charge density increasing with decreasing pH. In our research, nanoparticles prepared with different PEI stock solution pH (7-12) were tested (Figure 4.8, 4.9 and 4.10). Both size and zeta potential increase as the pH increases while entrapment efficiency reaches a maximum value of 38.7% at a PEI solution pH of 10. As discussed previously, the increasing pH results in decreasing charge density, decreasing the interaction between PEI and DS. The particle size becomes bigger as the electrostatic interaction decreases and peptone has a higher potential to interact with DS. Also overall negative surface charge increases since the density of cationic group decreases. If the PEI-DS interaction is too low (PEI pH > 10), the entrapment efficiency of peptone decreases.

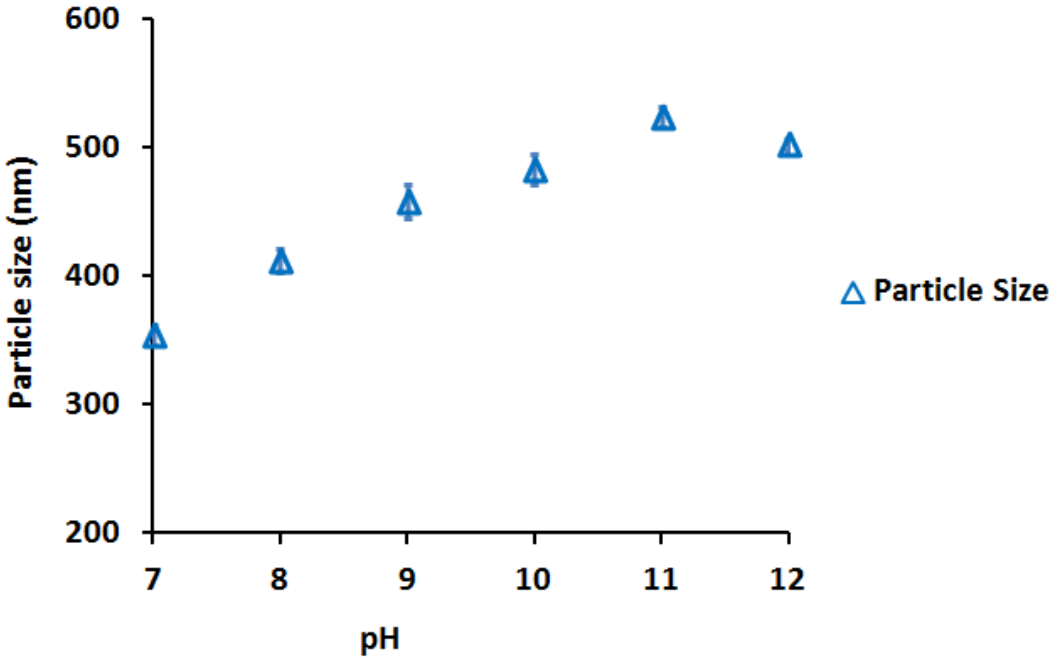

Figure 4.8 The effect of PEI pH on particle size (PEI: peptone mass ratio = 3:10)

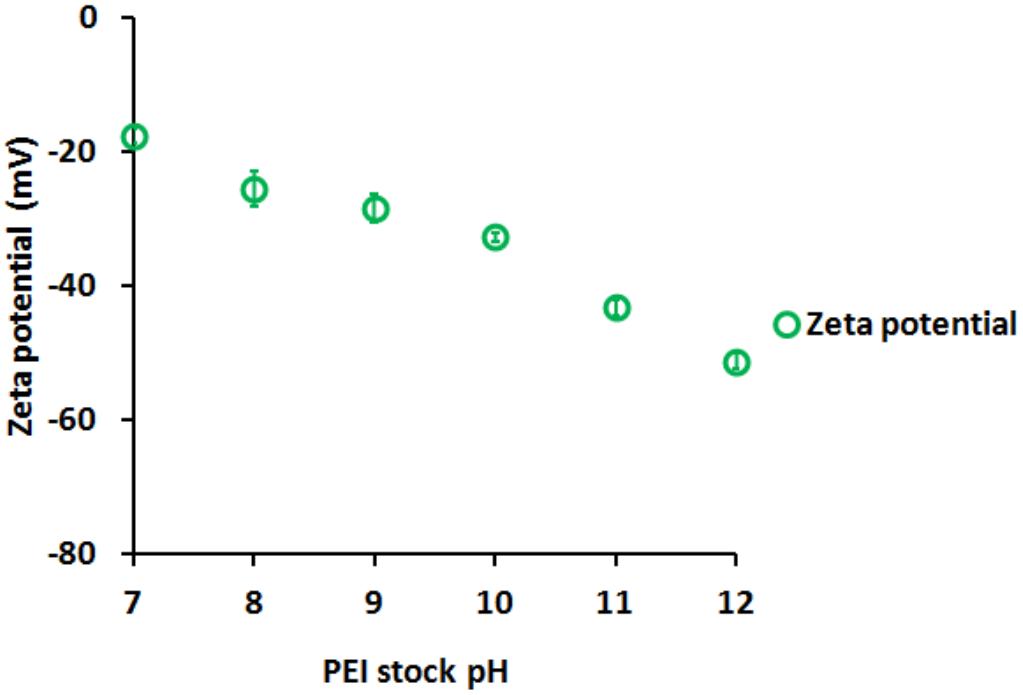

Figure 4.9 The effect of PEI pH on zeta potential (PEI: peptone mass ratio = 3:10)

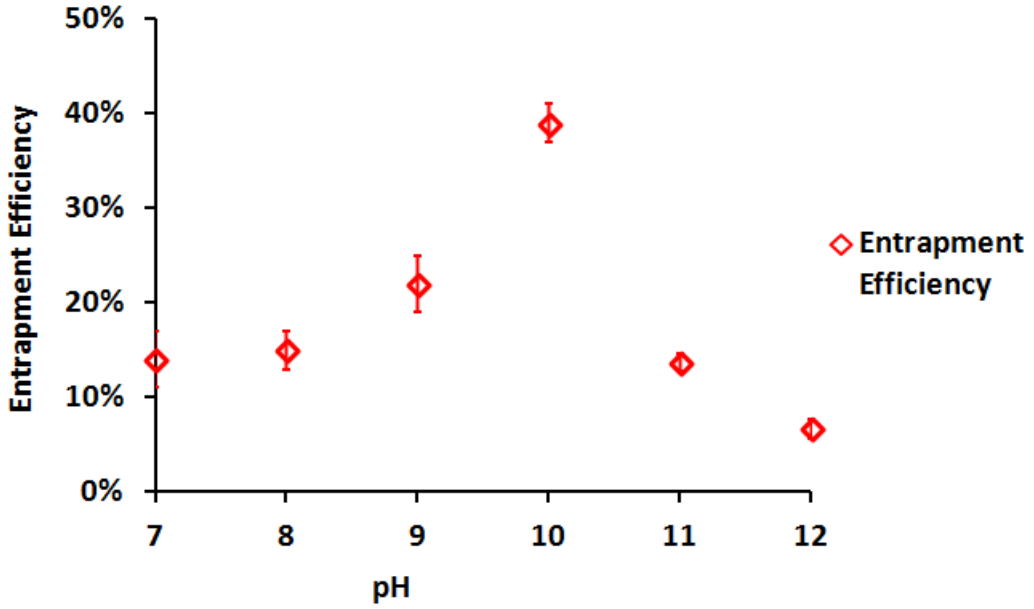

Figure 4.10 The effect of PEI pH on EE (PEI: peptone mass ratio = 3:10)

4.1.6 The effect of salinity on the stability of PECNP

The effect of salinity on the stability of the PECNPs was tested as the nanoparticles may be exposed to high salinity brineduring the MEOR treatment. It was found that the electrostatic attraction between polyelectrolytes could be screened by increasing the salinity, leading to changes and even disappearance of complex.[63]

Synthetic seawater was added to the nanoparticle suspension in a 1:1 ratio. The particle size of the nanoparticle was measured over time to monitor the effect of 50% w/w synthetic sea water on the stability of nanoparticles (Figure 4.11-4.12). The effect of salinity on the release of the peptone from the PECNP was also tested (Figure 4.13-4.14).

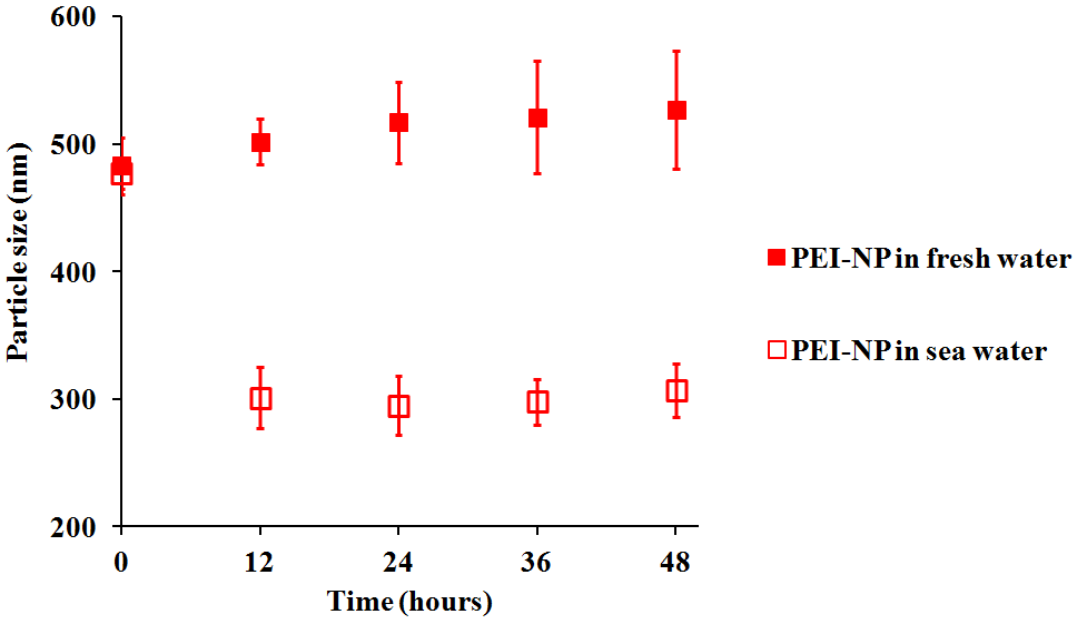

Figure 4.11 The effect of salinity on PEI-NP particle size (P101-11)

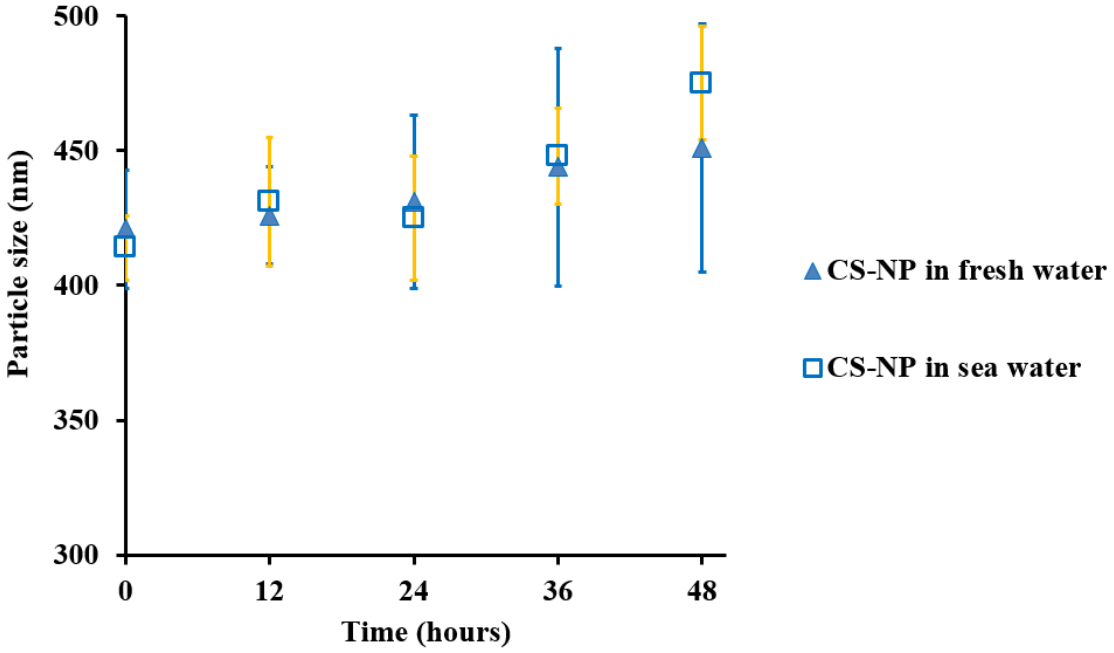

Figure 4.12 The effect of salinity on CS-NP particle size (C3-21)

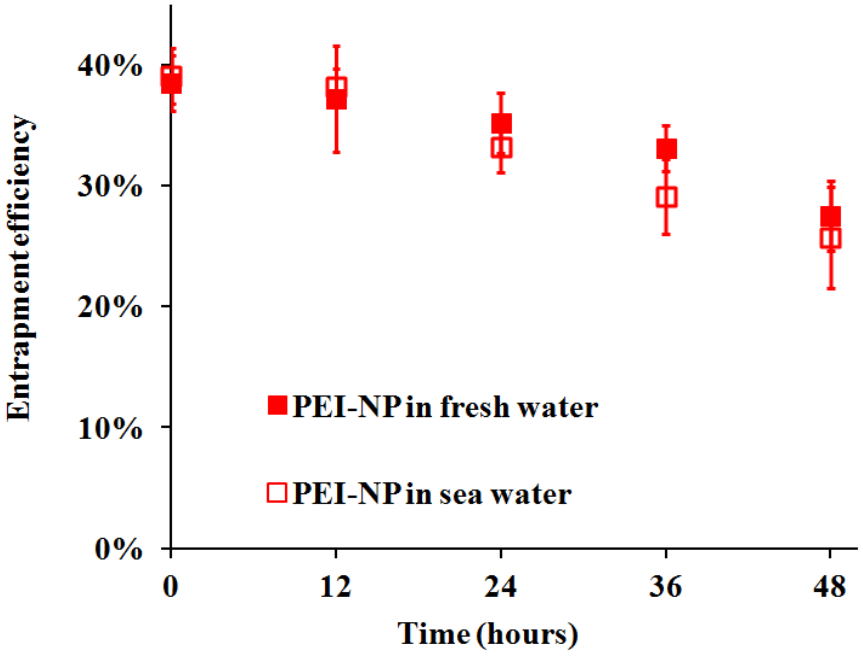

Figure 4.13 The effect of salinity on PEI-NP entrapment efficiency (P101-11)

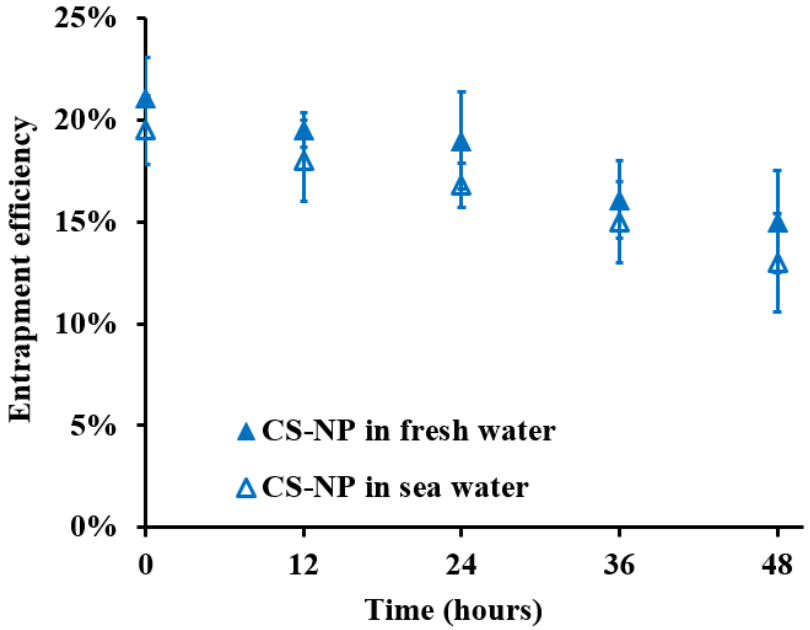

Figure 4.14 The effect of salinity on CS-NP entrapment efficiency (C3-21)

It is observed from Figures 4.11-4.14 that the 50% w/w synthetic sea water (salinity: 17,500 ppm) did not affect the entrapment efficiency of both PEI-NP and CS-NP. The particle size of CS-NP did not change when exposed to an intermediate salinity (17,500ppm) environment, comparing to the range of formation water salinity given by Robertson of 2,000-200,000 ppm.[113] However, the PEI-NP shrinks when synthetic sea water (SSW) is applied. The particle size decreased from approximately 500 nm to 300 nm. Moreover, the particle size of PEI-NP in SSW is stable up to 48 hours. With smaller particle size, the nanoparticle can be delivered into smaller pores to better improve the oil recovery. Therefore, the stability of the PEI-NP is not affected by the addition of salts, but the functionality is enhanced in a high salinity environment.

Dautzenberg and Kriz[114] designed a polyelectrolyte complex with PDADMAC /acrylamide copolymer and polymethacrylate. They gradually increased the salinity after the formation of polyelectrolyte complex. They observed that the particle size of the PEC complex increased when the concentration of NaCl [NaCl] was less than 11.5g/kg, when [NaCl] was higher than 11.5g/kg, a sharp decrease on size occurred. The [NaCl] in our research is 12.5g/kg, which is greater than 11.5g/kg, the observed decrease of particle size agrees with Dautzenberg and Kriz's findings. Zhang *et al.*[115] suggested that in a polyelectrolyte complex system, there is usually a difference in mobile ion concentrations into and out of complex, which result in an osmotic pressure between the complex and the surrounding solution. In order to reduce the osmotic pressure, the complex will swell naturally (dilution of the network charge density). When adding salt into the system, system, the difference between ion concentrations inside and outside of the gel matrix is reduced. Consequently, the swelling of complex decreases with increasing salt

concentration. Therefore, the addition of salts will reduce the particle size of PEC complex.

4.2Toxicity of the polycation and polyanion

The toxicity of PECNP was determined by monitoring the growth of oilfield microbes in aerobic and anaerobic conditions. The microbial growth in the selective media in which polycation/polyanion were added were compared with the ones incubated in complete media (positive control). Microbes were inoculated into three individual samples for each media. Both complete media and selective media incubated without inoculation of microbes were used as negative controls. Toxicity of the nanoparticle may be manifested as delayed growth, lower maximum growth rate and/or a lower maximum population at the stationary phase of the microbial growth curve. Toxicity tests were performed on aerobic and anaerobic oilfield microbes, and the growth curves are shown in Figure 4.15 and 4.16. No growth was observed in the negative controls; the data points of negative controls were omitted from the graph. In both aerobic and anaerobic condition, the microbes incubated with polycation/polyanion in the media have similar growth rates and similar populations at stationary phase to the microbes incubated with complete media.

A summary of the generation times (c) and growth rates (b) obtained from the growth curves in Figure 4.15 and 4.16 is shown in Table 4.9and 4.10. The microbes in the positive control group were incubated with sufficient nutrients and no toxic component was added. If the polyelectrolytes were harmless to the microorganisms, then the growth rate of the experimental treatments should be at least as high as that of the

positive control group. Accordingly, one-tailed t-tests were conducted using Microsoft Excel to determine if the respective means of the *b* and *c* values were significantly smaller in the selective media groups than in the positive control group. The null hypothesis was that means of each the polyelectrolyte treatments was equal to, or greater than the mean of the control treatments:

$$H_O: \mu \geq \mu_o$$

Where H_O represents the null hypothesis, μ is the mean of growth data from each of the selective media groups, and μ_o is the mean of growth data from the positive control group.

The alternative hypothesis (H_A) is that μ is less than μ_o.

$$H_A: \mu < \mu_o$$

One-tailed t-test results are listed in Table 4.11. The results are presented as t-statistic (t_{stat}), number of degrees of freedom (df) and p-value (p). All the p-values are greater than 0.05 and so the null hypothesis is not rejected – there is no statistically significant adverse effect of PEI or DS at these concentrations on the growth rate or generation time. Therefore, with the same generation time (c) and growth rate (b), we can conclude that polyelectrolytes are non-toxic to the oilfield microbes isolated from Wellington oilfield (Wellington, KS) at a concentration required for nutrient delivery. When PEI concentration increased to 6000 ppm, no growth of microorganisms was observed (Figure 4.17). DNA screening of isolated mixed culture and toxicity of

polyelectrolytes to other naturally occurring oilfield microbes should be tested in the future work.

The toxicity of PEI was tested and results are summarized in Figure 4.17. The growth kinetic information and t-test results was listed in Table 4.12 and 4.13. PEI 25K has been reported as a safe siRNA transfection reagent for pancreatic cancer cell lines at a PEI concentration of 1000 ppm.[102] This is similar to what we have observed on aerobic and anaerobic oil field microbes: PEI was non-toxic at concentrations required to deliver nutrients (3000 ppm). When PEI concentration exceeded 3000 ppm in the growth medium, it is observed from the one-tailed t-test results that p values for both growth rate and generation time are less than 0.05. The null hypothesis was rejected, there were significant difference of growth kinetics between selective medium groups and positive control group at these concentrations. When PEI concentration is higher than 3000 ppm, the growth of microbes will be inhibited.

Although DS is generally believed to be an enhancer of colorectal tumors in the rat Walton[116] and Ishioka,[117] the toxicity of DS to microbes has seldom been reported. In this research, the toxicity of DS was tested at different DS concentration from 3000 ppm to 12000 ppm. It was observed that DS was non-toxic to oilfield microbes up to 12000 ppm (Figure 4.16). The *b* and *c* values of microbial growth at different DS concentration can be found in Table 4.12. The calculated p-values for t-tes tare listed in Table 4.13. All the p-values are greater than 0.05. Therefore, the null hypothesis is accepted – there is no significant adverse effect of DS at these concentrations on the growth rate or generation time of microbes.

CS is reported to be non-toxic to mammalian cells since it is basically glucose polymer.[118] Moreover, starch is a common carbon nutrient for different types of bacteria, such as amylolytic bacteria[119] and *Lactobacillus* species.[120] Therefore, CS has the potential to be utilized by the microbes as a carbon nutrient source. The *b* and *c* values of microbial growth at different DS concentration can be found in Table 4.14. The calculated p-values for t-tests are listed in Table 4.15. The null hypothesis is accepted since all the p-values are greater than 0.05. There is no significant adverse effect of CS at a concentration up to 3000 ppm on the growth rate or generation time of microbes.

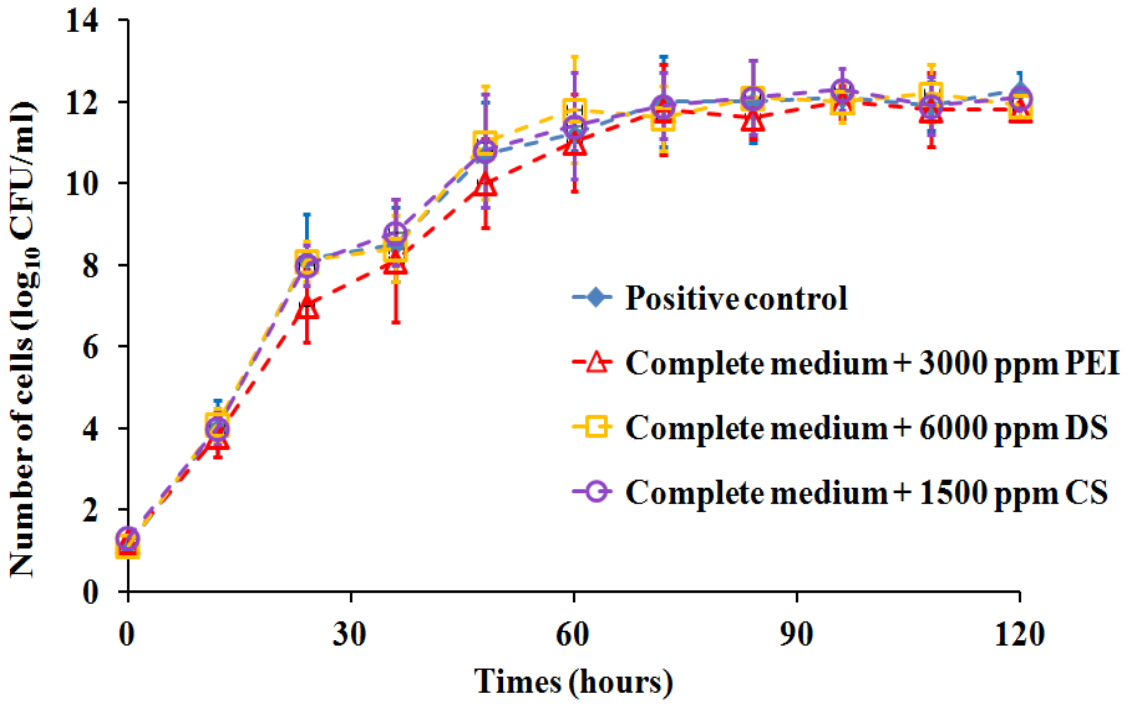

Figure 4.15 The toxicity of PECNP to mixed aerobic oilfield microbes (each point is the mean of three replicates, Error bars = 1 standard deviation)

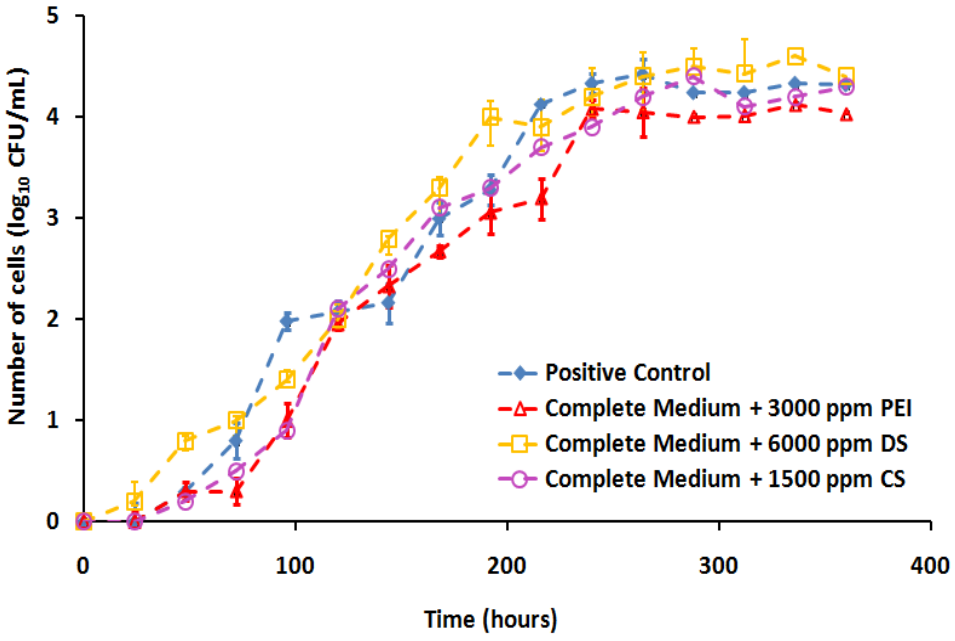

Figure 4.16 The toxicity of PECNP with anaerobic microbes (each point is the mean of three replicates, Error bars = 1 standard deviation)

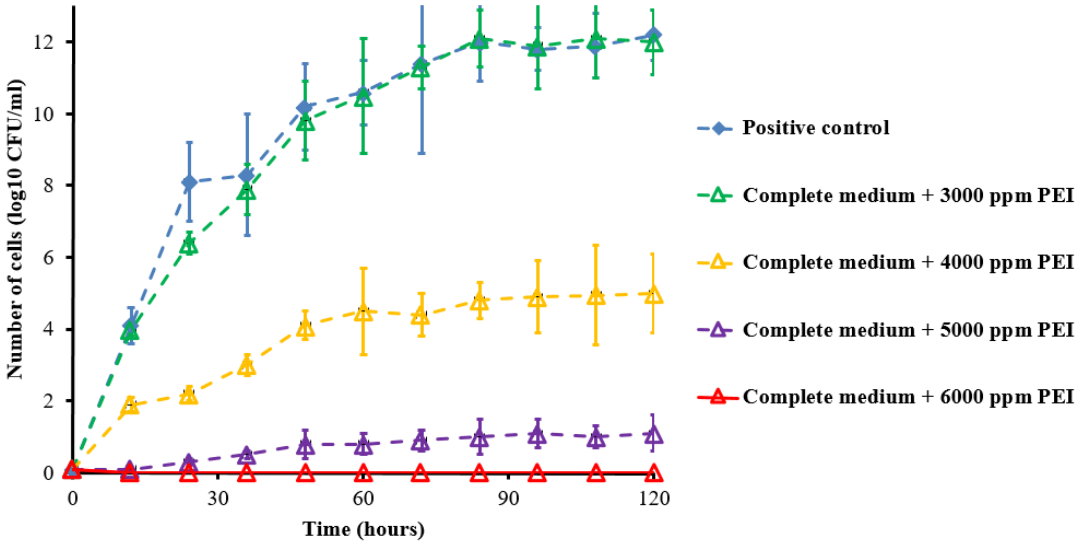

Figure 4.17 The toxicity of PEI at different concentration to aerobic microbes (each point is the mean of three replicates, Error bars = 1 standard deviation)

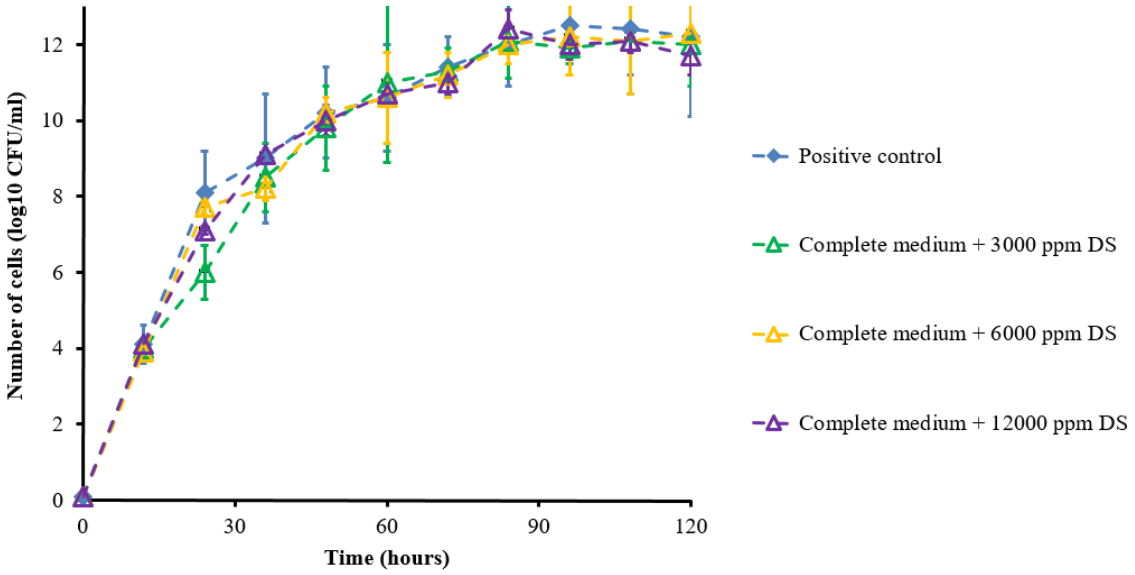

Figure 4.18 The toxicity of DS at different concentration to aerobic microbes (each point is the mean of three replicates, Error bars = 1 standard deviation)

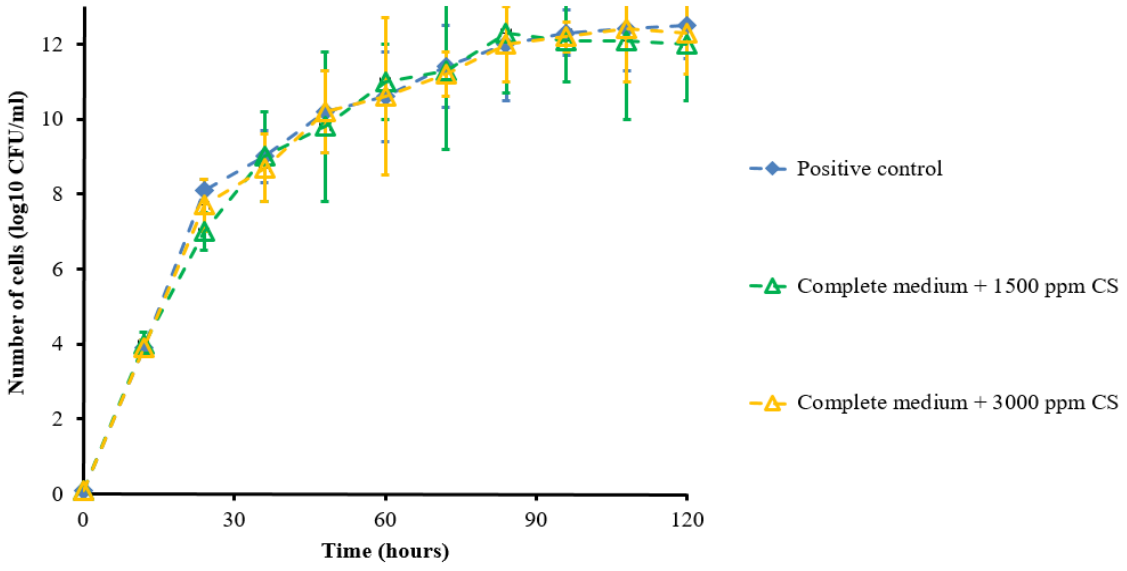

Figure 4.19 The toxicity of CS at different concentration to aerobic microbes (each point is the mean of three replicates, Error bars = 1 standard deviation)

Table 4.9Aerobic cell growth kinetics in peptone media with different polycation or polyanion added (errors were calculated as standard deviation of triplicate samples)

Group	Growth rate (logCFU/hour)	Generation time (min)
Complete medium	0. 71 ± 0.021	120 ± 5
Complete medium + 3000 ppm PEI	0.67 ± 0.045	120 ± 4
Complete medium + 6000 ppm DS	0. 71 ± 0.032	113 ± 8
Complete medium + 1500 ppm CS	0. 72 ± 0.032	117 ± 11

Table 4.10 Anaerobic cell growth kinetics of peptone media with different polycation or polyanion added (errors were calculated as standard deviation of triplicate samples)

Group	Growth rate (logCFU/hour)	Generation time (min)
Complete medium	0.46 ± 0.031	996 ± 10
Complete medium + 3000 ppm PEI	0.42 ± 0.034	978 ± 29
Complete medium + 6000 ppm DS	0.48 ± 0.070	1058 ± 37
Complete medium + 1500 ppm CS	0.45 ± 0.051	970 ± 44

Table 4.11 T-test results for toxicity test of polycations and polyanions (Both *b* and *c* values of aerobic and anaerobic microbes are analyzed)

Microbe type		Growth rate (b)			Generation time (c)		
		d_f	t_{stat}	p	d_f	t_{stat}	p
Aerobic	PEI	4	1.16	0.15	4	0.80	0.50
	DS	4	0.53	0.31	4	1.58	0.09
	CS	4	0.45	0.34	4	1.21	0.15
Anaerobic	PEI	4	1.38	0.12	4	0.76	0.25
	DS	4	0.53	0.31	4	2.06	0.13
	CS	4	0.29	0.39	4	1.04	0.18

Table 4.12 Aerobic cell growth kinetics in peptone media with concentrations (3000 ppm-6000 ppm) of PEI added (errors were calculated as standard deviation of triplicate samples)

Group	Growth rate (logCFU/hour)	Generation time (min)
Complete medium	0. 63 ± 0.053	116 ± 10
Complete medium + 3000 ppm PEI	0.61 ± 0.045	117 ± 12
Complete medium + 4000 ppm PEI	0. 24 ± 0.032	304 ± 28
Complete medium + 5000 ppm PEI	0.04 ± 0.041	1636 ± 77
Complete medium + 6000 ppm CS	No growth	No growth

Table 4.13 T-test results for toxicity test of PEI

PEI concentration	Growth rate (b)			Generation time (c)		
	d_f	t_{stat}	p	d_f	t_{stat}	p
3000 ppm PEI	4	0.77	0.24	4	0.67	0.27
4000 ppm PEI	4	18	2.6×10^{-5}	4	39	1.3×10^{-6}
5000 ppm PEI	4	45	6.8×10^{-7}	4	85	8.8×10^{-8}
6000 ppm PEI	No growth					

Table 4.14 Aerobic cell growth kinetics in peptone media with concentrations (3000 ppm-12000 ppm) of DS added

Group	Growth rate (logCFU/hour)	Generation time (min)
Complete medium	0.64 ± 0.031	115 ± 13
Complete medium + 3000 ppm DS	0.61 ± 0.052	116 ± 17
Complete medium + 6000 ppm DS	0.62 ± 0.047	117 ± 14
Complete medium + 12000 ppm DS	0.62 ± 0.022	120 ± 9

Table 4.15 T-test results for toxicity test of DS

DSconcentration	Growth rate (b)			Generation time (c)		
	d_f	t_{stat}	p	d_f	t_{stat}	p
3000 ppm DS	4	1.85	0.14	4	0.78	0.24
6000 ppm DS	4	1.56	0.11	4	0.62	0.28
12000 ppm DS	4	1.04	0.17	4	0.75	0.19

4.3 Polyelectrolytes as sole nutrient source

Since the CS, DS and PEI were demonstrated to be non-toxic to the oilfield microbes at concentrations required to deliver nutrients, the possibility of using those components of PECNP as the nutrient source was also investigated. In this study, we replaced the carbon source dextrose in the peptone medium with DS or CS (same carbon concentration), and nitrogen source peptone with PEI (same nitrogen concentration) to compare the growth of microbes with the positive control group incubated in complete media. Triplicate samples were prepared for each media. The calculated b and c values are listed in Table 4.16 - 4.17 and Figure 4.20-4.21. The growth rate decreases approximately 50% and the generation time increases when CS is applied as sole carbon source for aerobic microbes. Similar results are obserevd when DS is used as sole carbon nutrient for anaerobic microbes. However, the maximum microbial population at the stationary phase is not affected, which indicates that the microbial growth is inhibited, but not arrested. The delay could be due to differences in the ability of the microbe to metabolize the polyelectrolyte. When PEI was applied as sole nitrogen source to the aerobic oilfield microbes, no growth was observed, which suggests the isolated oilfield microbes cannot uptake PEI as sole nitrogen source.

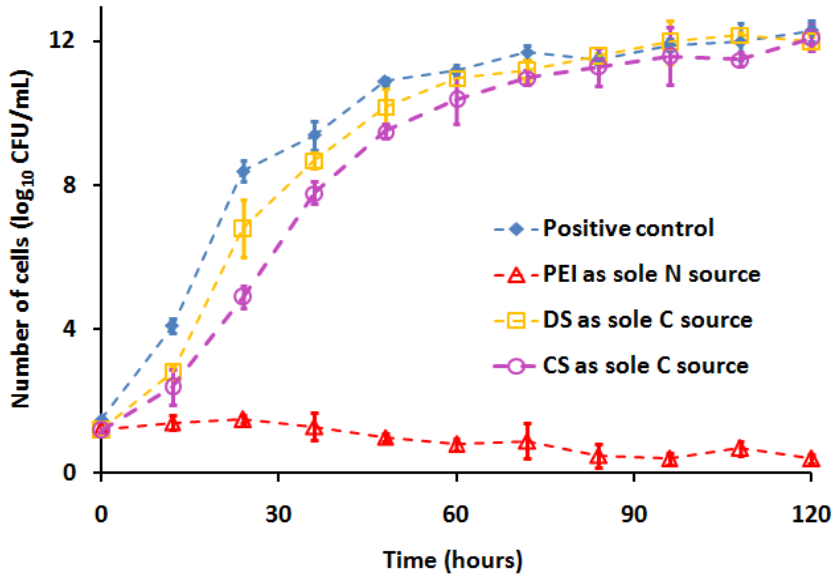

Figure 4.20 PEI, DS, CS as sole N or C source for aerobic oilfield microbes (three individual samples were prepared for each medium)

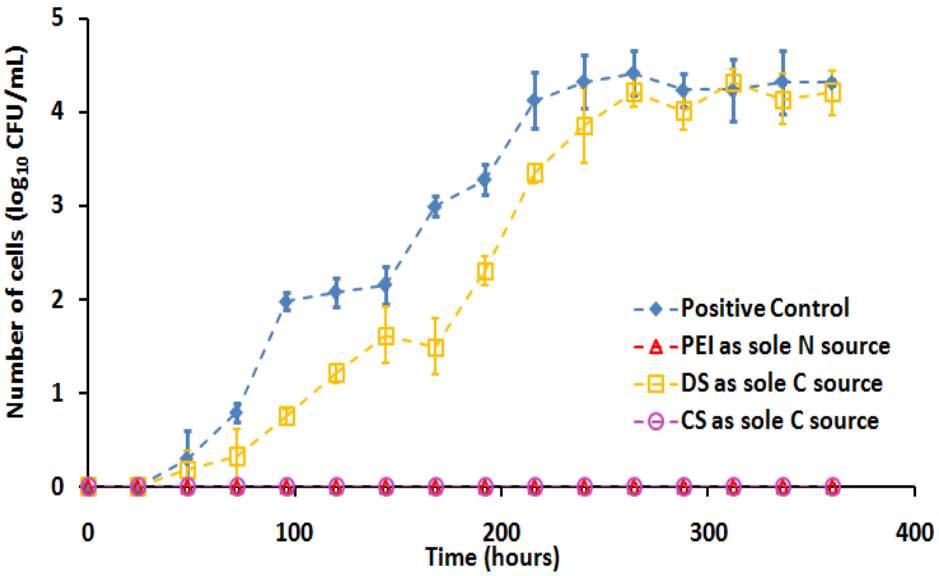

Figure 4.21 PEI, DS, CS as sole N or C source for anaerobic oilfield microbes (three individual samples were prepared for each medium)

Table 4.16 Aerobic cell growth kinetics in new nutrient media

Group	Growth rate (logCFU/hour)	Generation time (min)
Complete medium	0.71 ± 0.021	121 ± 2
PEI medium	No growth	No growth
DS medium	0.55 ± 0.063	120 ± 15
CS medium	0.47 ± 0.042	127 ±38

Table 4.17 Anaerobic cell growth kinetics in new nutrient media

Group	Growth rate (logCFU/hour)	Generation time (min)
Complete medium	0.45 ± 0.031	996 ± 10
PEI medium	No growth	No growth
DS medium	0.27 ± 0.067	1125 ± 58
CS medium	No growth	No growth

The results show that DS has the potential to be used as a carbon source for both aerobic and anaerobic oilfield microbes. CS can only be used as sole carbon source for aerobic oilfield microbes. PEI is not a capable nitrogen provider for either aerobic or anaerobic oilfield microbes.

4.4 Delayed growth test

The growth of both aerobic and anaerobic under media mixed with polyelectrolyte suspension were tested to evaluate the potential impact of PECNP on microbial growth. For the aerobic microbial growth test, two treatments were compared with positive control group (complete media). In the first group, microbe sonly used entrapped peptone in the polyelectrolyte suspension as sole nitrogen sources. No other nitrogen source was added to the incubation media. For the second group microbes can only utilize peptone and DS released from polyelectrolyte suspension as sole nitrogen and carbon source. No other nitrogen nor carbon source was added in the incubation media.

During the anaerobic test, PEI-NP was tested for microbial growth when nitrogen source was entrapped or both nitrogen and carbon source were entrapped inside the nanoparticles. CS-NP was only tested for the controlled release of nitrogen source since anaerobic oilfield mixture culture cannot use CS or DS as carbon nutrient (Section 4.3). The microbial growth curves of each group are shown in Figures 4.22 to 4.25. The calculated *b* and *c* values of delayed growth test are shown in Tables 4.18 and 4.19. The t-tests results for both PEI and CS NP were listed in Table 4.22 and 4.23. It is observed from the T-test data that all the p-values are smaller than 0.05. Therefore, the null hypothesis of no significant differences between positive control group and groups incubated with PECNP was rejected. There is statistical difference in between the growth of microbes with/without PECNP.

The microbial growth was delayed by applying nutrients in a polyelectrolyte nanoparticle system. A 10^2 magnitude decrease of microbial number for the first 72

hours was observed compared to groups incubated in the media with entrapped nutrients. The growth rates of both aerobic and anaerobic microbes incubated with both PEI-NP or CS-NP are approximately 1/3 to 1/2 of the positive control growth rate when the nutrients are entrapped inside the nanoparticle. The maximum aerobic microbial growth (stationary phase) was delayed by approximately 140 hours (6 days) when N source was entrapped, and 210 hours (9 days) when both C and N sources were entrapped, while the anaerobic microbial growth was delayed for 4 days (N entrapped) and 6 days (N and C entrapped).The delay of each treatment is calculated by the equation below:

$$Delay = t_{treatment} - t_p \qquad \text{Equation 4.1}$$

Where $t_{treatment}$ is the time for the NP treated group to reach stationary phase, t_p is the time for positive control group to reach stationary phase.

With the observed delay of growth, we can conclude that the nitrogen source peptone and carbon source DS were successfully entrapped by the nanoparticle, which prevented them from being taken up by the microbes in the first 4 to 5 days. The distance the nanoparticles could travel in the reservoir during this 4 days period was estimated using the pilot data published by Stephens and Brown.[121] In their research, the field chosen for pilot test was the North Blowhorn Creek Oil Unit which is located in Lamar County, Alabama. The injection rate for MEOR project was 7980 ft^3/day, the average net pay thickness was 12 ft. It is assumed that the flooded area by injection of PECNP is a perfect circle. The distance of PECNP travels in 4 days was calculated by the following equation:

$$L = \sqrt{\frac{4 \times I_j}{\pi h}} \qquad \text{Equation 4.2}$$

Where L is the distance traveled by the PECNP (ft), Ij is the injection rate (ft^3/day), and h is the net pay thickness.

It is calculated that the distance for PECNP travels in 4 days will be 58 ft. Therefore, 4 days is enough for the nanoparticles flow pass the near wellbore region in the reservoir. The observation agrees well with the hypothesis that nanoparticle systems have the potential to slow the release of nutrients and delay growth of oilfield microbes until the nutrients have propagated beyond the near wellbore region.

However, ideally there should be no microbial growth until the nanoparticle suspension has been transported away from the wellbore. On the NP treated groups in this test, the growth of microbes at the early time (0-24 hours) is inhibited but not arrested. That is because there is free peptone and DS in the PEI-NP system, the microbes will uptake the unentrapped nutrients during the early time. As in the case of CS-NP, although there is less than 5% of the free peptone in the system, the release of peptone in the CS-NP is faster than that of PEI-NP. As discussed in the Section 4.1.4, about 30% of entrapped peptone is released from CS-NP in the first 24 hours compare to 10% entrapped peptone in PEI-NP system. Further study on more stable and resuspendable nanoparticle is required to improve the function of PECNP system.

The growth of microbes and the release concentration of peptone of different nanoparticles were also plotted in the same graph to analyze the relationship between peptone release and number of microbes. The results are shown in Figures 4. 26 and 4.27.

In general, the number of microbes increased with increasing concentration of released peptone. It was also observed that when a sharp increase occurred in the released peptone concentration, there was also a sharp increase of microbial number in the next 12 hours (48 hour and 60 hour points in Figure 4.26 and 12 hour and 24 hour points in Figure 4.28). A possible explanation is that microbes requires time to uptake the released peptone and reproduce themselves. That's why there is a delay in the number of microbes when more nutrient is released from the nanoparticle.

Moreover, in the first 24 hours, the concentration of released peptone from PEI nanoparticle is significantly lower than that from CS nanoparticle. However, there is not much difference in the number of microbes. The free peptone in the PEI nanoparticle system might be the reason for this phenomenon. There are two sources of nitrogen nutrients in the PEINP system: one is the peptone entrapped in the PEINP, the other one is the free peptone. In the first 24 hours, microbes can uptake both released peptone and free peptone to maintain a similar number of cells as the CSNP group. Therefore, the CSNP plot (Figure 4.27) can more accurately represents the relationship between released peptone and number of microbes since the free peptone in the CSNP system is as low as 0.1% of initial peptone added into the system,

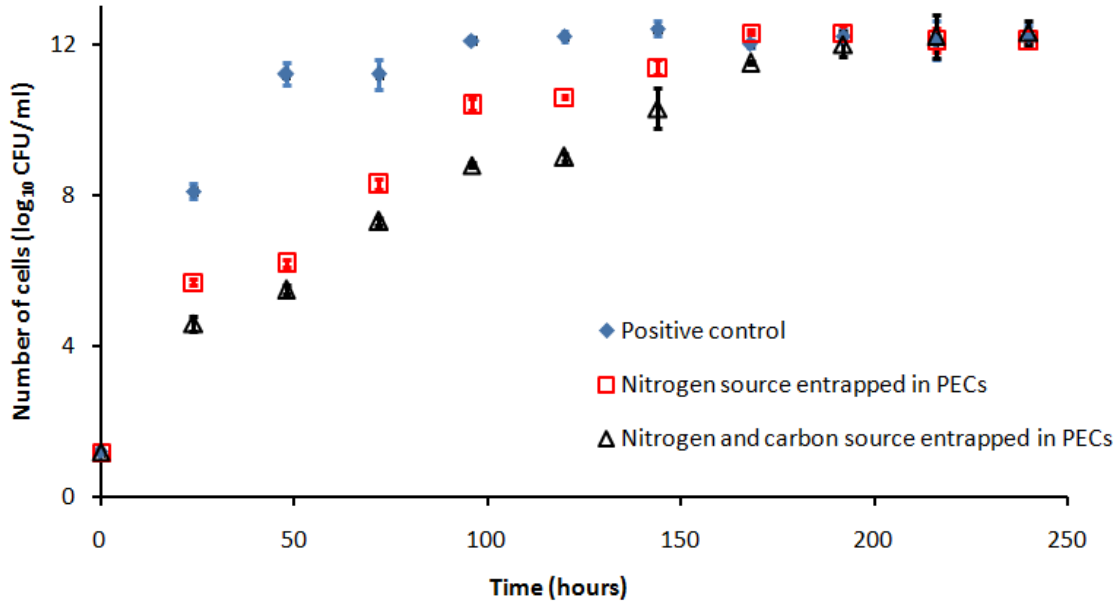

Figure 4.22 The delayed growth test of PEI-NP with aerobic microbes

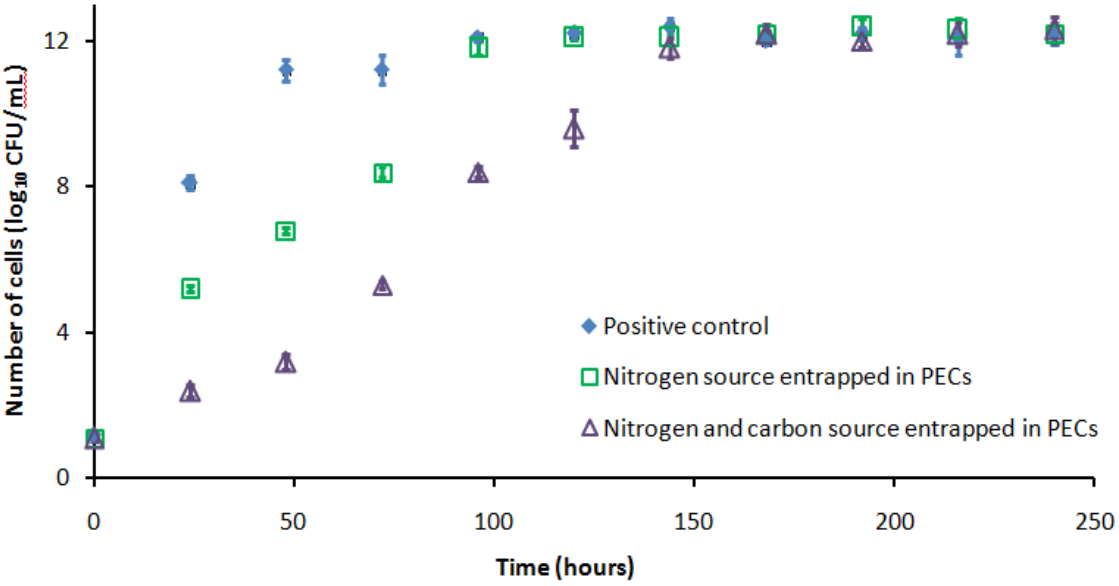

Figure 4.23 The delayed growth test of CS-NP with aerobic microbes

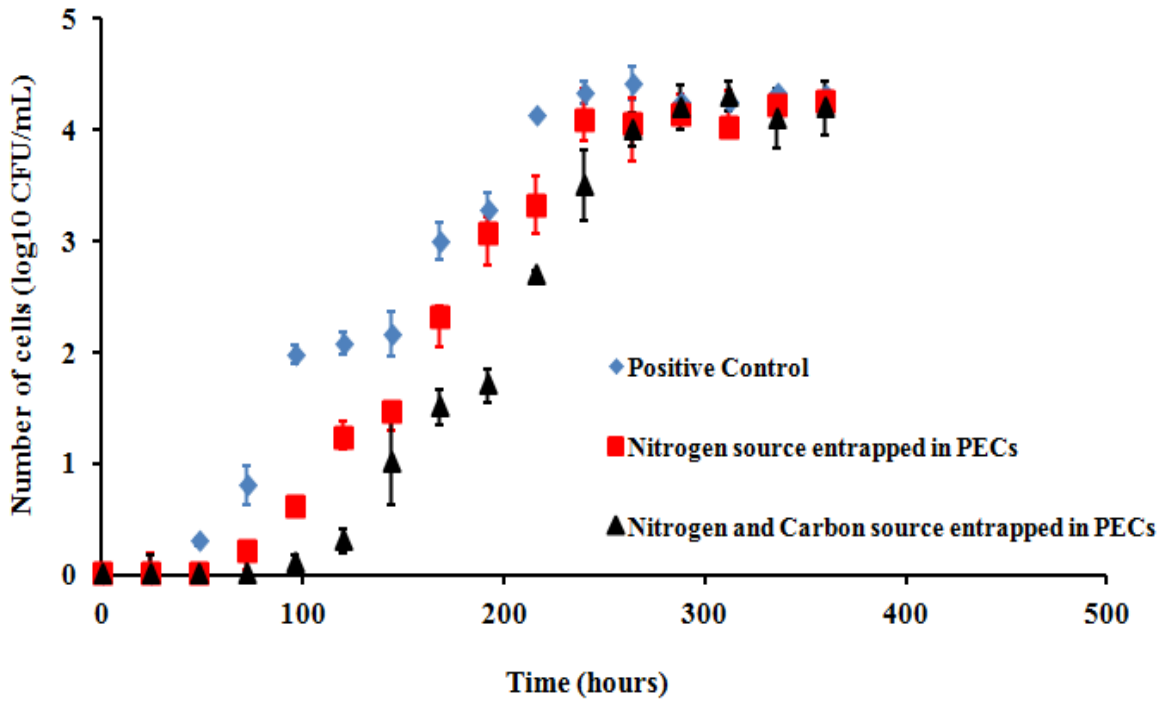

Figure 4.24 The delayed growth test of PEI-NP with anaerobic microbes

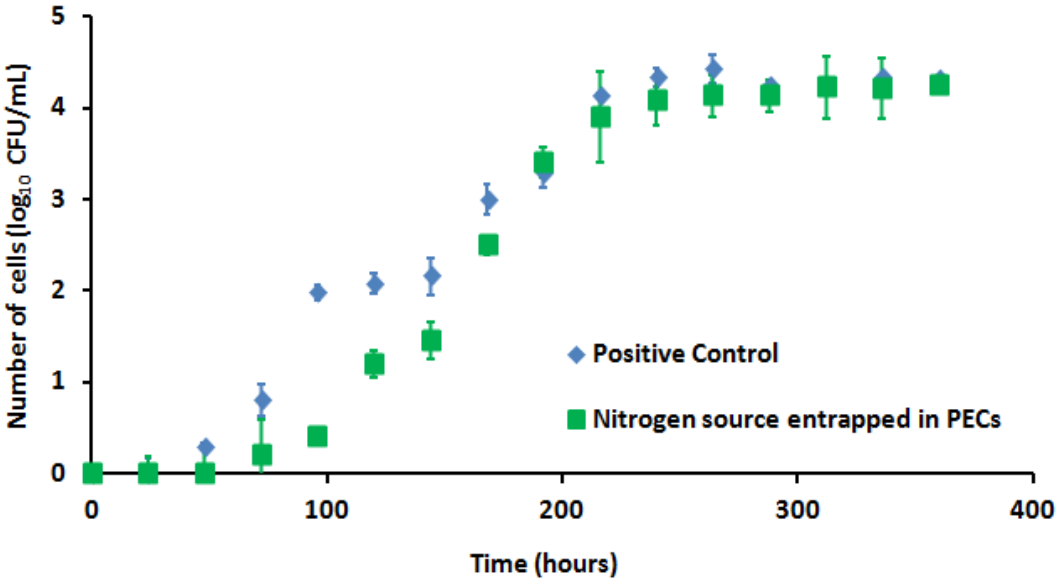

Figure 4.25 The delayed growth test of CS-NP with anaerobic microbes

Table 4.18 Aerobic cell growth kinetics of delayed growth tests

	Group	Growth rate, b (log_{10}CFU/hour)	Generation time, c (min)
PEI/DS/peptone NP	Positive Control	0.73	119
	N source entrapped	0.45	139
	N,C source entrapped	0.41	152
CS/DS/peptone NP	Positive Control	0.73	119
	N source entrapped	0.47	134
	N,C source entrapped	0.41	173

Table 4.19 Anaerobic cell growth kinetics of delayed growth tests (NA: Not applied)

	Group	Growth rate, b (log_{10}CFU/hour)	Generation time, c (min)
PEI/DS/peptone NP	Positive Control	0.41	1041
	N source entrapped	0.27	1148
	N,C source entrapped	0.23	1214
CS/DS/peptone NP	Positive Control	0.41	1041
	N source entrapped	0.33	1127
	N,C source entrapped	NA	NA

Table 4.20 T-test results for aerobic delayed growth test (Both b and c values of microbes incubated with PEINP and CSNP are analyzed)

Microbe type		Growth rate (b)			Generation time (c)		
		d_f	t_{stat}	P	d_f	t_{stat}	p
PEI NP	N entrapped	4	15.1	5.5×10^{-5}	4	1.65	0.01
	N&C entrapped	4	8.15	7.1×10^{-5}	4	5.45	1.5×10^{-3}
CS NP	N entrapped	4	10.21	3.8×10^{-5}	4	1.76	0.02
	N&C entrapped	4	5.57	6.5×10^{-5}	4	9.04	4.7×10^{-3}

Table 4.21 T-test results for anaerobic delayed growth test (Both b and c values of microbes incubated with PEINP and CSNP are analyzed)

Microbe type		Growth rate (b)			Generation time (c)		
		d_f	t_{stat}	P	d_f	t_{stat}	p
PEI NP	N entrapped	4	6.72	1.2×10^{-3}	4	2.85	0.02
	N&C entrapped	4	10.13	5.6×10^{-3}	4	5.87	3.3×10^{-3}
CS NP	N entrapped	4	5.21	1.4×10^{-3}	4	3.72	0.02
	N&C entrapped	4	8.86	2.7×10^{-3}	4	7.41	5.1×10^{-3}

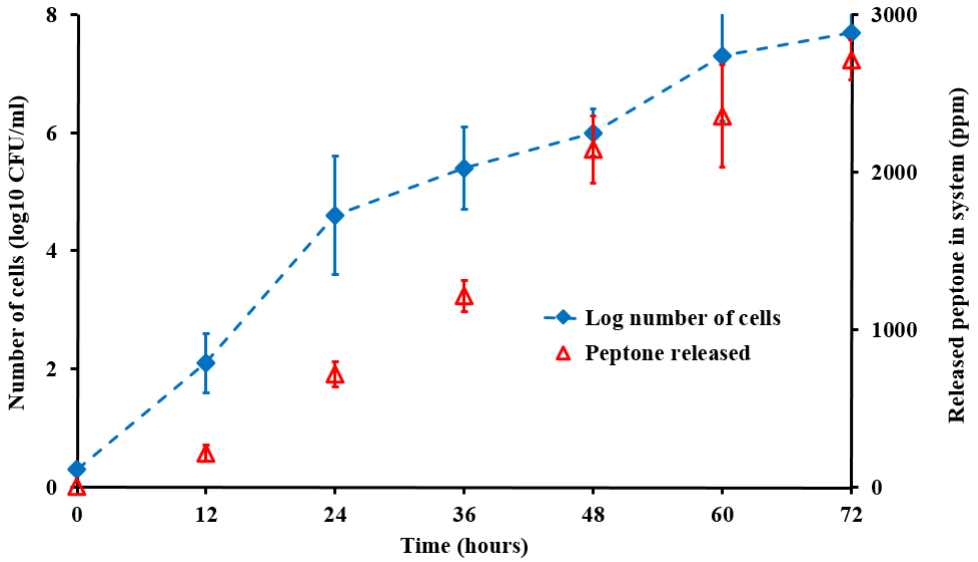

Figure 4.26 The relationship between peptone release concentration and microbial growth of microbes incubated with PEI nanoparticles

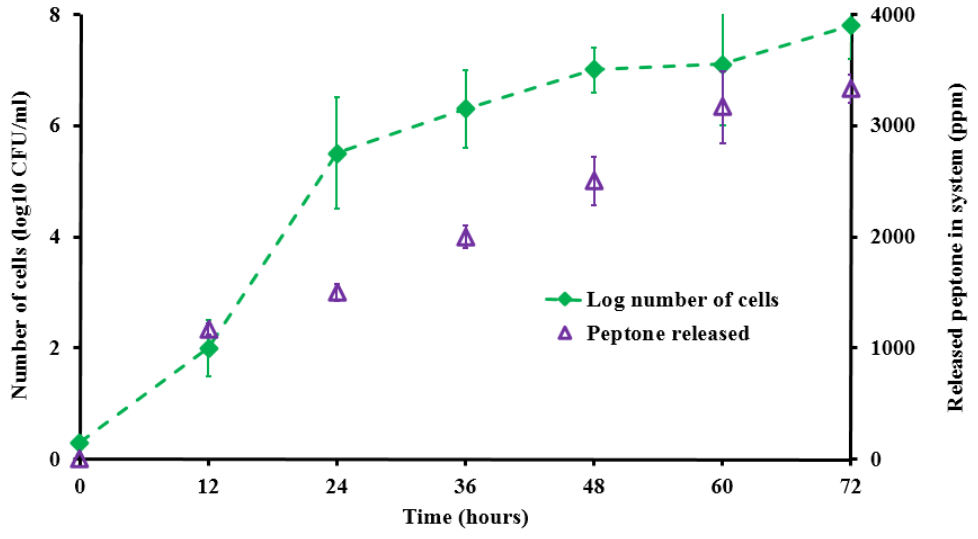

Figure 4.27 The relationship between peptone release concentration and microbial growth of microbes incubated with CS nanoparticle

4.5 Sand pack tests

Because the nanoparticle systems are designed for oilfield application purposes, a retention test is necessary to identify whether polyelectrolyte is absorbed on the rock surface or retained in pore throats[122,123] during the injection in the porous media. Low retention of nanoparticle is preferred to assure the delivery of nutrients far away from the near-wellbore region.

The results of sandpack tests are shown in Figures 4.28 to 4.31. Both PEI-NP and CS-NP were tested for the retention in the Berea sand and Ottawa sand by modified UV analysis and modified Bradford assay. A tracer test was conducted after the preparation of the sand pack to calculate the pore volume. Pore volume was calculated by comparing the area under the curve up to 1 PV and above the curve from 1 PV to C/Co = 1, if the areas are equal, the suspected 1 PV point is correct. All the calculated pore volumes are shown in Figures 4.28 to 4.31. The calculated retention and recovery of the nanoparticles can be found in Table 4.22.

Retention of peptone and nitrogen was almost 25 times higher in Berea than in Ottawa sand. Berea sand contains more clay than the Ottawa sand. The retention increases as the clay content increases. In Berea sand, the retention of nitrogen in CS-NP is as high as 526 μg/g sand, and the recovery of NP is low at about 50%. The retention of PEC nanoparticle is seldom reported. However, the retention of metallic nanoparticle is well studied.[122,124,125] Compared to the retention of silver (Ag) nanoparticles (~100,000 μg/g sand) reported by Hoppe[122], the retention of nutrient delivery nanoparticle in our research is approximately 200 times lower . Although both PECNP in our research and

Ag NP in Hoppe's experiments have similar zeta potential, -38 mV and -40 mV, respectively. The size of Ag NP is approximately 17 times smaller than PECNP with an average particle size of 30 nm. When the nanoparticle is 30 nm or smaller, they will have a size-dependent crystallinity that gives them properties drastically different from the nanoparticle with larger size.[126] Moreover, The retention of Ag NP is also related to dissolution process. The Ag NP dissolution could release Ag^+ into soil, which increases the adsorption of negatively charged Ag NP on soil. Therefore, the Ag NP data is less informative to study the retention of PECNP. More information is required to compare the retention of PECNP in our research to other polyelectrolyte nanoparticles.

Similarly, the recovery data of PECNP in porous media is almost nonexistent. The recovery of silica nanoparticle is extensively studied. Li and Cathles reported a 75% recovery of silica nanoparticle in porous media with 5.85 g/kg NaCl solution.[123] The particle size (300 to 500 nm) and zeta potential (-20 to -30 mV) of the published silica nanoparticle is similar to the PECNP in our research which makes the comparison more informative. The recovery of both peptone and nitrogen in our research is low compared to their study. However, they also mentioned that the recovery of the nanoparticles decreased as the concentration of NaCl increased. Synthetic sea water was chosen as a representative injection brine for this proof-of-concept study. The SSW used in our study contains approximately three times more NaCl than that of the study of Li and Cathles. The lower recovery of peptone in the porous media may be due to the higher NaCl concentration comparing to Li and Cathles' silica NP.

Although, as discussed in the beginning of this section, ideally no retention is preferred while the nanoparticle penetrating the porous media. In real cases, retention

always exists.[122] As the salinity and clay content increases in the porous media, the retention increases. Compared to the retention of published nanoparticles[122,123,127,128], the retention of our nanoparticles is low, especially in a saline environment. Many of the published nanoparticles have a retention higher than 1000 μg/g sand. In general, both PEI-NP and CS-NP designed in this research have the potential of application in the EOR projects for their relatively low retention and acceptable recovery in high salinity brine.

To further decrease the retention of the nanoparticle system, more studies on surface properties of both nanoparticles and porous media are required.[128]

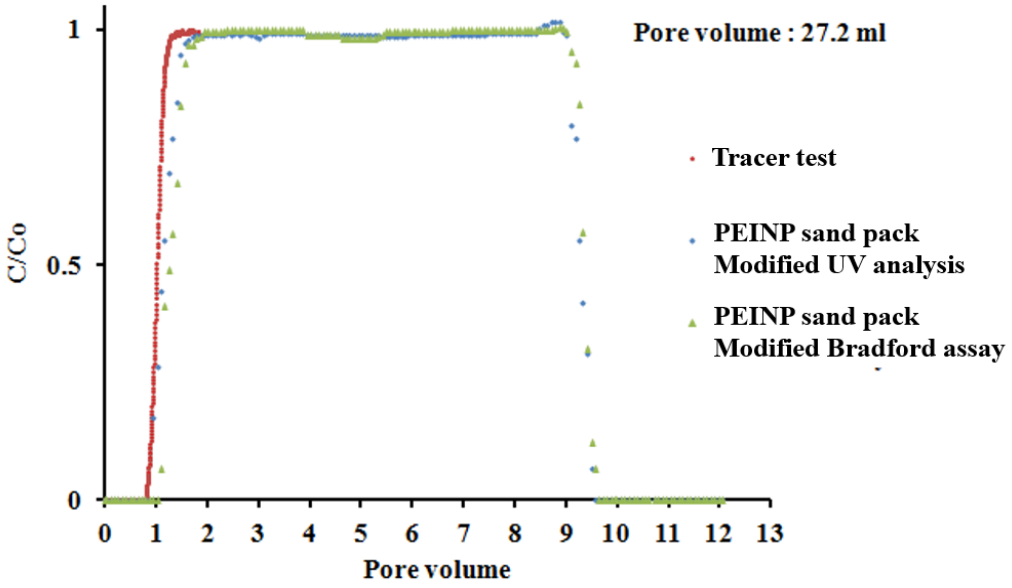

Figure 4.28 The retention test of PEI-NP in Ottawa sand

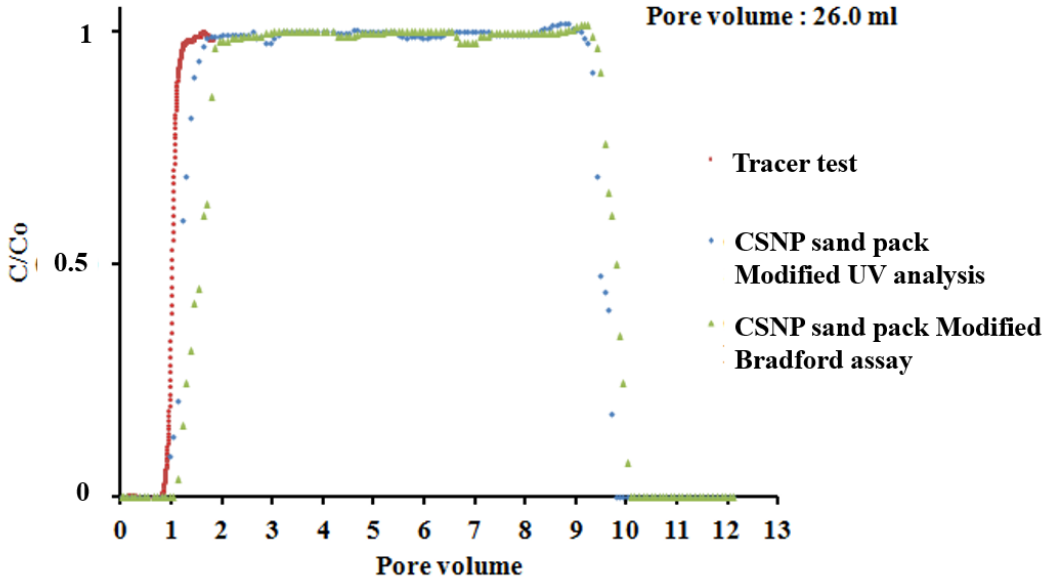

Figure 4.29 The retention test of CS-NP in Ottawa sand

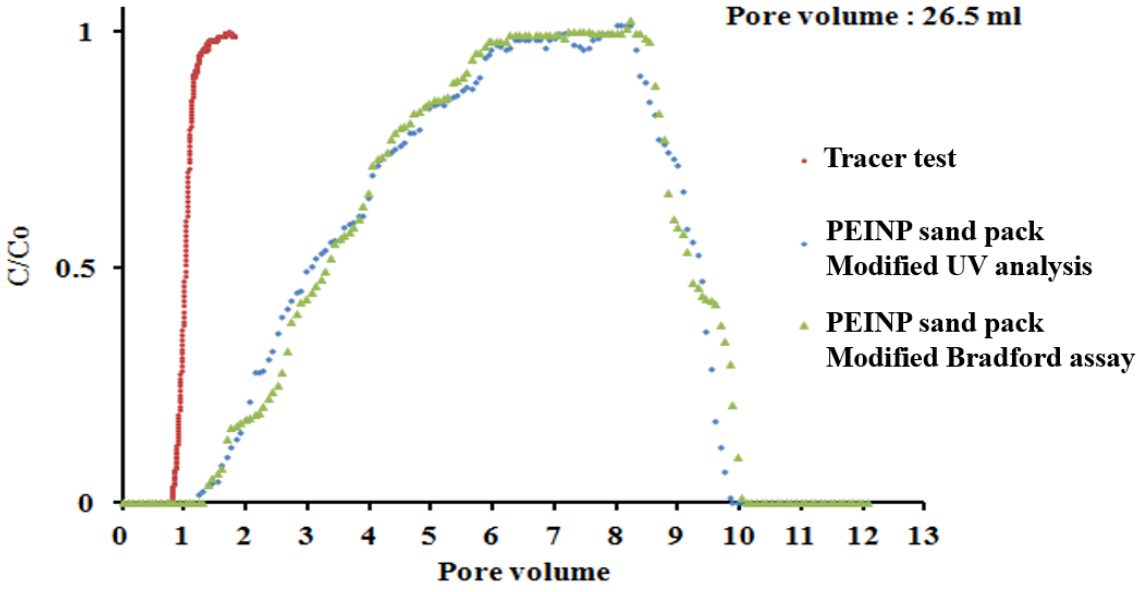

Figure 4.30 The retention test of PEI-NP in Berea sand

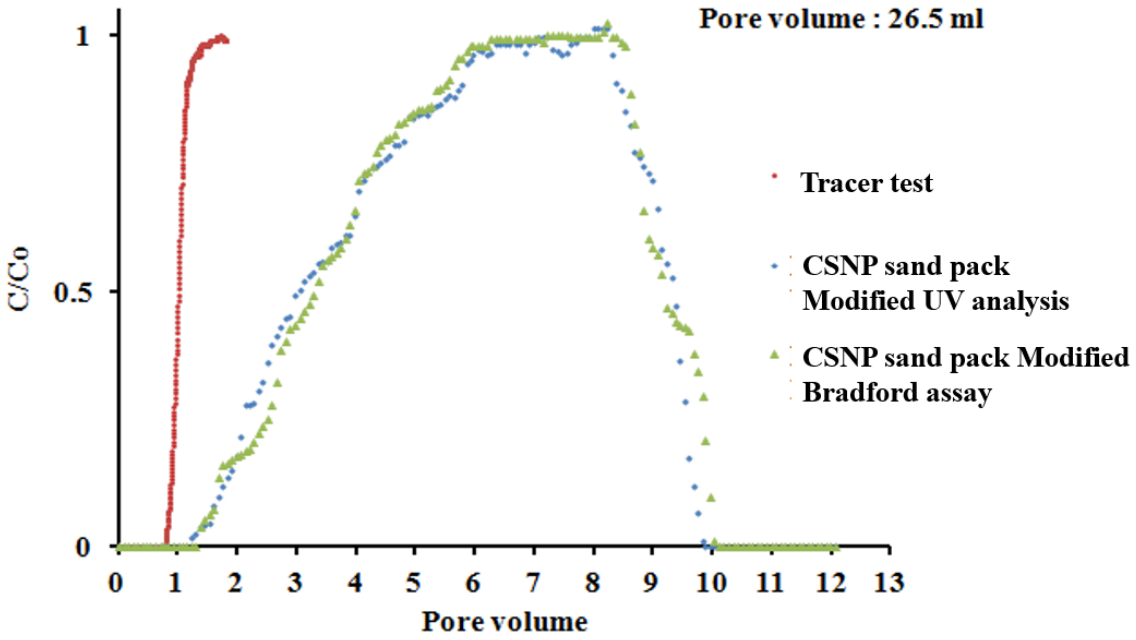

Figure 4.31 The retention test of CS-NP in Berea sand

Table 4.22 The retention and recovery of NP in different sand pack

	Group	Retention (μg/g sand)	NP recovery
Ottawa sand	Peptone in PEI-NP	10.1	90.5%
	Peptone in CS-NP	6.5	93.2%
	Nitrogen in PEI-NP	22.9	92.7%
	Nitrogen in CS-NP	15.1	95.1%
Berea sand	Peptone in PEI-NP	214.0	47.8%
	Peptone in CS-NP	230.2	51.2%
	Nitrogen in PEI-NP	488.9	48.9%
	Nitrogen in CS-NP	526.2	55.2%

5 Conclusion

In this work, polyelectrolyte complexes were formed using oppositely charged polyelectrolytes and a third component, nutrient (either ammonium or peptone).The entrapment of ammonium in the PEI-DS nanoparticle complex was proven unsuccessful as the size and zeta potential of ammonium nanoparticle increased more than 20% in 5 hours, and the entrapment efficiency dropped from approximately 50% to 14% in 3 hours. NH_4^+ is difficult to encapsulate because of its low molecular weight compared to protein and low electric charge compared to chromium. A nitrogen source with higher molecular weight and higher charge density was required to form PEC nanoparticles.

Peptone was used as a nitrogen source to replace ammonium in the nanoparticle system. Stable peptone-loaded PEC nanoparticles (500 nm diameter) can be prepared with different formulations which vary in PEI: peptone ratio and order of addition. PEI stock pH is important in the optimization of PECNP entrapment efficiency. A maximum EE of 38.6% was achieved at PEI pH = 10, PEI: peptone: DS mass ratio is 3:10:10, addition order DS-peptone-PEI (Recipe P101-11).

Resuspendable CS/peptone/DS nanoparticle was then developed to reduce the free peptone in the system. CS-NP was found to be a better delivery system for the nutrient propagation in MEOR as the resuspension process eliminated most of the free nutrients in the system. The free peptone concentration was reduced to less than 0.5% after resuspension with CS: peptone ratio of 5:3, and addition order of DS-peptone-CS.

After the optimization of PECNPs, the feasibility of applying these nanoparticles in field condition was tested. The stability of nanoparticles were monitored while

addition of synthetic sea water. Both PEI-NP and CS-NP were able to tolerate the sea water up to 48hours.

The potential for application of these nanoparticles in microbial enhanced oil recovery was investigated. First, the toxicity of nanoparticles on isolated oilfield microbes was tested. It can be concluded that both PEI-NP and CS-NP can be applied in MEOR since they are non-toxic at the concentrations required to deliver nutrients. The oilfield microbes can survive in an environment containing the polyelectrolytes used in the PECNP systems. The microbes can even use DS and CS as a carbon source for reproduction.

Second, the release of nutrients from the nanoparticles was tested. Bacterial growth was delayed by applying nutrients as a polyelectrolyte nanoparticle system, a 10^2 magnitude decrease of microbial number for the first 72 hours was observed. The growth of microbes was delay for at least 4 days up to 5 days which is sufficient for the nutrients flow beyond the near wellbore region in a typical reservoir. Polyelectrolyte nanoparticles have the potential toentrap and deliver nutrients in to the far field of the reservoir to prevent near wellbore plugging.

Finally, the retention of nanoparticle in the porous media was analyzed. Both PEI-NP and DS-NP are transported efficiently in sand with low clay content, the retention of optimized nanoparticles is significantly lower than other published nanoparticles. The clay content in the porous media is an important factor affecting nanoparticle retention; the retention of PECNP increases as the clay content increases.

Entrapment and controlled release of nutrients by polyelectrolyte nanoparticle was achieved. The optimized nanoparticles have potential to entrap nutrients and deliver them far from the near wellbore region to prevent near wellbore bioplugging.

6. Recommendations for Future Work

The optimization of different molecular weight of PEI and DS to form new PEI/peptone/DS NP with smaller particle size and higher entrapment efficiency is recommended. In field application, smaller particle size is desiredfor NPs to maximize the oil recovery and minimize the retention of the nanoparticles; higher EE is required to eliminate the effect of free nutrient components in the nanoparticle suspension. A protein with higher and more uniform molecular weight is suggested to reduce the particle size. Bovine serum albumin with a molecular weight of 66.5KDa may be able to be entrapped in the nanoparticle to achieve high entrapment efficiency.

Both carbon and nitrogen nutrients were successfully entrapped in the PECNP. However, it is still impossible to entrap phosphate salts such as monophosphate into the PECNP. A cheap and digestible polyphosphate is required as triphosphate is a metabolic product but not a nutrient source for most microbes.

DNA sequencing and classification of the isolated oilfield microbes is recommended since it is important to know the desired biosurfactant producers and biopolymer producers in the mixed culture, and modify the PECNP recipe to better stimulate the growth of desired microbes. Also it is important to test the toxicity of polyelectrolytes on each biosurfactant producer or biopolymer producer, and test the capability of polyelectrolytes as a sole nutrient source. In this way, it will be possible to extend the application of the nanoparticle delivery system to oil reserves other than Wellington oilfield.

More accurate methods of total carbon (TC) and total nitrogen (TN) analysis are recommended for the sand pack test. The modified UV analysis is a good testing method for the retention of the peptone in the nanoparticle suspension in the sand pack. However, the modified Bradford method is an inaccurate method for testing the total nitrogen retention in the sand pack since it is calculated from estimated nitrogen concentration of PECNP. Direct methods of testing of TC and TN with high accuracy are required for better understanding the retention if PECNP.

In Section 4.4, the delayed growth of oilfield microbes over time was discussed, a delay of the maximum microbial population up to 8 days was achieved. However, the delay of microbial growth over a distance during injection into porous media to realize the improvement of near wellbore bioplugging is required. Comparison of the formation of bioplugging with directly injected nutrients in porous media and delivery of nutrients by PECNP should be conducted. Diluted microbe suspension may be injected into the sand pack prior to the injection of nutrients. The injectivity change and profile of number of bacteria would be tested after the PECNP injection.

References

1 Armstrong, R. T. Microbial Enhanced Oil Recovery in Fractional-Wet Systems: A Pore-Scale Investigation. *Transport in Porous Media* **92**, 819-835 (2012).

2 Brown, L. R. Microbial enhanced oil recovery (MEOR). *Current opinion in microbiology* **13**, 316-320 (2010).

3 Jenneman G., K. R., McInerney M., Menzie D., Revus D. . Experimental studies of in-situ microbial enhanced recovery. *Journal of Petroleum Science and Engineering* **24**, 33-38 (1984).

4 Tzimas, E.; Cortes, C.; Peteves S. Enhanced Oil Recovery using Carbon Dioxide in the European Energy System. (European Commission Joint Research Centre, 2005).

5 Green, D. G.; Willhite, P. *Enhanced Oil Recovery*. Vol. 6 (Society of Petroleum Engineers, 1998).

6 Maudgalya, S.; McInerney, R. J. in *Production and Operations Symposium* (Society of Petroleum Engineer, Oklahoma City, Oklahoma, 2007).

7 Sen, R. Biotechnology in petroleum recovery: The microbial EOR. *Progress in Energy and Combustion Science* **34**, 714 – 724 (2008).

8 Sheehy, A. J. Microbial Physiology and Enhanced Oil recovery. *Developments in Petroleum Science and Technology* **31**, 37-44 (1991).

9 Banat, I. M. Biosurfactants production and possible uses in microbial enhanced oil recovery and oil pollution remediation: a review. *Bioresource Technology* **51**, 1-12 (1995).

10 Zhao, F.; Zhao, J.; Li, G.; Bai, X.; Han, S. and Zhang, Y. Heterologous production of Pseudomonas aeruginosa rhamnolipid under anaerobic conditions for microbial enhanced oil recovery. *Journal of Applied Microbiology* **118** (2015).

11 Aparna, A.; Smitha, H.; Screening, H. Production of Biosurfactant by Bacillus claussi. *Research in Biotechnology* **3**, 49-56 (2012).

12 Lazar, I.; Yen, T. F. Microbial enhanced oil recovery (MEOR). *Petroleum Science and Technology* **25**, 1353 –1366 (2007).

13 Yen, T. F. *Microbial Enhanced Oil Recovery*. (CRC Press, 1989).

14 Bryant, R.S.; Chase, K.; Bertus, K.; and Stepp, A. in *64th Technical Conference and Exhibit ion of the Society of Petroleum Engineers* 567-578 (San Antonio, TX, 1989).

15 Lazar, I. Microbial enhanced Oil Recovery. in *Elsevier Science* (ed E.C. Donaldson and J.B Clark) 485-530 (Amsterdam, Netherlands, 1991).

16 Beckman, J. W. The Action of Bacteria on Mineral oil. *Industrial Engineering Chemical News* **4**, 3 (1926).

17 ZoBell, C. E. Bacteria Release of Oil from Oil Bearing Materials, Part I and II. *World Oil* **126**, 36-47 (I), 35-41 (II) (1947).

18 Davis, J.B. Microbiology in the Petroleum industry. *Bacteriological Reviews* **18**, 215-238 (1954).

19 Senyukov, V.M.; Taldykina, N.N.; Shissherina, P.E.Microbial method of treating petroleum deposit containing highly mineralized stratal waters. *Mikrobiologiya* **39** (1970).

20 Lazar, I. in *European Symposium on Enhanced Oil Recovery* 279-287 (Inst itute of Offshore Engineering and Herriot-Watt Universit y, Edinburgh, 1978).

21 Zajic, J.E.; Jack, T.R.; Kosaroc, N. *Microbial Enhanced Oil Recovery*. (Penn Well Books, 1983).

22 Yarbrough, H. F. in *International Conference on Microbial Enhancement of Oil Recovery* (ed E.C. Donaldson and J.B Clark) 149-153 (Proceedings, Union County, Arkanas, 1983).

23 Donaldson, E.C.; Yen, T.F. in *Developments in Petroleum Science*. 227.

24 Ivanov, M.V.; Borzenkov, I.A.; Glumov, I.F.; Ibatulin, P.B. in *Elsevier* (ed A. Woodhead E. Premuzic) 373-381 (Amsterdam, 1993).

25 Hitzman, D. O. in *9th Symposium on Improved Oil Recovery. Society of Petroleum Engineers*.

26 McInerney, M. J. *Petroleum microbiology: Biofouling, souring and improved oil recovery*. 600-607.

27 Donaldson, E. C. Microbial enhancement of oil recovery- recent advances. *Development in Petroleum Science and Technology* **31**, 530 (1991).

28 Desouky, S. M. Modelling and laboratory investigation of microbial enhanced oil recovery. *Journal of petroleum science & engineering* **15**, 309 - 320 (1996).

29 Magot, M.; Patel, B. Microbiology of petroleum reservoirs. *Antonie van Leeuwenhoek* **77**, 103-176 (2000).

30 Ginn, T.; Nelson, K.; Scheibe, T.; Murphy, E. and Clement T. Processes en microbial transport in the natural subsurface. *Advances in Water Resources* **25**, 1017–1042 (2002).

31 Chisholm, J.; Knapp, R.; McInerney, M. and Menzie, D. in *Society of Petroleum Engineers Annual Technical Conference and Exhibition* (New Orleans, Louisiana, USA, 1990).

32 Abu-Ruwaida, A. S.; Haditirto, S. Isolation of biosurfactant-producing bacteria -- product characterization and evaluation. *Acta Biotechnologica* **11**, 315-324 (1992).

33 Adkins, J. P. Microbially enhanced oil recovery from unconsolidated limestone cores. *Journal of Geomicrobiology* **10**, 77-86 (1992).

34 Jack, T.R. in *Symposium on Applicat ions of Microorganisms to Petroleum Technology*. (ed T.E. Burchfield and R.S. Bryant) VII I-VII 13.

35 Hitzman, D. O. in *Development in Petroleum Science* (ed E.C. Donaldson) 11-20 (Amsterdam, 1991).

36 Madigan, M.; Parker, J. *Brock: Biology of microorganisms (Tenth ed.)*. (Prentice-Hall, 2003).

37 Bryant, R. Review of microbial technology for improving oil recovery. *SPE Reservoir Engineering* **4,** 1378-1389 (1989).

38 Jang, L.K.; Yen, T. F. in *SPE California Regional Meeting* (Long Beach, California, 1984).

39 Van Hamme, J. A. S.; Ward, O. Recent advances in petroleum microbiology. *Microbiology and Molecular Biology Reviews* **67** (2003).

40 Brooks, G. F.; Butel, J. S.; Morse, S. A. *Jawetz, Melnick, & Adelberg's Medical Microbiology*. (McGraw-Hill, 2007).

41 Hirai, Y. Survival of bacteria under dry conditions; from a viewpoint of nosocomial infection. *Journal of Hospital Infection* **19**, 191-200 (1991).

42 Marshall, S. L. Fundamental aspects of microbial enhanced oil recovery: A literature survey. (Floreat, Western Australia, 2008).

43 Georgiou, M. S. Microbial Enhanced Oil Recovery Research –Final Report prepared for U.S. Department of Energy. (Department of Petroleum Engineering, University of Texas, Austin, USA, 1993).

44 Cotter, P. D. Surviving the acid test: responses of gram-positive bacteria to low pH. *Microbiology and Molecular Biology Reviews* **67**, 429-453 (2003).

45 Crescente, C.; Abraiz, A.; Torsaeter, O.; Hultmann, L.; Stroen, A.; Rasmussen, K. and Kowalewski E. in *16th SPE/DOE Improved Oil Recovery Symposium* (Tulsa, Oklahoma, USA, 2008).

46 Pommerville, J. *Alcamo's Laboratory Fundamentals of Microbiologyy, 7th ed.*, (Jones and Bartlett Publishers, 2005).

47 Makkar, R. S. Biosurfactant production by microorganisms on unconventional carbon sources - A review. *Journal of Surfactants and Detergents* **2**, 237-241 (1999).

48 Joshi, S.; Nerurkar, A.; Desai, A. J. Statistical optimization of medium components for the production of biosurfactant by Bacillus licheniformis K51. *Journal of microbiology and biotechnology* **17** (2007).

49 Li, W. *Performance evaluation and characterization of a naturally occuring bacterial community for removing petroleum hydrocabons from oilfield produced water* Master of Science thesis, New Mexico Tech, (2010).

50 Nielsen, J.; Lid én, G. *Bioreaction engineering principles* (Kluwer Academic/Plenum Publishers, 2003).

51 Malthus, T. R. *An Essay on the Principle of Population*. (1798).

52 Baranyi, C. P. Single-cell and population lag times as a function of cell age. *Applied and Environmental Microbiology* **74**, 2534-2536 (2008).

53 Skarstad, K.; Boye, E. Cell cycle parameters of slowly growing Escherichia coli B/r studied by flow cytometry. *Journal of Bacteriology* **154**, 656-662 (1983).

54 Zwietering, M.H.; Rombouts, F. M. Modeling of the Bacterial Growth Curve. *Applied and Environmental Microbiology* **56**, 1875-1881 (1990).

55 Kennedy, M. J. Preservation records of microorganisms – evidence of the tenacity of life. *Microbiology* **140**, 2513-2529 (2014).

56 Baranyi, J. *Modelling and parameter estimation of bacterial growth with distributed lag time* PhD thesis, University of Szeged, (2010).

57 Langevin, D. Complexation of oppositely charged polyelectrolytes and surfactants in aqueous solutions. A review. *Adv. Colloid Interface Sci.*, 170–177 (2009).

58 Raiders, R.A.; Jenneman, G. E.; Knapp, R. M.; McInerney, M. J.; Menzie, D. E. in *60 th Annual Technical Conference and Exhibit ion of SPE* Sept. 22-25 (Las Vegas, NV, 1985).

59 Udipta Saikia, B.; Vendhan, V. A Brief Review On The Science, Mechanism And Environmental Constraints Of Microbial Enhanced Oil Recovery (MEOR). *International Journal of ChemTech Research* **5**, 1205-1212 (2013).

60 Nielsen, S. M. *Microbial Enhanced Oil Recovery – Advanced Reservoir Simulation* PhD thesis, Technical University of Denmark, (2010).

61 Al-Sulaimani, H.; Al-Wahaibi, Y.; Al-Bahry, S.; Elshafie, A.; Al-Bemani, A. Microbial biotechnology for enhancing oil recovery: Current developments and future prospects. *Biotechnology, Bioinformatics and Bioengineering* **1**, 147-158 (2011).

62 Rojas, O. J. Adsorbance of surfactant and polymer at interfaces. *Auburn University PhD Dissertation* (1998).

63 Koetz, J.; Kelly, S. *Polyelectrolytes and Nanoparticles*. (Springer Laboratory, 2007).

64 Li, D. Towards Rational Design of Polyelectrolyte-Surfactant complexes: Thermodynamics, microstructure and property. *University of Delaware Dissertation* (2013).

65 Berkland, C.; Cordova, M; Liang, J. T.; Willhite, G. P. Polyelectrolyte Complexes for Oil and Gas Applications. US patent (2008) US20080058229A1.

66 Barrat, J. L. in *Advances in Chemical Physics, Polymeric Systems* (ed I. Prigogine I. Prigogine , S. A. Rice) (Wiley, 2009).

67 Ghahfarokhi, R. B. *Fracturing Fluid Cleanup by Controlled Release of Enzymes from Polyelectrolyte Complex Nanoparticles* PhD thesis, University of Kansas, (2010).

68 Tiyaboonchai, W. *Development of a New Nanoparticle Delivery Vehicle Based on an Aqueous Polymer System: Polyethylenimine and Dextran Sulfate.* PhD thesis, University of Kansas, (2003).

69 Cordova, M. Cheng, Min; Trejo, Julieta; ,Johnson, S. J.; Willhite, G. P.; Liang, J. T. and Berkland, C. Delayed HPAM Gelation via Transient Sequestration of Chromium in Polyelectrolyte Complex Nanoparticles. *Macromolecules* **41**, 4398-4404 (2008).

70 Tiyaboonchai, W. Formulation and Characterization of DNA-Polyethylenimine-Dextran Sulfate Nano-Particles. *European Journal of Pharmaceutical Sciences* **19**, 191-202 (2003).

71 Barati, R. J.; Johnson, S. J.; McCool, S.; Green, D. W.; Willhite, P.; Liang J. T. Fracturing Fluid Cleanup by Controlled Release of Enzymes from Polyelectrolyte Complex Nanoparticles. *Journal of Applied Polymer Science* **121**, 1292-1298 (2011).

72 Hartig, S. H.; Dikov, M. M.; Prokop, A.; Davidson, M. Multifunctional Nanoparticulate Polyelectrolyte Complexes. *Pharmaceutical Research* **24**, 2353-2369 (2007).

73 Li, W.; Johnson, S. J.; Liang, J. T. Rate-limiting nutrient delivery system for microbial enhanced oil recovery. in *2014 Graduate Student Poster Contest* (University of Kansas School of Engineering, Lawrence, KS, 2013).

74 Kwak, C. T. *Polymer–Surfactant Systems*. (Marcel Dekker Inc, 1998).

75 Lindman, B.; Khan, A.; Marques, E.; Miguel, M.-G.; Picullel, L.; Thalberg, K. Phase behavior of polymer-surfactant systems in relation to polymer-polymer and surfactant-surfactant mixtures. *Pure & Applied Chemistry* **65**, 953–958 (1993).

76 Hansson, P.; Almgren, M. Interaction of Cn TAB with Sodium (Carboxymethyl)cellulose: Effect of Polyion Linear Charge Density on Binding Isotherms and Surfactant Aggregation Number. *The Journal of Physical Chemistry* **100**, 9038-9046 (1996).

77 Matulis D.; Bloomfield, V. A. Thermodynamics of cationic lipid binding to DNA and DNA condensation: roles of electrostatics and hydrophobicity. *Journal of the American Chemical Society* **124**, 7331-7342 (2002).

78 Tse, S. H. *The effects of ionic spacing and degree of polymeriazation on the stoichiometry of polyelectrolyte interactions in diluted aqeous solutions*, PhD Dissertation, University of Wisconsin (1979).

79 Arguelles-Monal, W. Study of the stoichiometric polyelectrolyte complex between chitosan and carboxymethyl cellulose. *Polymer Bulletin* **23**, 307-313 (1990).

80 Vanerek, A. Coacervate complex formation between cationic polyacrylamide and anionic sulfonated kraft lignin. *Colloids and Surfaces, A* **273**, 55-62 (2006).

81 Dumitriu, E. C. Inclusion and release of protein from polysaccharide-based polyion complexes. *Advanced Drug Delivery Reviews* **31**, 223-246 (1998).

82 de Vasconcelos , C. L.; dos Santos, D. E. S.; Dantas, T. N. C.; Pereira, M. R. and Fonseca, J. L. C. Effect of Molecular Weight and Ionic Strength on the Formation of Polyelectrolyte Complexes Based on Poly(methacrylic acid) and Chitosan. *Biomacromolecules* **7**, 1245–1252 (2006).

83 Shkinev, V. M. Enrichment of arsenic and its separation from other elements liquid phase polymer based retention. *Separation Science and Technology* **22**, 2165-2174 (1987).

84 De Geest, B. G.; Sukhorukov, G. B.; Demeester, J.; De Smedt SC, S. C. Release mechanisms for polyelectrolyte capsules. *Chemical Society Reviews* **36**, 636-649 (2007).

85 Yemuland, O. Synthesis and characterization of poly(ethyleneimine) dendrimers. *Colloid & Polymer Science* **286**, 747–752 (2008).

86 Kasturi, S. P. *Design, synthesis, and evaluation of synthetic particulate delivery systems in DNA and protein vaccine delivery* Doctor of Philosophy dissertation, University of Texas at Austin, (2006).

87 Boussif, O.; Zanta, M.A.; Mergny, M.D.; Scherman, D.; Demeneix, B.; Behr, J.P. in *Proceedings of the National Academy of Sciences*. 7297–7301.

88 Robbins, C. R. *Chemical and Physical Behavior of Human Hair*. (Springer, 2012).

89 Kirby, G. H. in *ASME Turbo Expo 2005: Power for Land, Sea, and Air*.

90 Moghimi, S. M. in *Nanotechnologies for the Life Sciences* (ed C. Kumar.) (Wiley-VCH, 2006).

91 Chen, Y.; Wang, F.; Benson, H. A. E. Designing chitosan-dextran sulfate nanoparticles using charge ratios. *AAPS PharmSciTech* **8**, 131-139 (2007).

92 Sarmento, B.; Veiga, F.; Ferreira, D. Development and characterization of new insulin containing polysaccharide nanoparticles. *Colloids and Surfaces B: Biointerfaces* **53**, 193-202 (2006).

93 Choi, S. G. Water mobility and textural properties of native and hydroxypropylated wheat starch gels. *Carbohydrate Polymers* **51**, 1-8 (2003).

94 Blanchet, D.; Vandecasteele, J. P. in *SPE ATCE comference* (New Orleans, Louisiana, USA, 2001).

95 Tulevaa, B. K. Biosurfactant Production by a New *Pseudomonas putida* Strain. *Zeitschrift für Naturforschung* **57c**, 356-360 (2002).

96 Huff, B. L. *Microbial and Geochemical Characterization of Wellington Oil Field, Southcentral Kansas, and Potential Applications to Microbial Enhanced Oil Recovery* Master thesis, University of Kansas, (2014).

97 Gray, V. L.; Muller, C.T.; Watkins, I. D.; Lloyd, D. Low tyrosine content of growth media yields aflagellate Salmonella enterica serovar Typhimurium. *Microbiology* **152**, 23-28 (2006).

98 Johnson, S. J.; Trejo, J.; Veisi, M.; Willhite, G. P.; Liang, J. T.; Berkland, C. Effects of divalent cations, seawater and formation brine on positively charged polyethylenimine/dextran sulfate/Cr(III) polyelectrolyte complexes and HPAM/Cr(III) gelation. *Journal of Applied Polymer Science* **115**, 1008-1014 (2009).

99 Bradford, M. M. Rapid and sensitive method for the quantitation of microgram quantities of protein utilizing the principle of protein-dye binding. *Analytical Biochemistry* **72**, 248–254 (1976).

100 Smoluchowski, M. Drei Vorträge über Diffusion, Brownsche Molekularbewegung und Koagulation von Kolloidteilchen. *Zeitschrift für Physik A Hadrons and Nuclei* **17**, 557-571 (1916).

101 *Reference Guide: Fisher Scientific accumet XL Series Benchtop Meters*. (Fisher Scientific, 2012).

102 Wirth, M. A simple and cost-effective method to transfect small interfering RNAs into pancreatic cancer cell lines using Polyethylenimine. *Pancreas* **40**, 144-150 (2011).

103 Gray, V. L.; Watkins, I. D.; Lloyd, D. Peptones from diverse sources: pivotal determinants of bacterial growth dynamics. *J Appl Microbiology* **104**, 554-565 (2008).

104 Rao, C. R. Some Statistical Methods for Comparison of Growth Curves. *Biometrics* **14**, 1-17 (1958).

105 Yan, L. Y.; Yu, T.; Shen, W. water-soluble oil-displacing agent with tracer properties for enhancing oil recovery. *RSC Advances* **5**, 42843-42847 (2015).

106 Zemel, B. *Tracers in the Oil Field*. Vol. 43 (Elsevier, 1995).

107 Bradford, M. M. A dye binding assay for protein. *Analytical Biochemistry* **72**, 248-254 (1976).

108 Sutton, S. Measurement of Cell Concentration in Suspension by Optical Density. *http://www.microbiol.org/resources/monographswhite-papers/measurement-of-cell-concentration-in-suspension-by-optical-density/*.

109 Christensen, J. How particles affect UV light in the UV disinfection of unfiltered drinking water. *American Water Works Association Journal* **95**, 179 (2003).

110 Say, R.; Ünlüer, O. B.; Ersöz; A. Resuable Pectinase Nano Polymeric Particles. *Journal of Biocatal Biotransformation* **3** (2014).

111 Tiyaboonchai, W. *Development of a New Nanoparticle Delivery Vehicle Based on an Aqueous Polymer System: Polyethylenimine and Dextran Sulfate* PhD thesis, University of Kansas, (2003).

112 Robertson, E. Low-Salinity Waterflooding to Improve Oil Recovery-Historical Field Evidence. in *2007 SPE Annual Technical Conference and Exhibition*

113 Dautzenberg, H. Response of polyelectrolyte complexes to subsequent addition of salts with different cations. *Langmuir* **19**, 5204–5211 (2003).

114 Zhang, Q.; Lin, D.; Yao, S. Effect and mechanism of sodium chloride on the formation of chitosan–cellulose sulfate–tripolyphosphate crosslinked beads. *Soft Matter* **9** (2013).

115 Walton, K. W. Investigation of the toxicity of a series of dextran sulphates of varying molecular weight. *Br J Pharmacol Chemother* **9**, 1-14 (1954).

116 Ishioka, T. Induction of colorectal tumors in rats by sulfated polysaccharides. Critical reviews in toxicology. *Critical Reviews in Toxicology* **17**, 215-244 (1987).

117 Amar-Lewis, E. Quaternized starch-based carrier for siRNA delivery: From cellular uptake to gene silencing. *Journal of Controlled Release* **185**, 109-120 (2014).

118 Thomsen, M. H.; Kiel, P. Batch fermentations on synthetic mixed sugar and starch medium with amylolytic lactic acid bacteria. *Applied Microbiology and Biotechnology* **74**, 540-546 (2007).

119 Sharon, G.; Ringo, J. M. Commensal bacteria play a role in mating preference of*Drosophila melanogaster*. in *Proceedings of the National Academy of Sciences of the United States of America*. 20051-20056 (2010).

120 Stephens, J. B.; Vadie, L. A. Utilization of Indigenous Microflora in Permeability Profile Modification of Oil Bearing Formations in *Proceedings of the 1996 10th Symposium on Improved Oil Recovery*. (1996).

121 Hoppe, M. Utermann. Retention of Sterically and Electrosterically Stabilized Silver Nanoparticles in Soils. *Environmental Science & Technology* **48**, 12628-12635 (2014).

122 Cathles, Y. V. Retention of silica nanoparticles on calcium carbonate sands immersed in electrolyte solutions. *Journal of Colloid and Interface Science* **436**, 1-8 (2014).

123 Hull, M. S. Uptake and retention of metallic nanoparticles in the Mediterranean mussel *Aquatic toxicology* **140** (2013).

124 Tsoukalas, D. Recent advances in nanoparticle memories. *Materials Science & Engineering. B, Solid-State Materials for Advanced Technology* **124-125**, 93-101 (2005).

125 Auffan, M. R.; Bottero, J. Y.; Lowry, G. V.; Jolivet, J. P.; Wiesner, M. R. Towards a definition of inorganic nanoparticles from an environmental, health and safety perspective. N. *Nature Nanotechnology* **4**, 634-641 (2009).

126 Jaisi, D. P.; Blake, R.E. Transport of single-walled carbon nanotubes in porous media: filtration mechanisms and reversibility. *Environmental Science & Technology* **42**, 8317-8323 (2012).

127 Liang, Y.; Simunek, J.; Vereecken, H.; Klumpp, E. Sensitivity of the transport and retention of stabilized silver nanoparticles to physicochemical factors. *Water Research* **47**, 2572-2582 (2013).

Appendix 1. Selective media used in this research

Table A1.1 PEI toxicity test medium (*Pseudomonas putida*)

	Concentration (g/kg)
$(NH_4)_2HPO_4$	1.5
K_2HPO_4	1.2
$MgSO_4$	0.2
Yeast extract	0.5
Sodium benzoate	3.0
PEI	3.0
H_2O	990.6

Table A1.2 DS toxicity test medium (*Pseudomonas putida*)

	Concentration (g/kg)
$(NH_4)_2HPO_4$	1.5
K_2HPO_4	1.2
$MgSO_4$	0.2
Yeast extract	0.5
Sodium benzoate	3.0
DS	6.0
H_2O	987.6

Table A1.3 CS toxicity test medium (*Pseudomonas putida*)

	Concentration (g/kg)
$(NH_4)_2HPO_4$	1.5
K_2HPO_4	1.2
$MgSO_4$	0.2
Yeast extract	0.5
Sodium benzoate	3.0
CS	5.0
H_2O	988.6

Table A1.4 PEI toxicity test medium (Aerobic mixed culture)

	Concentration (g/kg)
Peptone	10.0
NaCl	20.0
KH_2PO_4	2.5
Dextrose	5.0
NH4Cl	6.0
PEI	3.0
H_2O	953.5

Table A1.5 DS toxicity test medium (Aerobic mixed culture)

	Concentration (g/kg)
Peptone	10.0
NaCl	20.0
KH_2PO_4	2.5
Dextrose	5.0
NH4Cl	6.0
DS	6.0
H_2O	950.5

Table A1.6 CS toxicity test medium (Aerobic mixed culture)

	Concentration (g/kg)
peptone	10.0
NaCl	20.0
KH_2PO_4	2.5
Dextrose	5.0
CS	5.0
H_2O	957.5

Table A1.7PEI toxicity test medium (Anaerobic mixed culture)

	Concentration (g/kg)
peptone	10.0
NaCl	20.0
KH_2PO_4	2.5
Dextrose	5.0
$NaNO_3$	0.66
PEI	3.0
H_2O	958.8

Table A1.8DS toxicity test medium (Anaerobic mixed culture)

	Concentration (g/kg)
peptone	10.0
NaCl	20.0
KH_2PO_4	2.5
Dextrose	5.0
$NaNO_3$	0.66
DS	6.0
H_2O	955.8

Table A1.9CS toxicity test medium (Anaerobic mixed culture)

	Concentration (g/kg)
peptone	10.0
NaCl	20.0
KH_2PO_4	2.5
Dextrose	5.0
$NaNO_3$	0.66
CS	5.0
H_2O	956.8

Table A1.10Sodium benzoate medium

with PEI as sole nitrogen source

	Concentration (g/kg)
PEI	2.3
K_2HPO_4	3.2
$MgSO_4$	0.2
Yeast extract	0.5
Sodium benzoate	3.0
H_2O	990.8

Table A1.11Sodium benzoate medium

with DS as sole carbon source

	Concentration (g/kg)
$(NH_4)_2HPO_4$	1.5
K_2HPO_4	1.2
$MgSO_4$	0.2
Yeast extract	0.5
DS	6.8
H_2O	989.8

Table A1.12Sodium benzoate medium

with CS as sole carbon source

	Concentration (g/kg)
$(NH_4)_2HPO_4$	1.5
K_2HPO_4	1.2
$MgSO_4$	0.2
Yeast extract	0.5
CS	2.8
H_2O	993.8

Table A1.13peptone medium (Aerobic mixed culture)

with PEI as sole carbon source

	Concentration (g/kg)
PEI	4.4
NaCl	20
KH_2PO_4	2.5
Dextrose	5
H_2O	968.1

Table A1.14peptone medium (Aerobic mixed culture)

with DS as sole carbon source

	Concentration (g/kg)
Peptone	10
NaCl	20
KH_2PO_4	2.5
DS	9
H_2O	958.5

Table A1.15peptone medium (Aerobic mixed culture)

with CS as sole carbon source

	Concentration (g/kg)
Peptone	10
NaCl	20
KH_2PO_4	2.5
CS	3.7
H_2O	963.8

Table A1.16peptone medium (Anaerobic mixed culture)

with PEI as sole nitrogen source

	Concentration (g/kg)
PEI	4.4
NaCl	20
KH_2PO_4	2.5
Dextrose	5
$NaNO_3$	0.66
H_2O	967.4

Table A1.17peptone medium (Aerobic mixed culture)

with DS as sole carbon source

	Concentration (g/kg)
Peptone	10
NaCl	20
KH_2PO_4	2.5
DS	9
$NaNO_3$	0.66
H_2O	957.8

Table A1.18peptone medium (Aerobic mixed culture)

with CS as sole carbon source

	Concentration (g/kg)
Peptone	10
NaCl	20
KH_2PO_4	2.5
CS	3.7
$NaNO_3$	0.66
H_2O	963.1

Appendix 2 The entrapment efficiency of PEI-NP at different PEI pH

Table A2.1 The entrapment efficiency (EE) of different PEI/DS/peptone PECNP (PEI pH = 7)

Matrix for EE	Mass ratio of PEI											
Mass ratio of peptone	0.5	1	1.5	2	2.5	3	3.5	4	4.5	5	5.5	6
5	0%	0%	0%	2.8%	13.2%	9.3%	1.5%	2.4%	1.7%	0%	0%	0%
10	0%	0%	6.8%	10.1%	11.1%	9.1%	10.3%	16.4%	2.2%	0%	0%	0%
15	1.0%	1.5%	3.8%	8.6%	8.8%	1.5%	6.2%	8.5%	0%	0%	0%	0%
20	1.5%	1.7%	3.5%	9.7%	5.2%	0%	0%	0.7%	0%	0%	0%	0%
25	0.9%	0.8%	1.7%	2.8%	1.7%	0%	0%	0%	0%	0%	0%	0%
30	0%	0%	0%	0%	0%	0%	0%	0%	0%	0%	0%	0%
35	0%	0%	0%	0%	0%	0%	0%	0%	0%	0%	0%	0%
40	0%	0%	0%	0%	0%	0%	0%	0%	0%	0%	0%	0%

Table A2.2 The entrapment efficiency (EE) of different PEI/DS/peptone PECNP (PEI pH = 8)

Matrix for EE	Mass ratio of PEI										
Mass ratio of peptone	0.5	1	1.5	2	2.5	3	3.5	4	4.5	5	5.5	6
5	0%	0.8%	3.1%	0%	4.1%	1.4%	3.2%	1.8%	1.5%	0%	0%	0%
10	0%	2.8%	4.5%	9.3%	10.2%	14.5%	16.2%	16.4%	26.7%	0.3%	0%	0%
15	2.2%	1.9%	3.8%	9.0%	7.2%	12.3%	11.5%	22.1%	6.2%	0.3%	0%	0%
20	0%	0%	0.7%	7.5%	6.3%	8.1%	2.8%	0.5%	0%	0%	0%	0%
25	0%	0%	2.1%	8.2%	4.1%	2.4%	0%	0%	0%	0%	0%	0%
30	0%	0.2%	0.9%	1.7%	0%	0%	0%	0%	0%	0%	0%	0%
35	0%	0.1%	0.9%	0%	0%	0%	0%	0%	0%	0%	0%	0%
40	0%	0%	0.2%	0%	0%	0%	0%	0%	0%	0%	0%	0%

Table A2.3 The entrapment efficiency (EE) of different PEI/DS/peptone PECNP (PEI pH = 9)

Matrix for EE	Mass ratio of PEI										
Mass ratio of peptone	0.5	1	1.5	2	2.5	3	3.5	4	4.5	5	5.5	6
5	4.5%	4.2%	1.3%	1.6%	1.5%	2.3%	1.8%	1.9%	1.7%	0%	0%	0%
10	6.2%	5.5%	6.2%	12.1%	14.2%	15.2%	12.5%	16.5%	9.5%	0%	0%	0%
15	5.8%	6.2%	3.8%	13.8%	11.8%	14.3%	12.1%	9.6%	4.4%	0.2%	0%	0%
20	4.7%	6.1%	10.2%	16.5%	10.7%	10.3%	2.3%	2.7%	0%	0%	0%	0%
25	5.0%	5.8%	5.2%	12.0%	4.1%	14.2%	1.9%	0%	0%	0%	0%	0%
30	4.8%	7.2%	6.1%	12.2%	6.7%	29.2%	1.4%	0%	0%	0%	0%	0%
35	4.5%	3.2%	5.3%	12.6%	2.5%	13.0%	4.2%	0%	0%	0%	0%	0%
40	4.2%	2.3%	2.6%	10.4%	5.3%	8.7%	0%	0%	0%	0%	0%	0%

Table A2.4 The entrapment efficiency (EE) of different PEI/DS/peptone PECNP (PEI pH = 11)

Matrix for EE	Mass ratio of PEI											
Mass ratio of peptone	0.5	1	1.5	2	2.5	3	3.5	4	4.5	5	5.5	6
5	0%	0%	0%	0%	0%	0%	0%	0%	0%	0%	0%	0%
10	0%	7.3%	5.4%	8.7%	2.1%	13.7%	5.3%	0%	0%	0%	0%	0%
15	0%	9.2%	1.5%	4.3%	3.3%	3.5%	3.3%	0%	0%	0%	0%	0%
20	0%	9.0%	6.2%	2.6%	4.2%	0.8%	1.8%	0%	0%	0%	0%	0%
25	0%	11.2%	5.2%	4.3%	5.6%	0%	0%	0%	0%	0%	0%	0%
30	0%	4.4%	7.8%	1.7%	0%	0%	0%	0%	0%	0%	0%	0%
35	0%	7.6%	8.3%	0%	0%	0%	0%	0%	0%	0%	0%	0%
40	0%	0.4%	4.5%	0%	0%	0%	0%	0%	0%	0%	0%	0%

Table A2.5 The entrapment efficiency (EE) of different PEI/DS/peptone PECNP (PEI pH = 12)

Matrix for EE	Mass ratio of PEI										
Mass ratio of peptone	0.5	1	1.5	2	2.5	3	3.5	4	4.5	5	5.5	6
5	0%	0%	0%	0%	0%	0%	0%	0%	0%	0%	0%	0%
10	0%	1.2%	2.1%	0.5%	0.6%	0.5%	0.5%	2.0%	3.1%	5.3%	2.2%	2.5%
15	0%	0.8%	1.8%	0.7%	0.2%	0.1%	1.1%	1.3%	1.7%	2.7%	1.7%	1.4%
20	0%	0.7%	2.0%	0.5%	0%	0%	0%	0.1%	0.2%	0.3%	0%	0%
25	0%	1.0%	2.2%	0.6%	0%	0%	0%	0%	0%	0%	0%	0%
30	0%	0%	2.1%	0.5%	0%	0%	0%	0%	0%	0%	0%	0%
35	0%	1.1%	1.5%	0.4%	0%	0%	0%	0%	0%	0%	0%	0%
40	0%	0.9%	1.9%	0.3%	0%	0%	0%	0%	0%	0%	0%	0%

Appendix 3 Microbial growth curves indicate the growth phases of different microbes

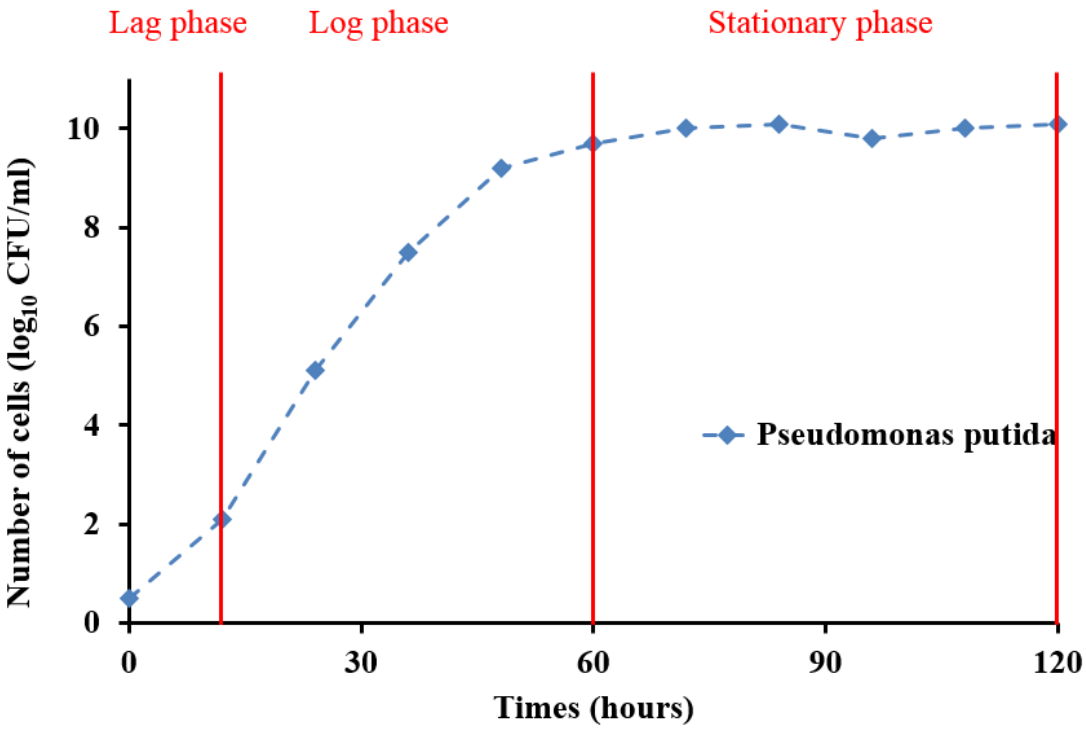

Figure A3.1 Microbial growth curve of *Pseudomonas putida* incubated at 40°C with peptone medium (lag phase: 0-12 hours, log phase: 12-60 hours, stationary phase: 60-120 hours)

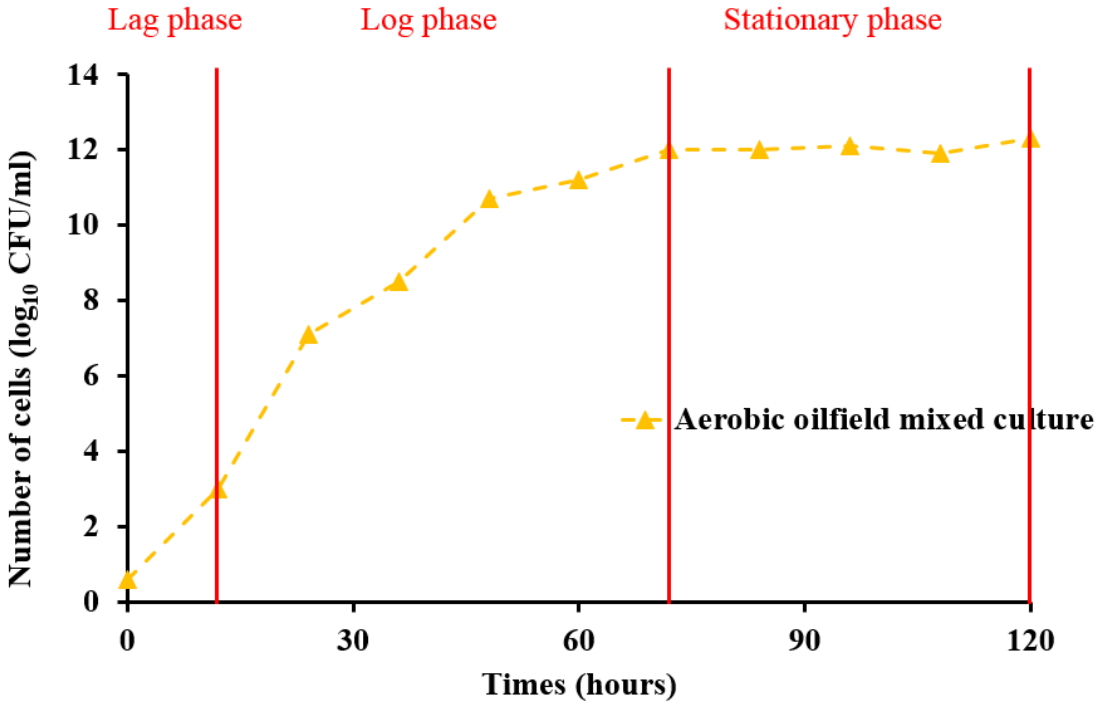

Figure A3.2 Microbial growth curve of aerobic oilfield mixed culture at 40°C with peptone medium (lag phase: 0-12 hours, log phase: 12-72 hours, stationary phase: 72-120 hours)

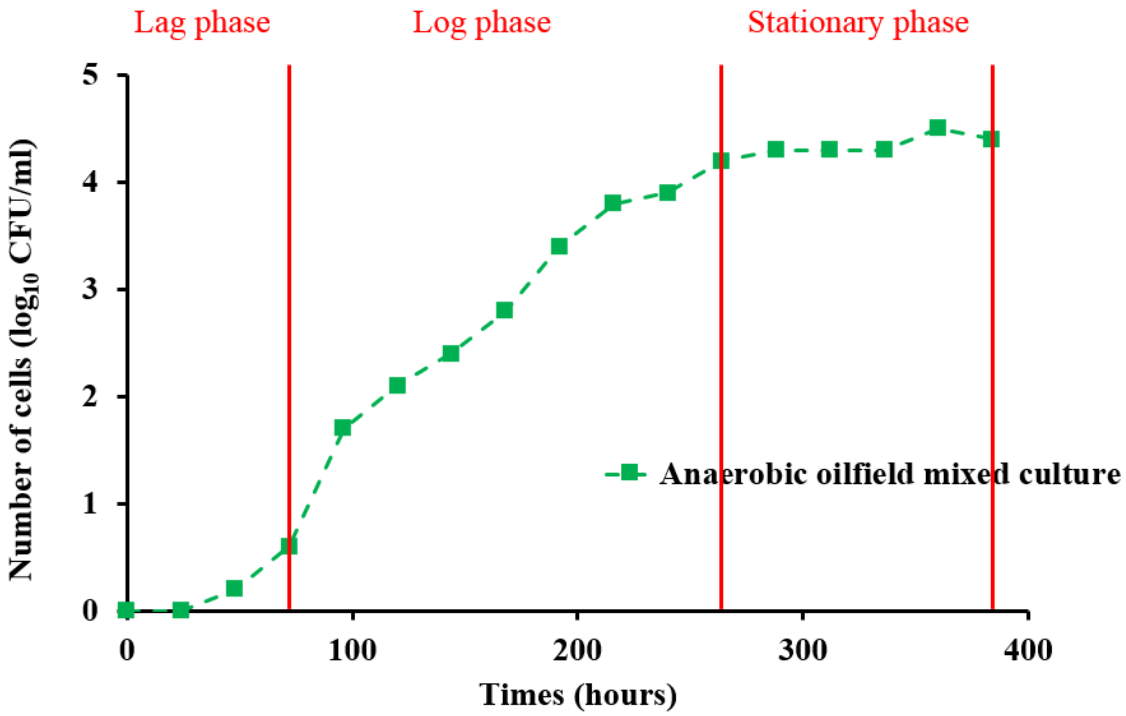

Figure A3.3 Microbial growth curve of anaerobic oilfield mixed culture at 40°C with peptone medium (lag phase: 0-72 hours, log phase: 72-264 hours, stationary phase: 264-384 hours)

Appendix 4. Comparison of different NP concentration testing methods

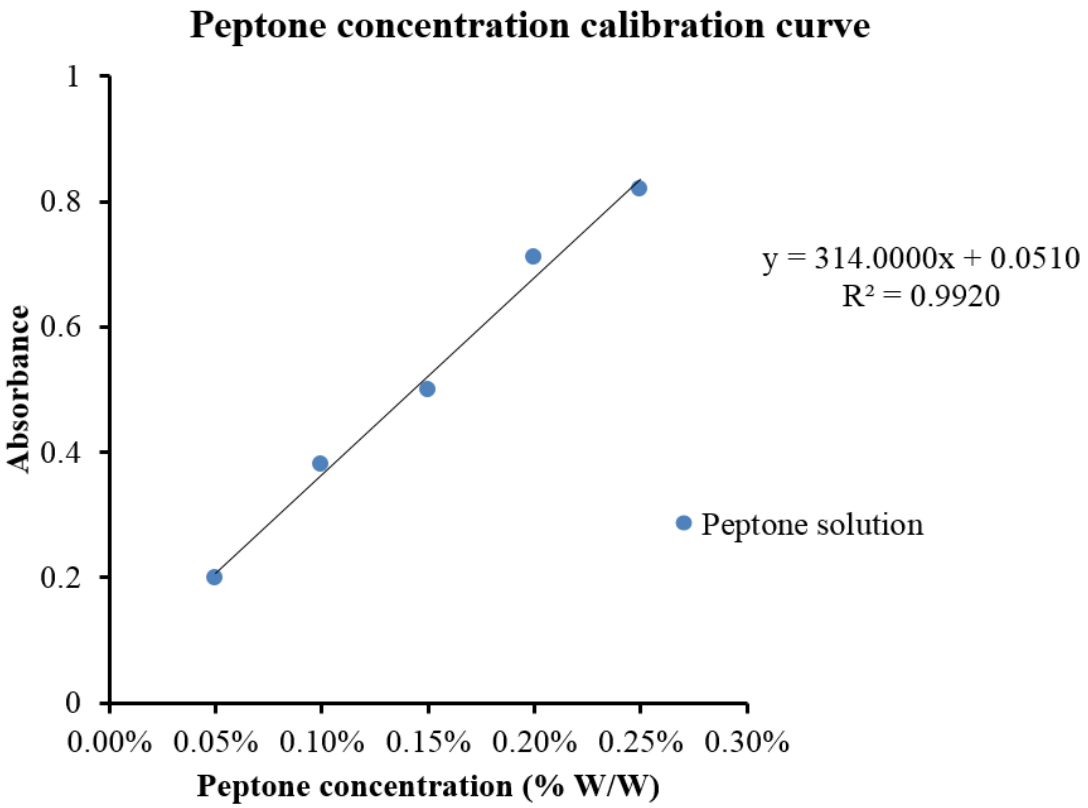

Figure A4.1 Standard calibration curve for peptone concentration at 270 nm [the calibration curve is tested at 25 ℃, pH = 6.1 (PEI pH =7)]

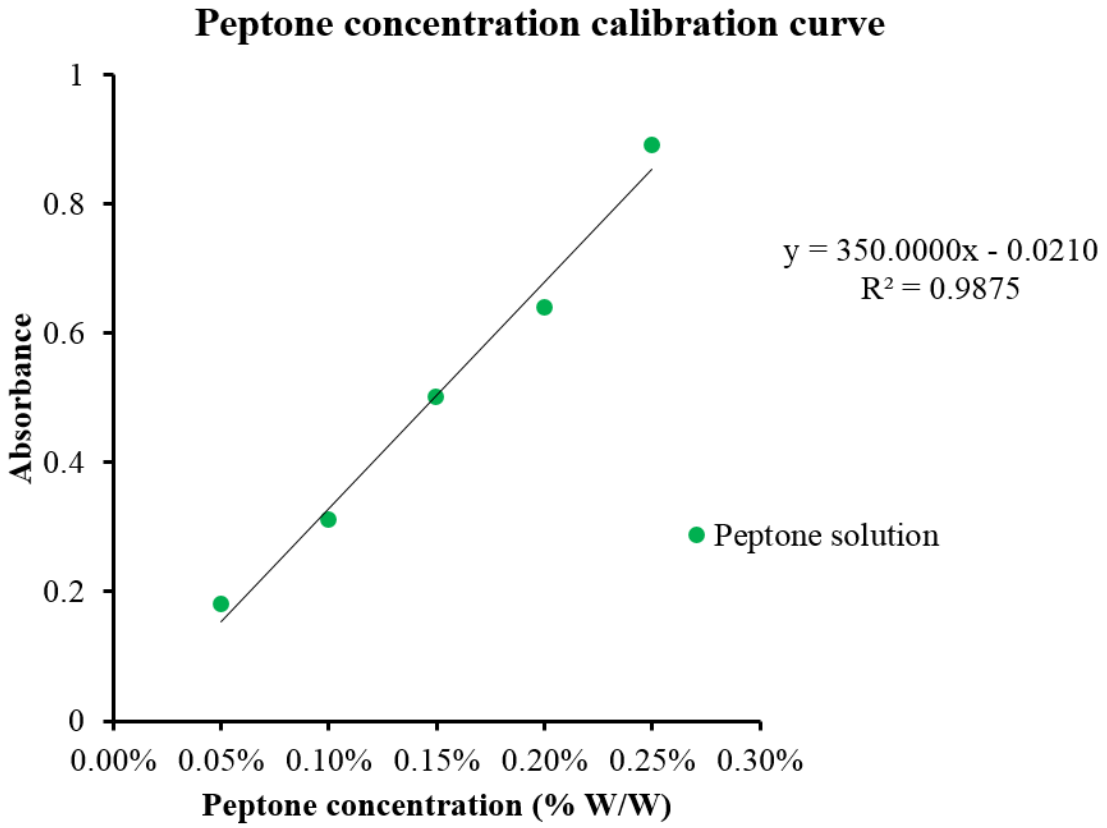

Figure A4.2 Standard calibration curve for peptone concentration at 270 nm [the calibration curve is tested at 25 ℃, pH = 6.5 (PEI pH =8)]

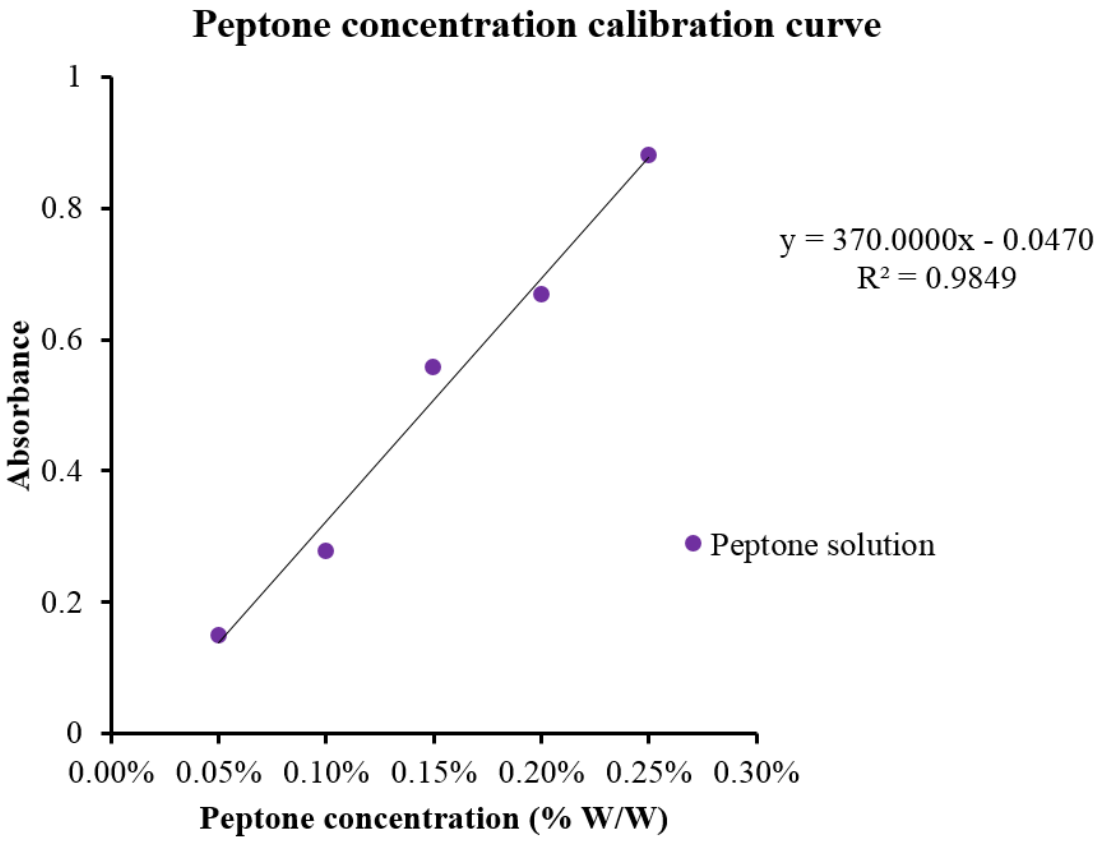

Figure A4.3 Standard calibration curve for peptone concentration at 270 nm [the calibration curve is tested at 25 ℃, pH = 7.1 (PEI pH =9)]

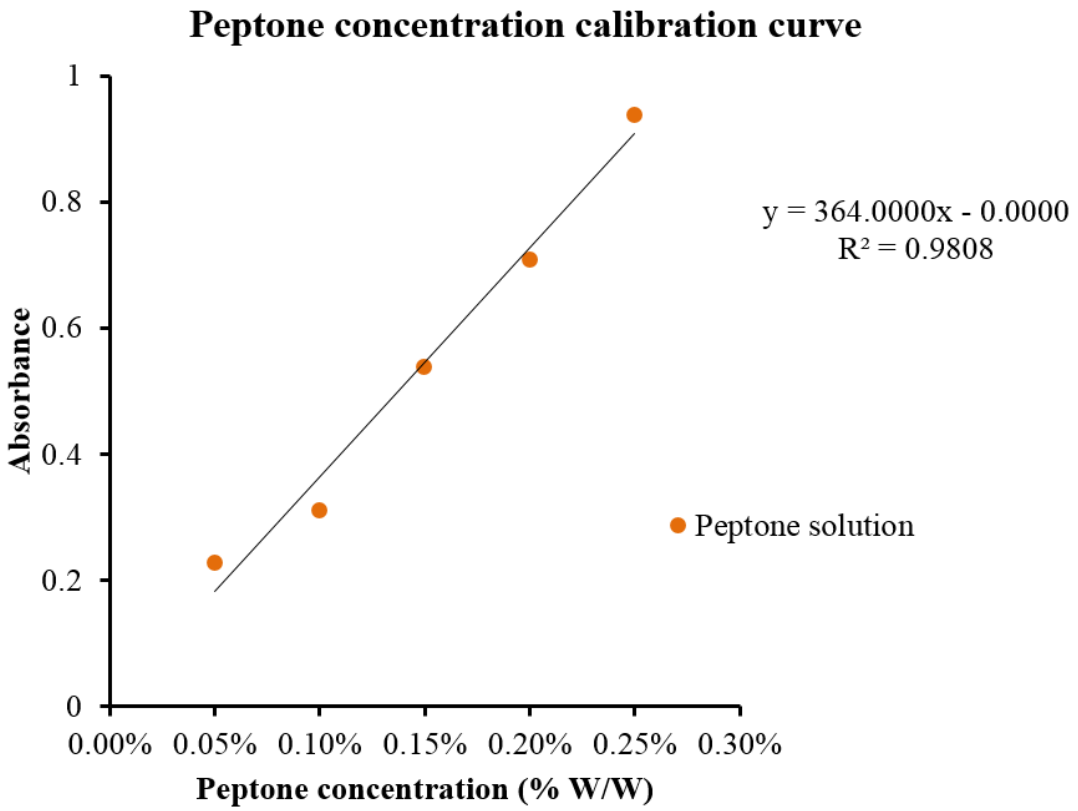

Figure A4.4 Standard calibration curve for peptone concentration at 270 nm [the calibration curve is tested at 25 ℃, pH = 7.9 (PEI pH =11)]

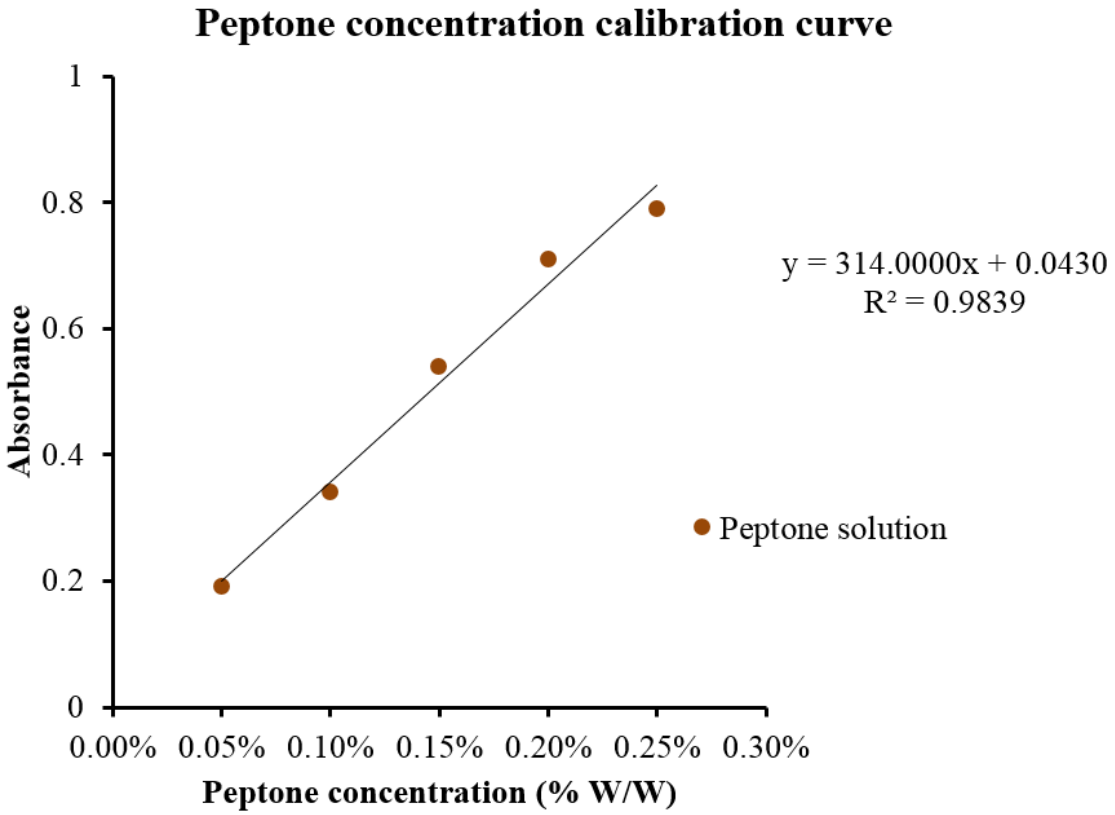

Figure A4.5 Standard calibration curve for peptone concentration at 270 nm [the calibration curve is tested at 25 ℃, pH = 8.3 (PEI pH =12)]

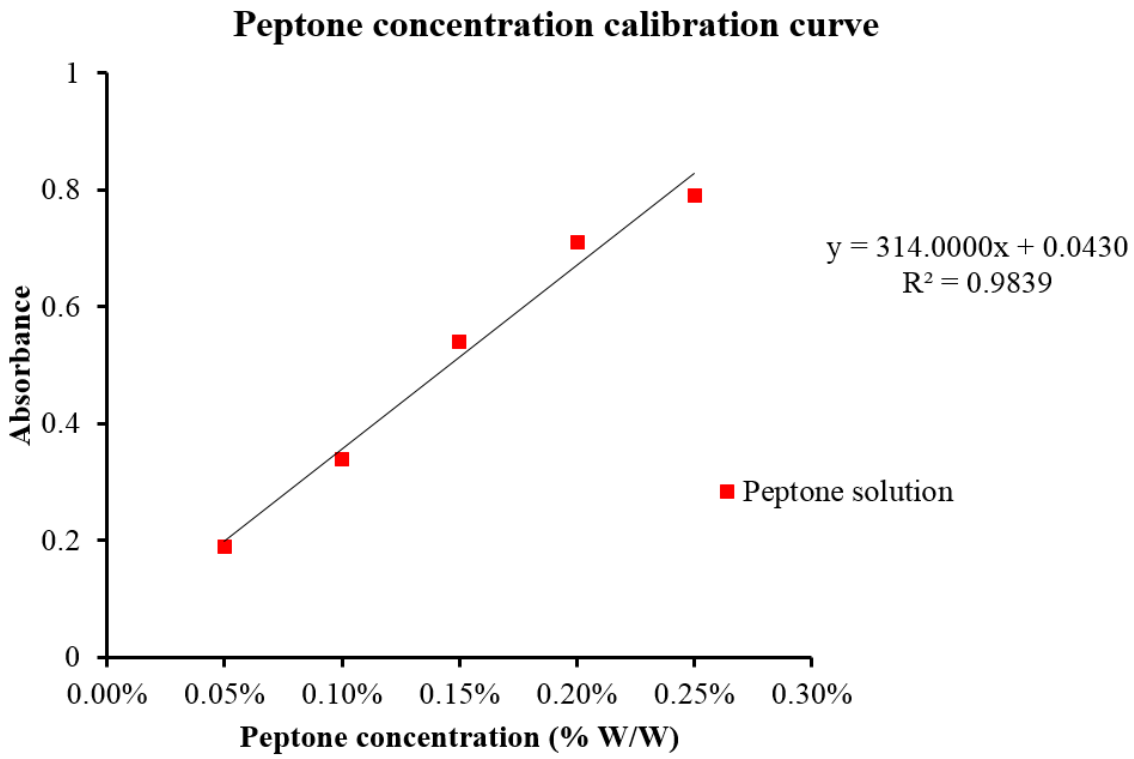

Figure A4.6 Standard calibration curve for peptone concentration at 270 nm [the calibration curve is tested at 40 ℃, pH = 7.4 (PEI pH =10)]